THE NATIONAL ACADEMIES PRESS

SHARE

Acoustic Beamforming: Mapping Sources of Truck Noise

DETAILS

BUY THIS BOOK

FIND RELATED TITLES

AUTHORS

Paul R Donavan; Yuriy A Gurovich; Kenneth J Plotkin; Daniel H Robinson; William K Blake; Transportation Research Board

Visit the National Academies Press at **NAP.edu** and login or register to get:

– Access to free PDF downloads of thousands of scientific reports
– 10% off the price of print titles
– Email or social media notifications of new titles related to your interests
– Special offers and discounts

NCHRP REPORT 635

Acoustic Beamforming: Mapping Sources of Truck Noise

Yuriy A. Gurovich
Kenneth J. Plotkin
Daniel H. Robinson
WYLE LABORATORIES INC.
Arlington, VA

William K. Blake
Bethesda, MD

Paul R. Donavan
ILLINGWORTH & RODKIN, INC.
Petaluma, CA

Subject Areas
Energy and Environment • Highway and Facility Design

TRANSPORTATION RESEARCH BOARD

WASHINGTON, D.C.
2009
www.TRB.org

NATIONAL COOPERATIVE HIGHWAY RESEARCH PROGRAM

Systematic, well-designed research provides the most effective approach to the solution of many problems facing highway administrators and engineers. Often, highway problems are of local interest and can best be studied by highway departments individually or in cooperation with their state universities and others. However, the accelerating growth of highway transportation develops increasingly complex problems of wide interest to highway authorities. These problems are best studied through a coordinated program of cooperative research.

In recognition of these needs, the highway administrators of the American Association of State Highway and Transportation Officials initiated in 1962 an objective national highway research program employing modern scientific techniques. This program is supported on a continuing basis by funds from participating member states of the Association and it receives the full cooperation and support of the Federal Highway Administration, United States Department of Transportation.

The Transportation Research Board of the National Academies was requested by the Association to administer the research program because of the Board's recognized objectivity and understanding of modern research practices. The Board is uniquely suited for this purpose as it maintains an extensive committee structure from which authorities on any highway transportation subject may be drawn; it possesses avenues of communications and cooperation with federal, state and local governmental agencies, universities, and industry; its relationship to the National Research Council is an insurance of objectivity; it maintains a full-time research correlation staff of specialists in highway transportation matters to bring the findings of research directly to those who are in a position to use them.

The program is developed on the basis of research needs identified by chief administrators of the highway and transportation departments and by committees of AASHTO. Each year, specific areas of research needs to be included in the program are proposed to the National Research Council and the Board by the American Association of State Highway and Transportation Officials. Research projects to fulfill these needs are defined by the Board, and qualified research agencies are selected from those that have submitted proposals. Administration and surveillance of research contracts are the responsibilities of the National Research Council and the Transportation Research Board.

The needs for highway research are many, and the National Cooperative Highway Research Program can make significant contributions to the solution of highway transportation problems of mutual concern to many responsible groups. The program, however, is intended to complement rather than to substitute for or duplicate other highway research programs.

NOTICE

The project that is the subject of this report was a part of the National Cooperative Highway Research Program conducted by the Transportation Research Board with the approval of the Governing Board of the National Research Council. Such approval reflects the Governing Board's judgment that the program concerned is of national importance and appropriate with respect to both the purposes and resources of the National Research Council.

The members of the technical committee selected to monitor this project and to review this report were chosen for recognized scholarly competence and with due consideration for the balance of disciplines appropriate to the project. The opinions and conclusions expressed or implied are those of the research agency that performed the research, and, while they have been accepted as appropriate by the technical committee, they are not necessarily those of the Transportation Research Board, the National Research Council, the American Association of State Highway and Transportation Officials, or the Federal Highway Administration, U.S. Department of Transportation.

Each report is reviewed and accepted for publication by the technical committee according to procedures established and monitored by the Transportation Research Board Executive Committee and the Governing Board of the National Research Council.

The Transportation Research Board of the National Academies, the National Research Council, the Federal Highway Administration, the American Association of State Highway and Transportation Officials, and the individual states participating in the National Cooperative Highway Research Program do not endorse products or manufacturers. Trade or manufacturers' names appear herein solely because they are considered essential to the object of this report.

THE NATIONAL ACADEMIES
Advisers to the Nation on Science, Engineering, and Medicine

The **National Academy of Sciences** is a private, nonprofit, self-perpetuating society of distinguished scholars engaged in scientific and engineering research, dedicated to the furtherance of science and technology and to their use for the general welfare. On the authority of the charter granted to it by the Congress in 1863, the Academy has a mandate that requires it to advise the federal government on scientific and technical matters. Dr. Ralph J. Cicerone is president of the National Academy of Sciences.

The **National Academy of Engineering** was established in 1964, under the charter of the National Academy of Sciences, as a parallel organization of outstanding engineers. It is autonomous in its administration and in the selection of its members, sharing with the National Academy of Sciences the responsibility for advising the federal government. The National Academy of Engineering also sponsors engineering programs aimed at meeting national needs, encourages education and research, and recognizes the superior achievements of engineers. Dr. Charles M. Vest is president of the National Academy of Engineering.

The **Institute of Medicine** was established in 1970 by the National Academy of Sciences to secure the services of eminent members of appropriate professions in the examination of policy matters pertaining to the health of the public. The Institute acts under the responsibility given to the National Academy of Sciences by its congressional charter to be an adviser to the federal government and, on its own initiative, to identify issues of medical care, research, and education. Dr. Harvey V. Fineberg is president of the Institute of Medicine.

The **National Research Council** was organized by the National Academy of Sciences in 1916 to associate the broad community of science and technology with the Academy's purposes of furthering knowledge and advising the federal government. Functioning in accordance with general policies determined by the Academy, the Council has become the principal operating agency of both the National Academy of Sciences and the National Academy of Engineering in providing services to the government, the public, and the scientific and engineering communities. The Council is administered jointly by both the Academies and the Institute of Medicine. Dr. Ralph J. Cicerone and Dr. Charles M. Vest are chair and vice chair, respectively, of the National Research Council.

The **Transportation Research Board** is one of six major divisions of the National Research Council. The mission of the Transportation Research Board is to provide leadership in transportation innovation and progress through research and information exchange, conducted within a setting that is objective, interdisciplinary, and multimodal. The Board's varied activities annually engage about 7,000 engineers, scientists, and other transportation researchers and practitioners from the public and private sectors and academia, all of whom contribute their expertise in the public interest. The program is supported by state transportation departments, federal agencies including the component administrations of the U.S. Department of Transportation, and other organizations and individuals interested in the development of transportation. **www.TRB.org**

www.national-academies.org

COOPERATIVE RESEARCH PROGRAMS

FOREWORD

By Christopher J. Hedges
Staff Officer
Transportation Research Board

This report documents the use of the acoustic beamforming technique to pinpoint and measure noise levels from heavy truck traffic. The system uses an elliptical array of more than 70 microphones and data acquisition software to measure noise levels from a variety of noise sources on large trucks—including the engine, tires, mufflers, and exhaust pipes. The results validate the feasibility of beamforming technology, offer new insight into the distribution of truck noise sources, and provide valuable input to the design and testing of quieter pavements and noise barrier systems. This report will be of interest to anyone concerned with understanding and mitigating highway noise levels.

Heavy trucks are significant contributors to overall traffic noise levels, and transportation agencies need to better understand the location and relative levels of the principal noise sources (e.g., exhaust, mechanical, tire–pavement, and aerodynamic) on heavy vehicles in order to more successfully mitigate traffic noise impacts.

Typical measures used to mitigate highway traffic noise include noise barriers, land use planning, and insulation of structures. Some transportation agencies are investigating additional measures, such as quiet pavements. Newer acoustical measurement and mapping techniques such as beamforming show promise for isolating the location and extent of the primary noise sources emanating from heavy trucks. Under NCHRP Project 08-56, a research team led by Wyle Laboratories designed and fabricated an elliptical beamforming array and tested a proof-of-concept design on stationary and moving trucks in a controlled setting. The tests were validated using known sound sources such as loudspeakers mounted on the vehicles. The resulting data were analyzed in the laboratory, and the tests validated the array's ability to localize and evaluate individual noise sources from the test vehicles. Following the proof-of-concept testing, the beamforming technique was used to measure truck noise sources under actual operating conditions on US 301 in Maryland. A total of 59 heavy truck and 4 medium truck pass-bys were measured, analyzed, and interpreted. The results showed acoustic beamforming to be a very appropriate method for truck noise measurement and enabled the research team to optimize the microphone array and software for this purpose. The system was effective in isolating and measuring noise sources for both stationary and moving trucks with frequencies between 250 and 2000 Hz. The report includes a number of recommendations, including the updating of current traffic noise models, development of a national database for traffic noise models on different pavement types, and the further application of the study results to evaluate pavement and noise barrier designs.

CONTENTS

S U M M A R Y

Acoustic Beamforming: Mapping Sources of Truck Noise

Heavy trucks are significant contributors to overall traffic noise levels. At highway speeds, the noise level produced by heavy trucks is about 10 dB greater than that of light vehicles. As a result, every heavy truck in the traffic flow contributes the same amount to the average noise level values as 10 light vehicles. Because of this significant contribution, a thorough understanding of the trucks as a noise source is crucial to the prediction and mitigation of traffic noise. Noise from heavy trucks originates from a variety of sources, which include exhaust stack outlet, muffler shell, exhaust pipes, engine block, air intake, cooling fan, tires, and aerodynamics. The relative contributions of these sources vary with vehicle type, operating condition, and (for tire noise) the type of pavement.

For modeling and abatement of traffic noise, the barrier performance of sound walls depends on the distribution of noise source heights. Because trucks contribute the tallest noise sources, highway noise walls are typically designed so the top of the exhaust stack is obscured from the receiver's sight under the assumption that exhaust noise is a major source. The current treatment of truck noise for highway conditions is often simplistic, placing about 50% of the source strength at a height of 12 ft (3.7 m) and the other half at ground level, independent of vehicle speed or pavement type.

A number of recent observations, however, challenge the current treatment of trucks and led to the need for new research. First, as a result of the federal regulations in the United States, truck noise levels have been incrementally lowered over the past few decades. In achieving this lower level of noise performance, engine and exhaust noise have been effectively addressed.

From recent studies performed in Europe, tire–pavement noise has been found to have a much larger contribution, 63% to 84%, at highway speeds. A few studies have also shown that noise levels are strongly dependent on truck tire type. From research work related to the application of quieter pavements, reductions in traffic noise have been measured consistent with the reduction of tire–pavement source levels when pavement modifications have been made, which goes beyond what would be predicted based on the current treatment of truck noise as being split evenly between tire–pavement and elevated sources on trucks.

For all these reasons, it is essential to have more information about truck noise sources than can be observed in typical passby measurements. The objective of this study was to use noise-source mapping techniques to accurately localize, identify, and quantify the noise sources on typical commercial trucks operating in the actual roadway environment. The scope of work for this project included design, development, experimental demonstration, and validation of a practical technology for truck noise-source localization and distribution under actual operating conditions.

Findings

Current noise-source identification techniques were reviewed and assessed for their suitability for the type of measurements necessary in the study. Traditional truck noise-source measurement methods—such as component wrapping, removal, and substitution—are labor intensive and can realistically be performed only on a relatively small number of vehicles in controlled tests. The sound intensity method, involving a special probe placed near different source regions of the vehicle, is typically applied either in laboratory settings or in controlled near-field measurements but cannot be employed in uncontrolled situations. Another method used for sound source identification is near-field acoustic holography. It employs an array of microphones that is also typically used in stationary, laboratory test conditions or is suspended along side of the tested vehicle. However, the microphone array must be physically as large as the source region of interest and cannot be employed in uncontrolled passby applications with moving vehicles.

The more compelling method of localizing noise sources is acoustic beamforming, which uses a stationary array of microphones to focus measurement on a specific point near the actual source and to scan this focus point electronically over the object of interest. The measurements can be performed in the far field, and the associated computer algorithm can account for both the moving source and Doppler frequency shift, as well as provide tracking of the vehicle by evaluating several time periods during the passby, thus increasing the accuracy of the result. Beamforming techniques have been used for localizing noise sources on trains and automobiles and in other applications. However, several issues had to be resolved before this technique could be employed for the truck application, including the spatial resolution for the low frequencies of interest for truck noise, the optimal array dimensions and configuration, the number of array microphones needed, as well as a few practical application concerns.

Based on the analysis of existing research and current practices, as well as the study team's experience in the preceding truck noise studies, beamforming was found the most appropriate noise source mapping method for truck application and was further developed and optimized for this application in the current study.

As the result of the development, an experimental 70+ microphone elliptical array was designed and fabricated for truck testing. The elliptical shape was found optimal because vertical resolution of the noise source image is more important than horizontal resolution for traffic noise barrier design and also because of certain inherent horizontal resolution of the noise source image during a passby. The microphone array parameters assuring the optimal performance were selected for implementation in the array hardware. Associated beamforming software was developed and implemented using a computerized data acquisition system.

The experimental microphone array and noise-source mapping technique was validated through proof-of-concept testing. It was performed at low-speed and high-speed truck testing facilities for a representative sample of trucks with different characteristics to validate the measurement system performance and verify its parameters. Multiple sound distribution images were obtained during the testing for truck noise sources—such as engine compartment, tires, and exhaust—in the effective frequency range from approximately 250 to 2000 Hz. The test results confirmed that the developed system provided adequate noise mapping and localization for typical noise sources on various trucks, both stationary and moving with the speed up to 50 mph (80 km/h).

With a few minor modifications, the measurement system was further applied to quantify noise sources for a wide range of trucks under actual road conditions on an in-service highway. One hundred vehicle passbys (heavy and medium trucks, and buses) were recorded using the measurement system in a single day of data acquisition. Individual vehicle speed during passbys varied from 55 to 70 mph (88 to 112 km/h). Figure S-1 shows the microphone array setup for the roadside noise measurements.

Figure S-1. Microphone array setup for roadside noise measurements.

The results of these measurements for 59 heavy truck passbys and 4 medium truck passbys were analyzed in detail, with acoustic images and spatial noise source distributions obtained to define and interpret the noise source levels and sound paths from the engine, tires, exhaust, and other body components. Individual trucks, as well as statistical metrics for the truck passbys, were evaluated. Figure S-2 shows a typical acoustic image of a truck with prevailing tire noise (a) and a vertical distribution of the overall A-weighted sound levels measured during the truck passby (b).

The results of the study indicate that, for majority of the measured trucks (55 heavy and 4 medium trucks), the highest noise levels were generated close to the pavement at approximately 0.6 m (2 ft) elevation. For these trucks, the measurement data did not reveal significant noise sources at the height of vertical exhaust stacks.

Four of the heavy trucks measured (7.3%) exhibited significant noise generation in the area of the vertical exhaust stack at about 3.6 m (12 ft) above the road surface, with the sound levels exceeding that produced by the tire–pavement interaction at low frequencies (below 500 Hz). Figure S-3 shows an acoustic image of a truck with the exhaust noise dominating the tire noise (a) and a vertical distribution of the overall A-weighted sound levels measured during the truck passby (b).

The study also showed that statistical vertical distributions (mean and maximum) of truck noise sources can be effectively simulated by a simple system of two uncorrelated sources located
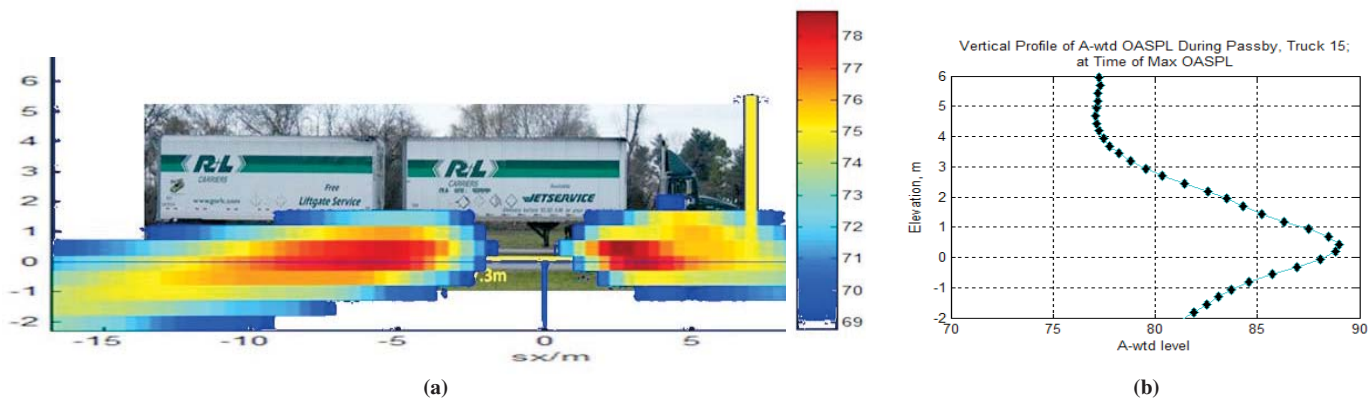
Figure S-2. Tire noise dominates in this truck passby: (a) source image and (b) vertical distribution of the overall A-weighted sound levels.
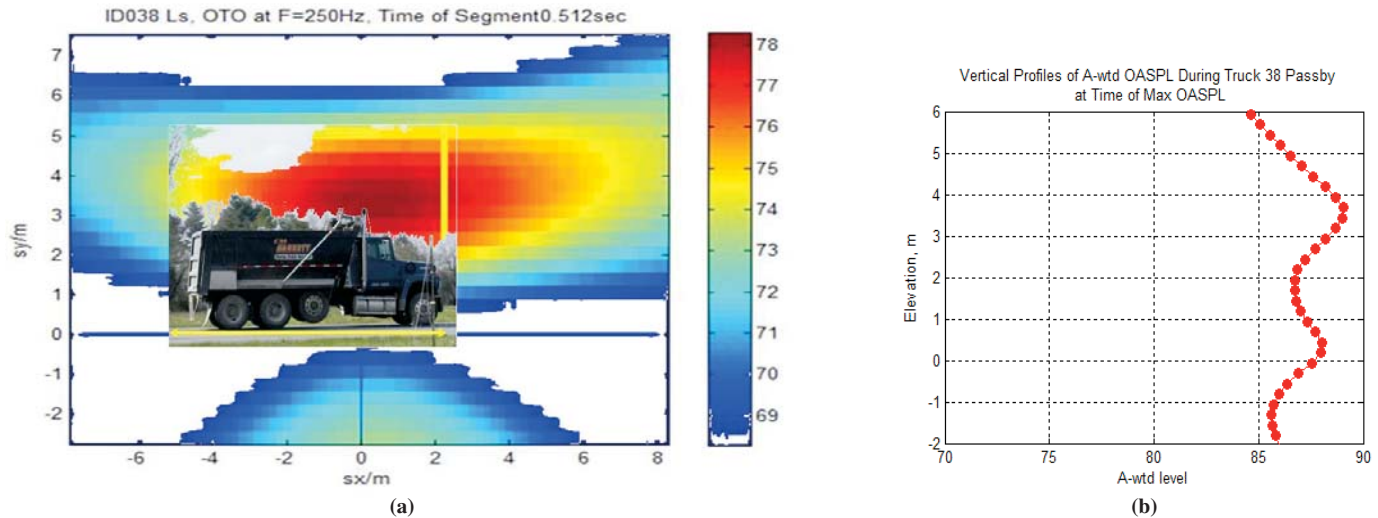
Figure S-3. *Exhaust noise dominates tire noise in this truck passby: (a) acoustic image and (b) vertical profile of overall A-weighted sound levels.*

near the pavement and at the exhaust stack elevation. These results can be used for developing a model for the truck noise propagation.

Conclusions

Overall, the results of the study validated the beamforming measurement technique in the truck noise application. It is confirmed that the measurement system developed in the course of the project performed effectively in mapping and localizing typical noise sources for stationary and moving trucks in actual road conditions in a wide frequency range from 250 to 2000 Hz. Sound distribution images and maps obtained during truck passbys permitted examination of the time histories and spatial distributions of sources, as well as an analysis of the noise paths from the engine, exhaust, muffler, tires, and other body components for various trucks.

Statistical analysis of the vertical distribution of noise sources indicated that for the majority of truck passbys measured at highway speeds on an in-service highway, tire–pavement interaction was the dominant source generating sound close to the pavement. A small proportion of heavy trucks, however, exhibited significant noise generation in the area of the vertical exhaust stack, dominating at low frequencies and elevations around 3.6 m (12 ft). These results are in general agreement with the conclusions of the California Department of Transportation study that used a commercial beamforming microphone array. The two studies provided essentially similar results in terms of sources identified, their relative contributions, and lack of higher elevation sources except in a few cases.

For the noise prediction modeling purposes, the current study indicated that a simple system of two uncorrelated sources, one located near the pavement and another at the exhaust stack elevation, can generally be used for simulating statistical vertical distributions (mean and maximum) of truck noise sources.

Recommendations

Based on the key findings and conclusions for the project, the following future research and testing needs can be identified:

- Conduct nationwide roadside truck noise measurements on a wider range of pavement types in multiple states to establish a new truck noise source database (source height distributions and spectral content) for traffic noise models. Additional analysis of subsampling of the full beamforming microphone array may be necessary, based on the data obtained in the current project, to expand the technique, simplify the array, and speed up data collection for wider scale measurements at a practical degree of effort.
- The noise source distributions for trucks obtained in the current study, although based on a relatively small sample of the truck population, can be applied (if deemed appropriate) as interim source height adjustments to the reference emission levels in the FHWA Traffic Noise Model.
- Traffic noise prediction models updated using the noise source distributions obtained in the current study can serve as a resource for state and federal agencies to examine the effectiveness of highway noise mitigation strategies, such as the use of quieter pavements or barrier design.
- Novel information obtained for noise source distributions on trucks, as well as the measurement technique developed in the course of the study, are recommended to truck manufacturers for further studies of potential source- or path-targeting treatments.
- The beamforming measurement technique developed during the course of the study is also recommended for use in the analysis of noise-generating mechanisms and noise abatement measures for automobiles, buses, and motorcycles, as well as other noise sources such as construction equipment, etc.
- The approach developed in the study can be used for exploring in greater detail the effects of varying pavement types and terrains on noise generated by different vehicle types, including the effects on vertical noise source distribution and tire–pavement interaction.

C H A P T E R   1

Background

1.1 Introduction

Heavy trucks are significant contributors to overall traffic noise levels. At highway speeds, the noise level produced by heavy trucks is about 10 dB greater than that of light vehicles (*1*). As a result, every heavy truck in the traffic flow contributes the same amount to the average noise levels as 10 light vehicles. Because of their contribution, a thorough understanding of trucks as a noise source is crucial to the prediction and mitigation of traffic noise. In addition to the overall noise level of truck passbys, the location and relative strength of the principal noise sources (e.g., exhaust, powertrain, tire–pavement, and aerodynamic) on individual trucks is important. For modeling and abatement of traffic noise, the barrier performance of sound walls depends on the assumed distribution of source heights. In some states, highway sound walls are designed so the top of the exhaust stack is obscured from sight under the assumption that exhaust noise is a major source. For abating truck noise through quieter pavements, the amount of expected noise reduction depends on the contribution of tire–pavement noise relative to other sources such as powertrain, exhaust, and possibly aerodynamic noise. The current treatment of truck noise for highway conditions is simplistic, placing about 50% of the source strength at a height of 12 ft (3.7 m) and the other half at ground level.

Recently, a number of observations have challenged the current treatment of trucks and led to the need for new research. First, truck noise levels are one of the very few noise sources regulated at the federal level in the United States. Over the past few decades, the regulated noise level has been incrementally lowered to the point where trucks are expected to meet the same level requirement as light vehicles under engine noise–dominated test procedures. In achieving this lower level of noise performance, engine and exhaust noise have been addressed. As older trucks are replaced, these sources are expected to play less of a role in total truck noise emissions under highway conditions than tire–pavement noise. In the

United States, source height distributions were last measured in the mid-1990s using the technology available at that time (*2, 3*). Those measurements were made when the current regulated level had been in place for 8 years. They do not reflect changes in the fleet that may have occurred in the subsequent decade.

A second factor challenging the current treatment of truck noise is recent research that has been performed in Europe. From these studies (*4, 5*), tire–pavement noise has been found to make a much larger contribution, 63% to 84%, to total truck noise at highway speeds. From the European work (*6*) and some research in the United States, a strong dependence on truck tire type has also been determined. The more aggressive tread tires often used on the drive axles are found to be as much as 10 dB louder than those used on the steering or trailer axles. With such large differences between tire types, it is expected that tire–pavement noise could be quite pronounced for some trucks, depending on tire selection.

The third set of observations comes from research work conducted in conjunction with the application of quieter pavements. In a number of recent projects, reductions in traffic noise have been measured consistent with the reduction of tire–pavement source levels when pavement modifications have been made (*7–9*). Even statistical passby measurements for trucks have shown reductions with pavement modifications almost as great as indicated by tire–pavement noise source level reductions (*10*). The reduction in truck noise source levels goes beyond that which would be predicted based on the current 50-50 split between tire–pavement and other, elevated noise sources on trucks.

1.2 Heavy Truck Noise Sources

Noise from heavy trucks originates from a variety of sources:

- Exhaust stack outlet
- Muffler shell

- Exhaust pipes
- Engine block
- Intake
- Fan
- Tires
- Aerodynamics

The relative contributions of these sources vary with vehicle type and operating condition, and (for tire noise) the type of pavement. Most sources are fairly localized, although installation details (i.e., engine compartment configuration) can affect the effective position and size of mechanical sources. Tire and aerodynamic noise are distributed, with tire noise near the ground along the length of the vehicle.

Source distribution is important in several ways:

- Source height is a major parameter in the design of roadside barriers.
- Source height is an important parameter for calculation of the effect of the ground on sound propagation.
- Truck dimensions are not small compared to standard reference measurement distances of 50 ft (15 m)—typical U.S. practice—or 25 ft (7.5 m)—typical European practice. Measurements conducted by Wyle during development of roadside test procedures (*11*) showed that propagation of truck noise at distances less than 50 ft (15 m) does not necessarily follow the 6 dB per distance doubling rule expected for simple sources.

The relative contribution and spatial distribution of truck noise sources can be quite complex and display significant variation from truck to truck, from site to site, and with truck speed due to the following factors:

- Exhaust system sources including the outlet and sound radiation from the muffler and exhaust pipe shells depend not only on the location and orientation of the system (e.g., vertical or horizontal) but also on the amount of deterioration or modification.
- Powertrain noise including radiation from the engine block, cooling fan, and intake will depend on powertrain configuration as well as its state of maintenance and loading.
- Tire noise will depend strongly on tire type and on pavement type with either of these contributing differences of up to 10 dB or more.
- The presence of exterior shrouds and air deflectors may also affect aerodynamically generated noise.

Because of all these parameters, it is important to have more information about each specific truck being evaluated than that which can be observed in typical uncontrolled passby measurements along the side of a roadway. Vehicle speed,

exhaust configuration, and pavement type can all be determined by using typical statistical passby test methods. Other key parameters, such as tire type, engine configuration, vehicle loading/operating condition, and general state of maintenance and/or modification, cannot be obtained in uncontrolled roadside testing. The state of compliance with the federally regulated noise emission levels also cannot be determined. For these reasons, evaluation of truck noise sources must include a combination of controlled passby and random, statistical passby data.

1.3 Source Identification Methods

During development of EPA's heavy truck noise regulations (*12*), extensive studies were conducted on truck noise sources. Source identification was typically obtained by combinations of near-field measurements, component wrapping, removal of components, and substitution of components (*13*). Stationary tests (idle-max-idle and dynamometer) and moving tests at various power settings (including coastby) further mapped out the contributions of various sources. That type of testing provided good results. For example, Wyle's light vehicle source study (*14*) mapped source and subsource characteristics over a full range of power and revolutions per minute (rpm), and yielded designs that were demonstrated to work on the road (*15*). Such testing is, however, labor intensive, and source analysis was performed on a relatively small number of vehicles. Substantially higher productivity can be achieved with remote sensing methods, such as acoustic holography, beamforming, and acoustic intensity measurements.

A number of studies reported in the current literature have addressed localizing noise sources on moving ground vehicles. Much of this work initially addressed high-speed trains. More recently, applications to motor vehicle passbys are appearing. A technique that has been proven successful in identifying and quantifying motor vehicle noise is the mapping of sound intensity. Typically, this technique is applied in a laboratory setting such as a chassis dynamometer where the sound intensity probe can be placed near different source regions of the vehicle. The resultant data can then be processed into sound intensity contour maps to assess source regions. Although this methodology is commonly used in a stationary laboratory setting, it has also been successfully used to map the source regions of moving tires (*16*). For controlled vehicle testing, this method could be extended to mapping the source regions of an entire vehicle. Such mapping would provide a direct linkage to the sound intensity method of tire–pavement noise measurements currently being applied in the California Department of Transportation (Caltrans) work and the Federal Highway Administration (FHWA) studies. The method could not be employed in uncontrolled situations, but was used in this study as a more sophisticated controlled test technique,

supplementing the classic near-field, component wrapping, and component substitution methods.

Another microphone array method used for source identification is acoustic holography. This method is also typically used in stationary laboratory test conditions. However, it has been used to identify source regions of tire–pavement noise under on-road operating conditions. In this application, the acoustic array is suspended along side and moving with the test tire (*17, 18*). Using a combination of near-field acoustic holography and far-field calculations based on Helmholtz's integral equation, it is possible to obtain a complete description of the sound field of the source, where both magnitude and phase of the sound pressure field are known at any point. The results of these works clearly indicated the source regions and compared well with similar localization studies performed using sound intensity. One of the features of acoustic holography is that the plane of the source distribution can be propagated very close to the source or farther away from the source, to typical passby measurement distances. However, unlike beamforming, the array used for acoustic holography must be physically as large as the source region of interest. In addition, acoustic holography is not suitable for passby applications when the array is stationary and the source is moving. As with sound intensity, this method could not be employed for uncontrolled passby testing, although it may be useful for some aspects of source localization under controlled conditions.

The more compelling method of localizing sources has been the application of acoustic beamforming, as detailed by Crewe et al. (*19*). Beamforming techniques in a horizontal direction have also been employed in French research specifically on truck sources (*6*). Acoustic beamforming uses an array of microphones to focus measurement on a specific point on an imaginary source plane near the actual source. This focus point is electronically swept across this plane, and the noise level is determined. In more advanced approaches, which should be used in the case of moving vehicles, the source plane moves with the vehicle and points are scanned over the time the vehicle goes by. Such an advanced approach requires that the algorithm accounts for both the moving source plane and Doppler shifting of the sound during the passby. In this manner, several slices in time can be evaluated near the position of interest, such as the time when the maximum passby noise level occurs. Unlike the more simple methods that consider only one instant during the passby, beamforming, by tracking the source and averaging over several instances, has a more accurate result. Because of tracking capability, this type of beamforming can also be exploited to evaluate source directivity as the vehicle approaches and recedes from the measurement position. Beamforming algorithms can also be provided for either spherical or planar cases. For the planar case, the array is assumed to be far enough from the source plane so that there is no path length difference for different points on the source plane (acoustic plane wave assumption). For the more complex spherical case, path lengths are assumed to be different and are accounted for properly by including spherical divergence. Because of the large physical size of the source plane for trucks, spherical beamforming which tracks the vehicle during the passby is likely the only appropriate approach to consider.

Based on the analysis of existing literature, research, and current practices, as well as the study team's experience in the preceding truck noise studies, beamforming is considered the most promising noise mapping method for trucks. It is capable of mapping both vertical and horizontal noise source distributions and implicitly carries with it spectral information about sources under actual operating conditions. Unlike the sound intensity and acoustic holography techniques, this method is also capable of identifying and tracking large moving sources during uncontrolled vehicle passby testing.

Although beamforming techniques are promising for localizing truck noise sources under passby conditions, several issues needed to be resolved before this technique could be selected for the truck application, namely:

- The spatial resolution of the technique for the frequencies of interest for truck noise. In the successful applications in the literature, the revealing "pictures" of sound are typically higher in frequency, above 1500 Hz. In part because of the longer wavelengths and the limitations of the array, at frequencies below 1000 Hz the source regions may appear quite large and source identification uncertain.
- Source-to-array distance. For controlled tests, distance can be optimized to be relatively close to the vehicle. For roadside measurements, practical issues of safe access, ambient conditions, and not distracting drivers limit how close the array can be positioned to the lane of travel.
- Practical concerns such as the effect of large vehicle wakes, random turbulence, and other background noise.

A study (*20*) performed by Illingworth & Rodkin, Inc. (I&R) under contract to Caltrans in 2005 focused on the ability of beamforming technology to localize sources on different types of trucks under several modes of operation. The results of this work addressed many of the application issues mentioned previously. The data from the Caltrans project was used to optimize the methodology with regard to the number of array microphones needed and the configuration of the array itself. The signal processing required for the beamforming algorithm was developed by Dr. William Blake for both the Caltrans study and this NCHRP study and includes spherical divergence, source tracking, and Doppler shift, as described in more detail in Section 3.2.1.

A significant part of the demonstration of a relatively new technique such as beamforming is to demonstrate that it yields

correct results and agrees with measurements from established methods. The work of Crewe et al. (*19*) provides some of that demonstration. Their test vehicle was, however, rather simple—a minivan whose dominant noise source was tire–pavement noise. Two non-tire noise sources were identified: the vehicle's horn and a speaker placed in the top near part of the engine compartment. The distribution of noise sources on heavy trucks is, in general, considerably more complex and requires additional technique verification.

1.4 Objective and Scope of Research

The objective of this study was to use acoustic measurements and noise source mapping techniques to accurately identify, locate, and quantify the noise sources on typical commercial truck and tractor-semitrailer combinations operating in the U.S. roadway environment.

The scope of work for this project was divided into nine tasks that generally define and demonstrate a technology for truck noise source localization, plan and execute measurements to better understand truck noise source distributions under actual operating conditions, and document the results throughout the project. These tasks are detailed in Chapter 2.

The interim report for the project, submitted in July 2007 in accordance with Task 4, presented the results of the literature search, development of the experimental design, and proof-of-concept tests (Tasks 1 through 3). Upon an NCHRP review and approval of the interim report, the roadside test plan was developed and implemented in Tasks 5 and 6. This final report incorporates the interim report material revised per the NCHRP comments (Tasks 1 through 4), includes the results of the roadside truck testing (Tasks 5 and 6), summarizes the key findings of the study (Task 7), and identifies the future research and testing needs (Task 8).

C H A P T E R   2

Research Approach

Task 1. Analyze Literature, Research, and Current Practice

A review was conducted of current noise source identification techniques. Emphasis was on beamforming, which had been demonstrated to be generally suitable for this type of measurement. A major objective of the literature review was to quantify frequencies, distances, array sizes, etc., to ensure that the array developed for this project would reflect the current state of the art. The recent work by I&R for Caltrans provided key data for analysis of these issues, particularly for investigating array size, frequency range, and spatial resolution.

Results of the review of current noise source identification techniques are presented in Chapter 3.

Task 2. Develop Experimental Design

Two separate experimental tasks were proposed in this project to develop a practical measurement technique for quantifying truck noise sources. The first experimental task was the design and validation of a noise source mapping technique through proof-of-concept tests on a limited number of trucks and pavements, with emphasis on validating the noise mapping method. This proof-of-concept test was completed in Tasks 2 and 3 and is described in Chapter 3.

Task 3. Perform Proof-of-Concept Test

The technology demonstration was accomplished through the proof-of-concept testing with the assistance of International Truck and Engine Corporation (IT) at their proving grounds in Fort Wayne, Indiana, in July 2006. A limited but representative sample of trucks was selected from the vehicle test matrix developed in the previous task and available at IT. The beamforming tests were conducted on a stationary truck operating under different conditions, were validated using known sound sources such as loudspeakers added to the vehi-

cle, and then were conducted with trucks performing a series of passby procedures. Beamforming measurements were conducted for a number of test configurations.

The proof-of-concept test data were post-processed and analyzed in a laboratory. This analysis included an experimental evaluation of various performance characteristics of the array measurement system, comparison with the theoretical parameters specified earlier for the array in the design stage, as well as example results for truck passbys at low- and high-speed tracks with localization and identification of individual noise sources for the tested trucks.

Task 4. Submit Interim Report

The interim report summarizing the results of Tasks 1 through 3 was submitted in July 2007. It presents the results of the literature search, development of the experimental design, and the proof-of-concept tests. Following a review and meeting with the NCHRP, comments by the NCHRP were accommodated in the experimental design and testing plan for the remaining tasks. Work on the subsequent tasks proceeded following NCHRP approval.

Task 5. Execute Testing Plan

The second experimental task of the project, application of the validated method to quantify noise sources on typical heavy trucks, was accomplished through noise mapping of a number of trucks under actual roadside conditions on an in-service highway. Prior to the mapping, the necessary adjustments to the technique identified during the proof-of-concept testing of Task 3 were performed. The roadside testing was conducted in April 2008 with the beamforming system collecting data for a wide range of trucks and various operating conditions on a selected highway (US 301). One hundred vehicle passbys were recorded in one day of testing using the measurement system developed.

Task 6. Document and Analyze Results

The roadside test data were again post-processed in a laboratory. The analysis included an experimental evaluation of the spectral content of the measured truck pass-bys and the vertical distribution of the noise from truck sources, as well as statistical assessment for multiple pass-bys. The results of the testing are presented and discussed in Chapter 3.

Task 7. Summarize Key Findings

The key findings of the study are summarized and presented in the Summary of this report.

Task 8. Identify Future Research and Testing Needs

Potential areas for follow-up research to and application of the truck noise source mapping technique developed in the study for further truck testing are identified and presented in Chapter 4.

Task 9. Submit Final Report

This final report incorporates the interim report material revised according to the NCHRP comments, includes the new results for the roadside truck testing, summarizes the key findings of the study, and identifies the future research and testing needs.

C H A P T E R   3

Research Findings

3.1 Review of Beamforming for Vehicle Noise Source Identification

A recent development in microphone array application for localization of sound sources of moving motor vehicles (*21*) showed that 124 microphones arranged in a two-dimensional snowflake array made it possible to locate sound sources during car passbys with a resolution of 1 to 1.3 ft (0.3 to 0.4m) in a frequency range of 500 to 4500 Hz. With an overall array size of approximately 12 by 12 ft (3.7 m by 3.7 m) and a distance of 8 ft (2.4 m) between the array and test object, the two-dimensional distributions of the sound pressure level were measured during passbys of an automobile at speeds from 50 to 110 mph (80 to 180 km/h). In the frequency range between 300 and 500 Hz, however, the array's spatial resolution was worsened by a factor of 2. Also, even with a simple, stationary point source in front of the center of the array, the false sources of lower magnitude, so-called ghost images, begin to appear in the resulting source maps at frequencies of 1000 Hz and above despite the array side lobes suppressed by the 10 to 15 dB array gain. Barsikow suggests that the frequency range of the array could be extended by increasing the number of microphones to a total of about 160 (*21*).

Commercial beamforming wheel arrays, instrumentation, and software packages were developed by Brüel & Kjær (*22, 23*). The wheel arrays consist of a number of spokes (from 7 to 15), each holding up to six microphones. Three typical wheel-array designs of 42, 66, and 90 channels with different performance levels cover different applications from general purpose to automotive components to entire vehicle. The geometry of each array is optimized for minimum side lobe levels over a certain frequency range.

A 90-channel Brüel & Kjær wheel array with a PULSE beamforming software package were used by I&R for truck noise testing on IT's endurance track performed for Caltrans in 2005 (*20*). Useful results were obtained, but there were lim-its associated with the system being general purpose, rather than optimized for the specific type of measurements needed for moving trucks.

In general, however, the circular spiral arrays (*24–28*) offer adequate side lobe suppression with a minimum number of sensors. As such, this class of arrays can be used to provide affordable performance over a broad frequency range. The circular spiral microphone array was used as the baseline for the beamforming design in the current study.

3.2 Development of Experimental Design

3.2.1 Noise Mapping Technique Development

Specific parameters that were considered relative to the beamforming technique developed in this study included the system requirements for heavy trucks (e.g., frequency range of interest, horizontal and vertical spatial resolution required, source to array distance) and design parameters for beamforming measurement application (e.g., number of microphones, array size and geometry, sample size and averaging time, processing software). A factor considered, both as a requirement and a design parameter, was the frequency resolution. One final factor is that, for highway barrier design purposes, vertical resolution is much more important than horizontal.

The design of candidate array options was built on lessons learned during the array-based demonstration tests of truck noise source localization conducted by Blake and Donavan under Caltrans sponsorship in 2005 (*20*).

The current design study had four major objectives:

- Extend the directivity gain to lower frequencies than used in the Caltrans demonstration of 2005.
- Meet or exceed the array gain performance of the Brüel & Kjær array used in the 2005 test.

- Optimize array performance for an affordable 70-element array.
- Tailor array shape to optimize:
  – Vertical directivity through vertical array aperture;
  – Horizontal directivity through combined array aperture and cross-range spreading loss during vehicle passby;
  – Array height (vertical aperture) for assembly/disassembly in the field controlled by available facility;
  – Side lobe suppression to minimize "false" source localizations at the high end of frequency range of interest.

The low frequency limit on array design was found to be 250 Hz, which should localize sources (potentially exhaust muffler related) to the upper or lower half of the cab area. Degraded performance is unavoidable at lower frequencies, given practicalities of array handling in the field.

The beamforming software package was developed to calculate both two-dimensional source image distributions projected in a vertical plane at the truck side and one-dimensional vertical sound source distributions determined at a distance of 20 ft (6 m). All processing was done in the frequency–time domain in which the received signal is sectioned into roughly 15 time segments of 0.1 to 0.15 s duration. Within each time segment, the spectrum of the sound at each array microphone was digitally computed in equivalent 1 Hz bands. These spectral levels are used to compute either sound pressure levels or inter-element cross-spectral densities. The processed sound pressure levels are used to evaluate the vertical profiles. The cross-spectral densities are used to localize in elevation (up and down) and cross-range (left or right) to give the two-dimensional source map in the vertical plane. To do this step, the array is digitally steered to its left and to its right. Because the arrival direction of the sound "looks" at the truck both approaching and leaving the array zone, an adjustment in Doppler shift is made at each frequency and for each arrival angle of the sound from the truck. Additionally, a correction is made for the range geometry spreading loss (i.e., $1/r^2$) at each of the time segments. The array is mathematically modeled as an acoustic lens that focuses on various points in the vertical plane in order to "scan" for the sources. The narrow band images, determined for 1 Hz band width, were summed to obtain images and sound levels in one-third octave frequency bands. All microphone signals, the photocell signals, and a recording time code were simultaneously recorded to provide accurate time resolution of the images at each moment of the passby. A digital photograph of a truck was geometrically scaled to the image plane dimensions using a pre-determined scale factor.

3.2.2 Microphone Array Design

The design strategy for the microphone array in this study needed to accommodate many factors, among them:

- Develop a circular spiral baseline array that approximates or surpasses the Brüel & Kjær array directivity for the truck application as used in the demonstration runs of 2005.
- Reduce the element number to 70 or 72, depending on the numbers of spokes and circles in the array.
- To ensure comparable side lobe structure with a reduced number of elements, reduce array circular area proportionately. This proportionate reduction provides comparable aperture area per element.
- Deform the circular spiral array by expanding the vertical aperture using the chart of spot width vs. frequency (see Figure 4) developed for the study, to select a trial major axis of the ellipse. Maintain element number and array area while deforming.
- Selectively introduce tilt of the spokes and spiral angle, to improve side lobe suppression as necessary. Figure 1 illustrates the essential geometry of an array of the type used in this study.

The notional array that is illustrated in Figure 1 represents one of the possible approximations to the array previously used in the Caltrans demonstration tests (*20*). This array performance was the baseline for the current design study. The circular array for this application, however, provides unnecessary localization in the horizontal direction and insufficient localization in the vertical direction. Given the intrinsic horizontal localization afforded by the passby itself, a deformed array was considered to optimize the effective localization vertically and horizontally for enhanced performance at low frequencies. Deformation of the parent circular array into an ellipse provides a means to tailor these arrays for truck passby. This facet of the array design represents one of the new products of the current project. The spiral angle and the spoke configuration introduce spatial irregularity into the circular array, which allows required side lobe suppression.

All of the arrays shown in Figure 2 have the same area (i.e., $AB = D^2$) and all have the same area density of elements. Figure 3 shows that the lobe structures of these arrays at 1000 Hz are virtually unaffected, as apparent from the illustration. The projection of the lobe structure has a shape outline that follows the outline of the array, but is rotated 90 degrees relative to it (i.e., an increase in array length along the x-axis results in a narrower beam in x; conversely, a reduction in array length along the y-axis results in a wider beam in y). (In this example, x represents the vertical axis and y represents the horizontal axis on a plane parallel to the array plane.)

Figure 4 provides a chart that gives the approximate lobe width, here called "spot width," as it refers to the localization in the truck side plane 20 ft (6 m) from the array plane. As shown, lengths on the order of 12 ft (3.7 m) are required to localize to within ±5 ft (1.5 m).
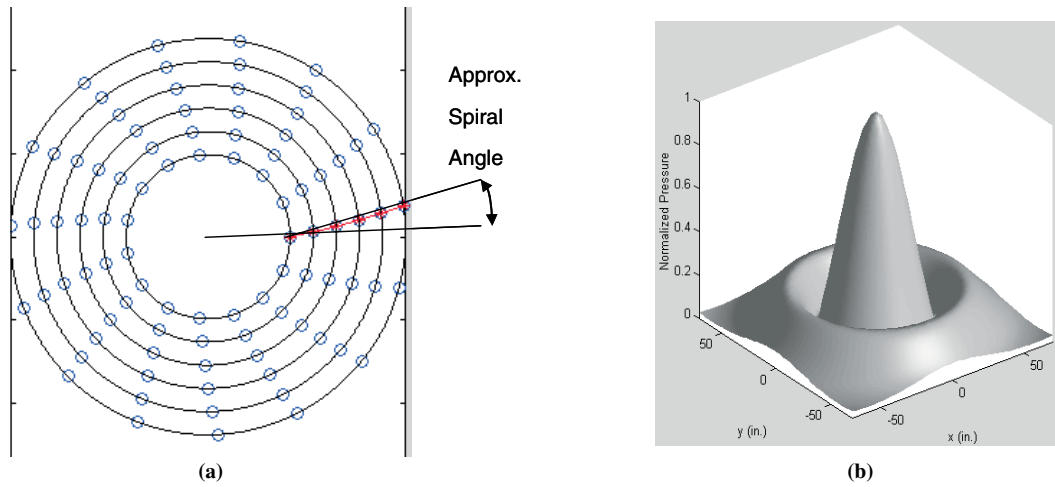
Figure 1. Notional 90-element circular spiral array with 15 spokes of 6 elements each and inner and outer radii of 19.7 and 47.6 in. (0.5 m and 1.2 m), respectively: (a) array pattern, (b) directivity pattern of array projected on x,y plane parallel to array plane and situated 20 ft (6 m) in front of it.

In Figure 5, the spot width is illustrated for the major and minor axes of the alternative arrays shown in Figure 2 [i.e., Ellipse 1, Ellipse 2, and the 7 ft (2.1 m) circular array] as a reference. Given the design requirement of constant area for all arrays, the degradation in horizontal beam width for the benefit of vertical discrimination is clearly seen.

3.2.3 Balance Between Array Aperture and Spherical Spreading Loss

As the truck sources pass by the microphone array, there is a sound level change at the array microphones that is simply due to the spherical spreading loss resulting from the varying

D= 7 ft

A= 9.1 ft

B= 5.37 ft

A= 11.8 ft

B= 4.1 ft

(a) Circular   (b) Ellipse 1   (c) Ellipse 2
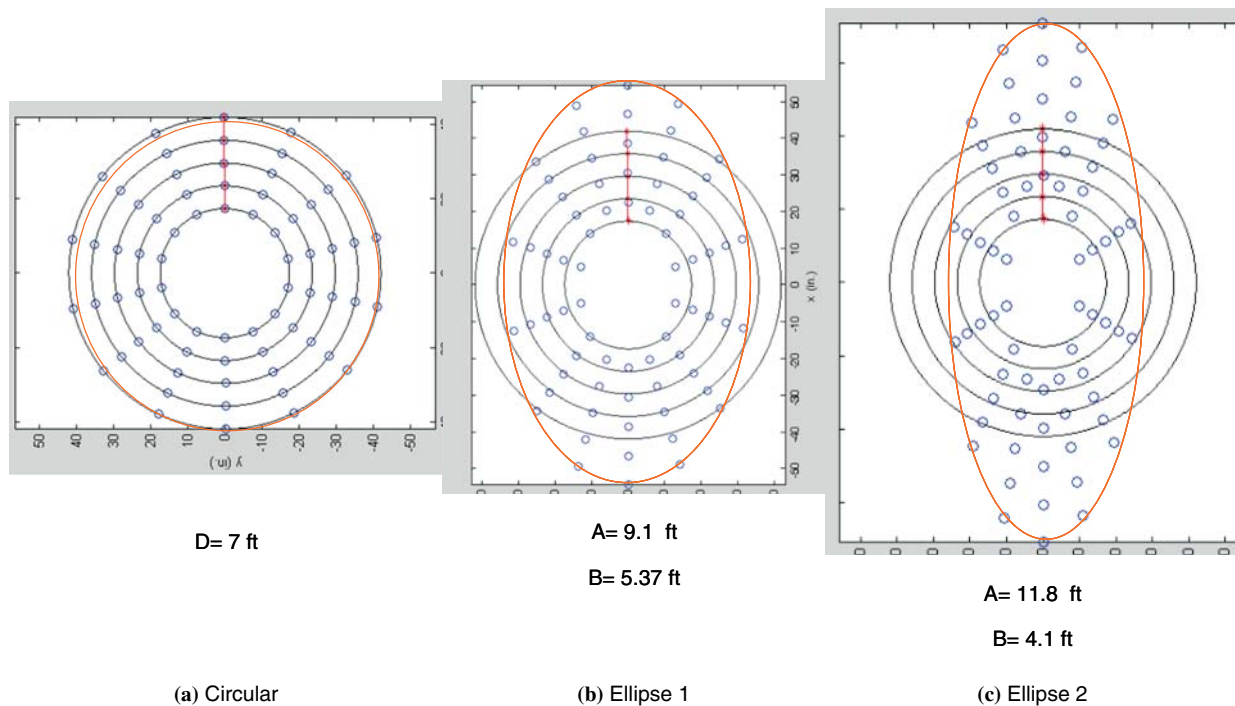
Figure 2. Patterns for various arrays of 70 elements distributed around 14 spokes of 5 elements each: (a) circular spiral, (b) Ellipse 1, (c) Ellipse 2. A is the major axis, B is the minor axis. The spiral angle is 0.5 degrees.

(a) Circular

(b) Ellipse 1

(c) Ellipse 2
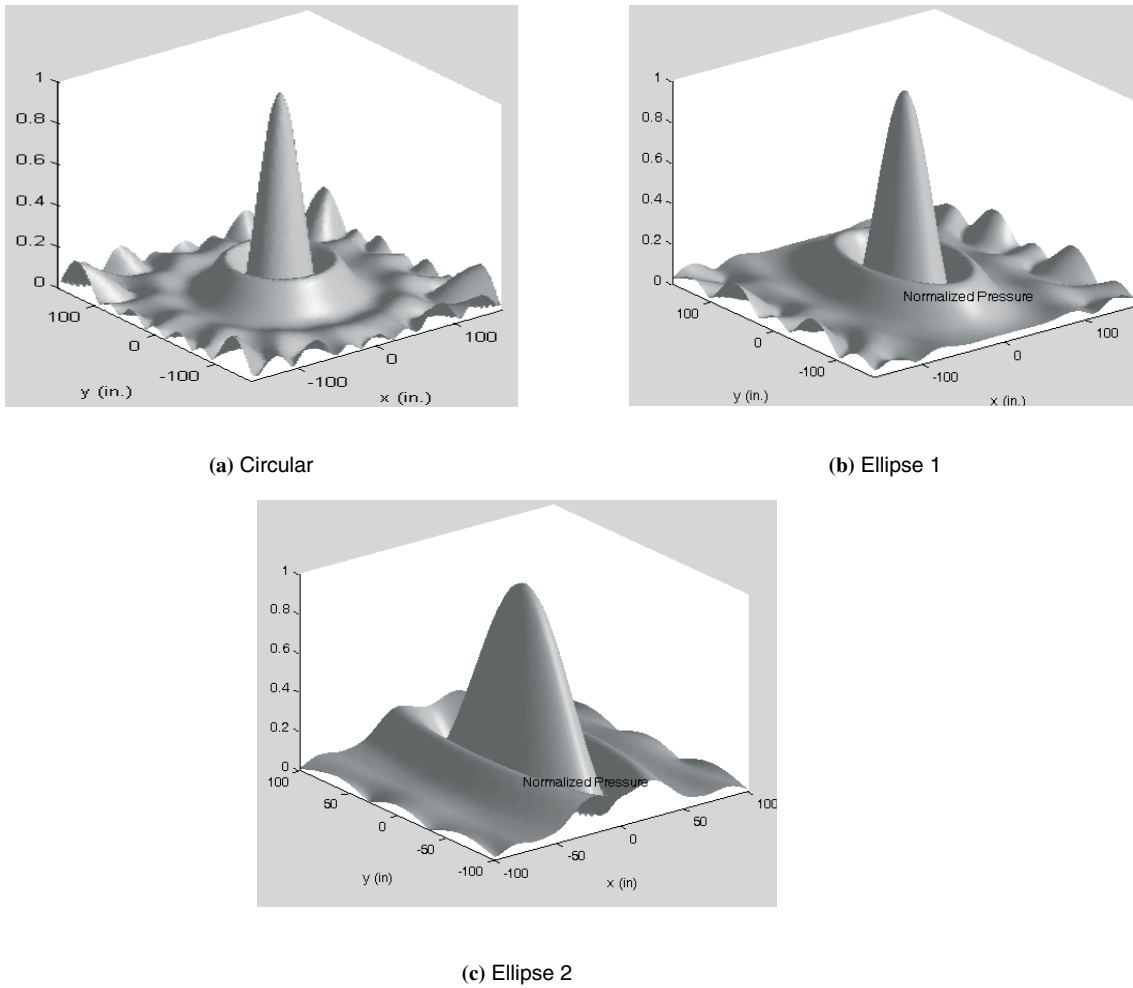
Figure 3. Directivity pattern projections on the parallel x,y plane 20 ft (6 m) in front of the array plane shown in Figure 2 at 1000 Hz.
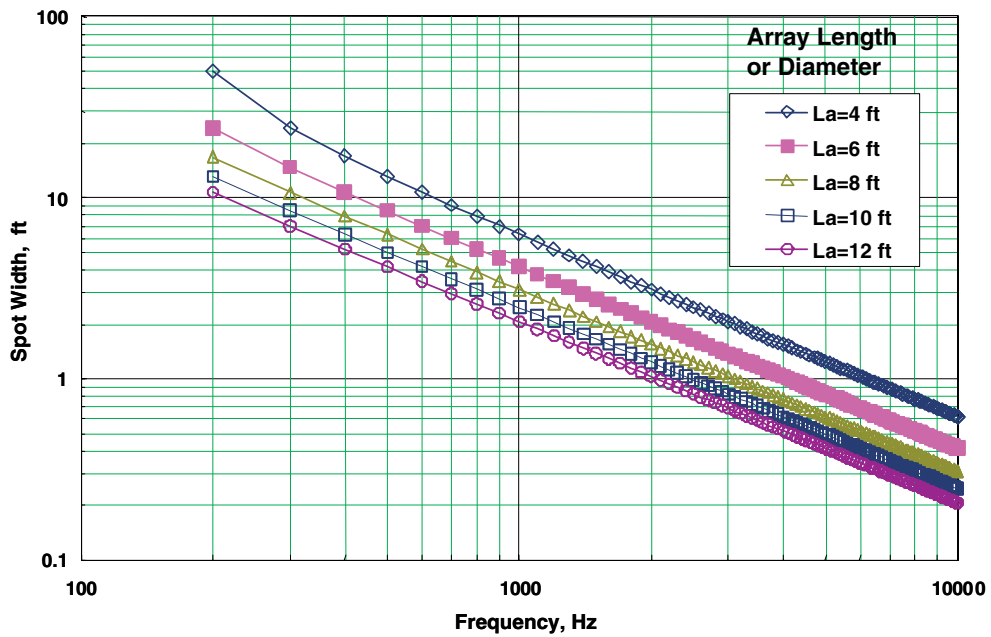
Figure 4. Width of the focus spot of arrays of various lengths or diameters as function of frequency at range of 20 ft (6 m).
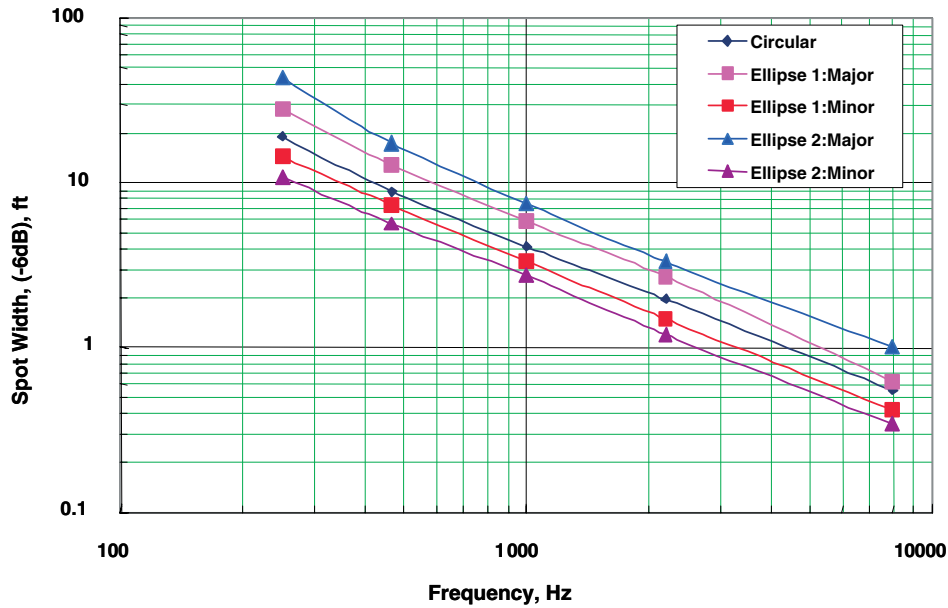
Figure 5. Total width of the −6 dB-down focus spots for major and minor axes of arrays shown in Figure 2.

distance. Ignoring possible effects of source directivity, which are probably of little concern in the 250 Hz region of interest, this variation in the sound level provides some localization along the truck. Figure 6 illustrates this effect. The −6 dB-down points for the passby are indicated along with the −6 dB-down points (at 250 Hz) for the three arrays that are shown in Figure 2. Although the combined effect of spreading loss and directivity gain has not been calculated, the approximate sound profile can be estimated. Figures 7 and 8 provide these approximate profiles for Ellipses 1 and 2. In all cases, the closest point of approach (CPA) is 20 ft (6 m).

These sketches show that spreading loss provides added discrimination as the horizontal directivity is reduced to provide for an increased vertical dimension of the array. One cannot arbitrarily increase the horizontal dimension because this would result in degradation of the side lobe structure.
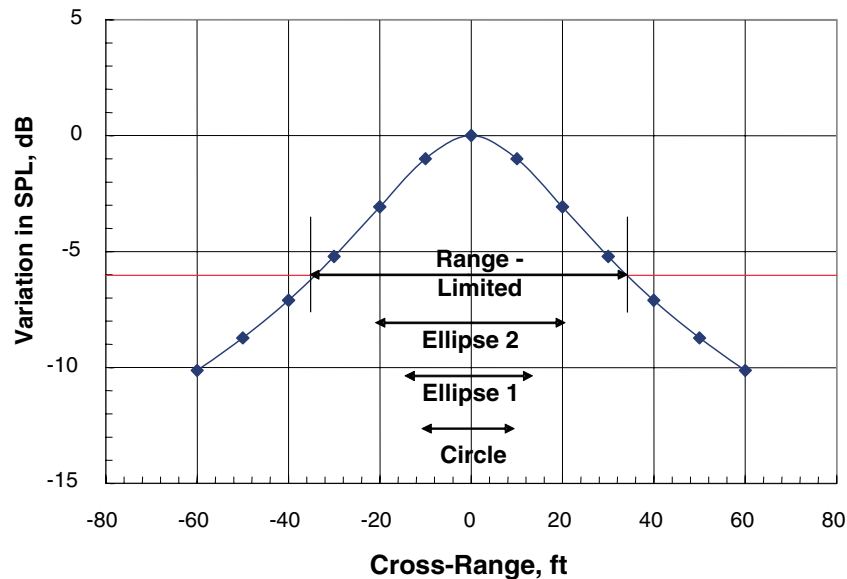
Figure 6. Horizontal profile of sound pressure level (SPL) due to passby of simple source at 20 ft (6 m) from array compared with cross-range apertures of array alternatives at 250 Hz.
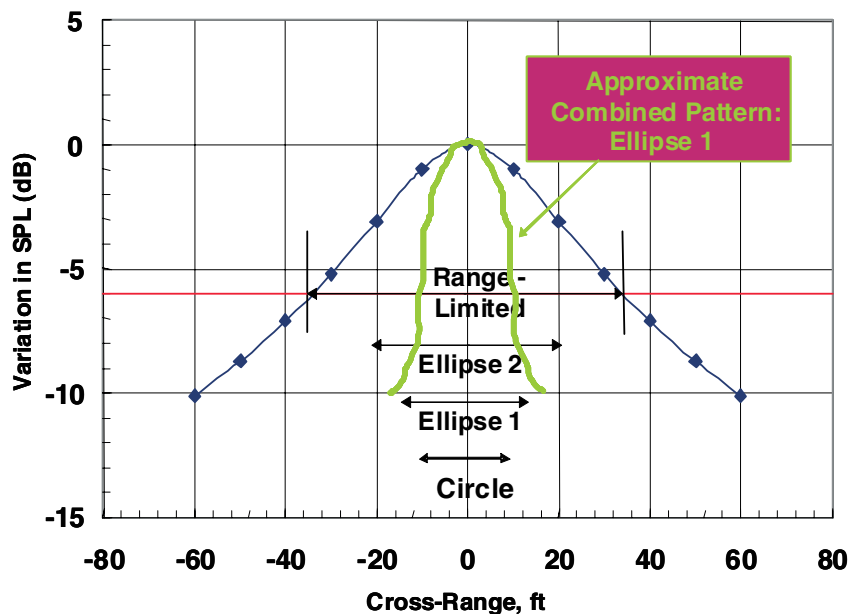
Figure 7. Approximate profile of sound pressure level for simple source passing by Ellipse 1 array at 250 Hz.

Table 1 summarizes these results for 250 and 465 Hz. The frequency of 465 Hz was used because it was one of the analysis bands used in the 2005 Caltrans study, and the study team anticipated that some future design evaluations might need to be compared to data obtained at this frequency. The numbers in parentheses are the lobe widths for the array alone, without benefit of the spreading losses. These values are theoretical, and comparison with the experimental ones is provided in Section 3.5.1 (see Figure 39). The lobe width for a hypothetical point array (a single omni-directional microphone) is also shown in the table for comparison.

3.2.4 Design Conclusions

The following conclusions were drawn from the design analysis described previously for the frequency band of highest A-weighted sound levels of emissions (during cruise):

- A 70-element elliptical array provides adequate aperture with acceptable side lobe suppression.
- The aspect ratio 1.7 of an elliptic aperture array provides beam patterns that are geometrically similar to the array shape at all frequencies of interest.
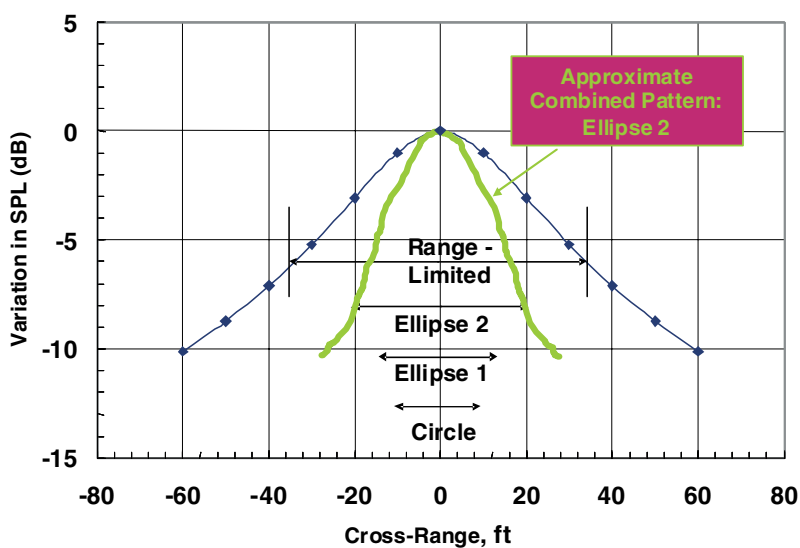
Figure 8. Approximate profile of sound pressure level for simple source passing by Ellipse 2 array at 250 Hz.

18

- Vertical directivity provides a beam focus spot 50 in. (1.3 m) wide (−6 dB-down) at 465 Hz.
- The array provides excellent side lobe suppression of approximately −14 dB over the range of 250 to 2250 Hz, and approximately −11 dB at 8000 Hz.
- A minimum spiral angle is needed to suppress side lobes, so element supports may be radial.
- Side lobes at high frequencies seem well distributed (i.e., appear amorphous), which minimizes the likelihood of unwanted highlights that may lead to false source images.

Table 1. Width of net focus spots for array alternatives including cross-range spreading.

Frequency (Hz)	Direction	Lobe Width (ft) for Array Design*			
		Circular	Ellipse 1	Ellipse 2	Point
250	Vertical	19	14.5	10.8	30
	Horizontal	18 (19)	21 (28)	25 (43)	30
465	Vertical	9	7.3	5.6	30
	Horizontal	8 (9)	12 (13)	15 (18)	30

* Numbers in parentheses represent values for the array alone

With regard to low-frequency performance, the following conclusions were drawn:

- With a 12 ft (3.7 m) major (vertical) axis of the ellipse, the vertical beam half height (−6 dB) is about 4.5 ft (1.4 m) at 250 Hz. This beam size will allow imaging resolution to the upper half of a large truck cab.
- The horizontal effective beam width during passby, including both beam width and spherical source spreading loss, would be about 9 ft (2.7 m) for the minor axis [horizontal dimension of 4.1 ft (1.2 m)].

The elliptical array described herein represents a new result of this study. Based on the design study for the Ellipse 2 array optimized for the current application, a 70-element array (schematically shown in Figure 9) was selected for experimental engineering and implementation through the proof-of-concept testing, as described in the following sections.
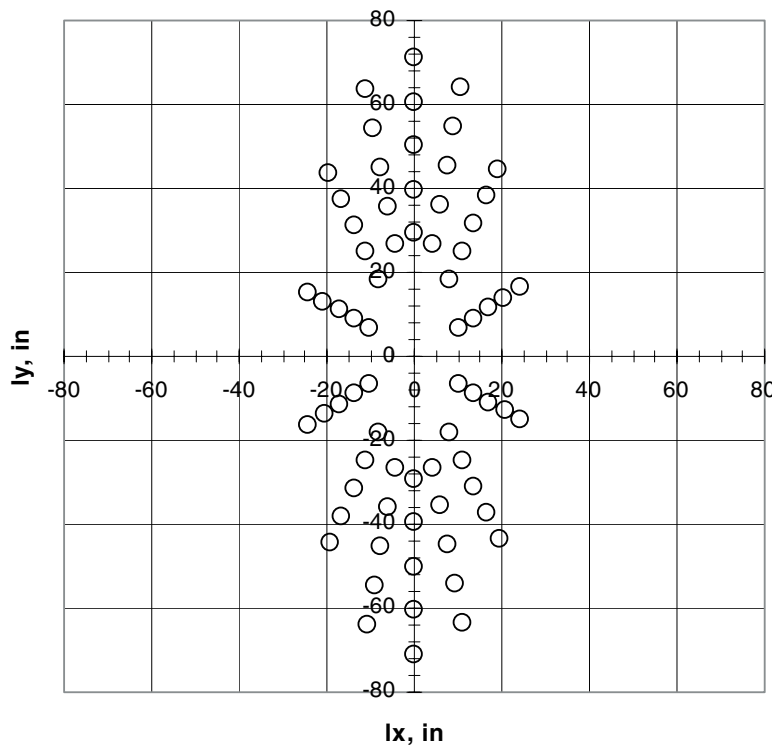
Figure 9. 70-element elliptical array.

3.3 Experimental Microphone Array Engineering

3.3.1 Mechanical Design

As the result of the development described in the previous sections, a 70-microphone elliptical array was designed, with an aspect ratio of 1.7, a width of 4 ft (1.2 m), and a height of 12 ft (3.7 m). This design should provide source resolution down to 250 Hz with side lobe suppression of −12 to −14 dB.

The microphone array assembly and data acquisition system were further developed by Wyle. Due to the significant size of the array aperture, it was assembled on a metal frame consisting of three separate sections vertically mounted together and installed on a four-wheel metal base. The sections, each approximately 4 ft by 3 ft (1.2 m by 0.9 m), could be easily disassembled for shipping. Fourteen PVC pipe spokes, each holding 5 microphones, were mounted on the frame sections, providing the 70-microphone elliptical pattern that was designed. The identical lower and upper frame sections hold five spokes each, with five microphones mounted equidistantly on each spoke. The middle frame section holds four spokes with five microphones each. During the field tests of the array, additional microphones were mounted along the central vertical axis of the middle frame section, raising the total number of microphones to 73 or 77 for some tests. The assembly with additional microphones is shown in Figure 10.

3.3.2 Data Acquisition System

The array was equipped with the 0.24 in. PCB Piezotronics Series 130 array microphones with 0.25 in. ICP® preamplifiers Model 130P10 or integral ICP® preamplifiers. The microphones/preamplifiers were inserted in holes predrilled in the spokes of the array, each provided with a 3.5 in. windscreen. Prior to array assembly, the microphones were phase-calibrated in pairs using a Brüel & Kjær Type 51AB sound intensity calibrator.

The data acquisition system was completed using a National Instruments Model PXI-1044 embedded controller chassis with 12 data acquisition cards providing analog-to-digital conversion for a total of 80 data channels for signal recording. The measurement signals from the array microphones were individually fed into the PXI channels through 50 ft (15 m) long microphone cables. A controller onboard the PXI chassis enables synchronization of all the data acquisition cards, providing simultaneous recording across all channels. The software for running the system in real time and transferring data from the PXI to a laptop computer for post-processing was developed by Dr. William Blake and Wyle.

During the proof-of-concept testing described in Section 3.4, one of the PXI channels was used for recording the time signal from an ESE Model ES-292 GPS-based time code generator
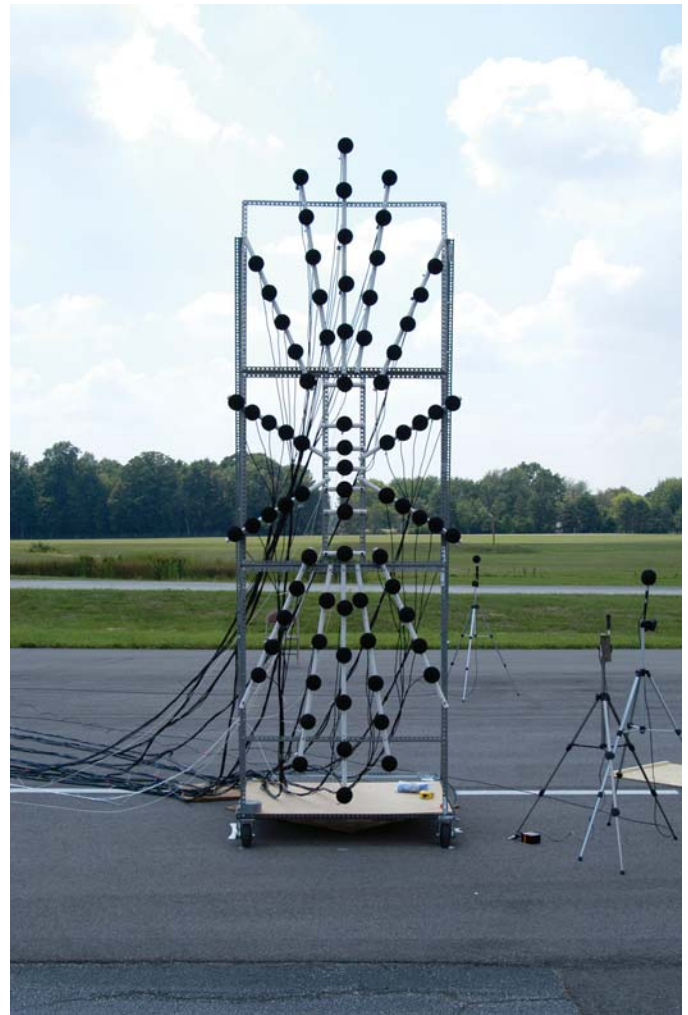
Figure 10. Experimental microphone array (note seven additional microphones in the array center).

(IRIG). Another channel received a signal from a pair of photocells installed on tripods near the microphone array to register truck passbys. The photocells were Banner Engineering Model SM31EL/SM31RL mini-beam emitter and receiver. Another PXI channel was used for recording signals from IT's vehicle tracking system. The system includes a Banner Engineering Model Q45BB6DLQ infrared linear position sensor attached to the front bumper of the truck. This photosensor detects white strips painted every 5 ft (1.5 m) along the track pavement and telemeters a series of signals to a remote receiver. The signals from the receiver were fed into the PXI. Truck speed was then determined by the distance between the strips and the time between the voltage pulses received in the signals.

3.3.3 Preliminary Testing

Prior to full-range proof-of-concept testing scheduled at IT's facilities in Ft. Wayne, Indiana, a preliminary testing of the experimental beamforming microphone array was performed

Figure 11. Preliminary testing of experimental microphone array (lower section).

locally in Virginia. The overall goal was to ensure that the microphone array, data acquisition system, and software worked properly prior to the actual proof-of-concept testing. The test was performed in a residential outdoor area, on a grassy lawn free of obstructions. Only the lower section of the array with 25 microphones was tested using a Mackie Model SRM450 loudspeaker with a pink noise generator, as well as a lawnmower and a gas-powered string trimmer as noise sources in static positions in front of the array. These noise sources were placed alone and in combinations at varying distances from the array, both at on-axis and off-axis locations relative to the array. The data were then processed with the beamforming software, to make sure that the different sources could be correctly identified. One of the test settings is shown in Figure 11. The resultant images of the loudspeaker at two different frequencies are shown in Figure 12.
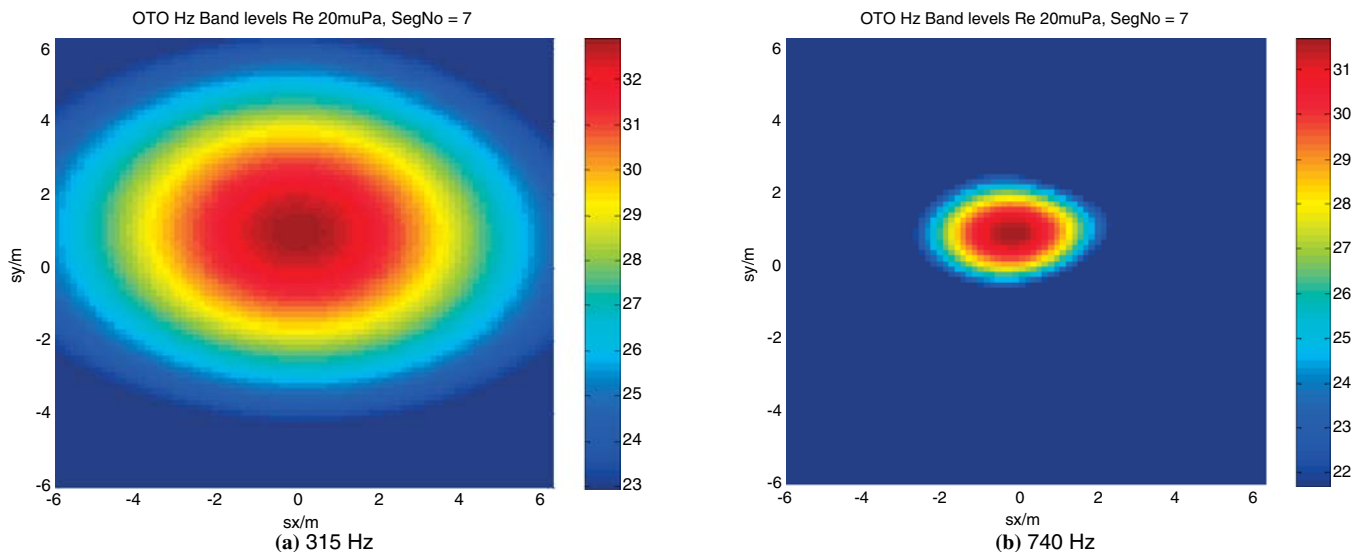
The preliminary testing results indicated that the array performed generally as expected for a truncated assembly. Lacking vertical symmetry, its directivity in both vertical and horizontal axes was found reasonable for an array of this size. The study team also concluded that the array setting in both vertical and horizontal directions (level and square) is important for image localization and reducing distortion of the images obtained. Overall, the preliminary testing served as a first practical verification of the experimental beamforming array performance.

3.4 Proof-of-Concept Testing

The proof-of-concept tests were conducted during two 1-week periods in July 2006 at IT's Truck Development and Technology Center (TDTC) in Ft. Wayne, Indiana. The TDTC is a controlled environment with test tracks and shop facilities for working on truck setups. IT provided access to its outdoor testing facilities, coordination with its ongoing testing activities, and a representative sample of trucks selected from the vehicle test matrix. IT also provided a professional driver for the tests and technicians to perform all work on the trucks.

The first week of testing was conducted at the low-speed passby sound pad. After a 1-week interval of preliminary data processing and analysis, the second week of tests was conducted at the high-speed proving grounds/endurance track. Both test phases were documented using digital videotape recording. Weather at the test sites was monitored to avoid testing during periods of rain or high winds.

3.4.1 Low-Speed Tests

The microphone array, data acquisition system, and other equipment were transported to and assembled at IT's low-

(a) 315 Hz

(b) 740 Hz

Figure 12. Loudspeaker image at frequency of (a) 315 Hz and (b) 740 Hz.
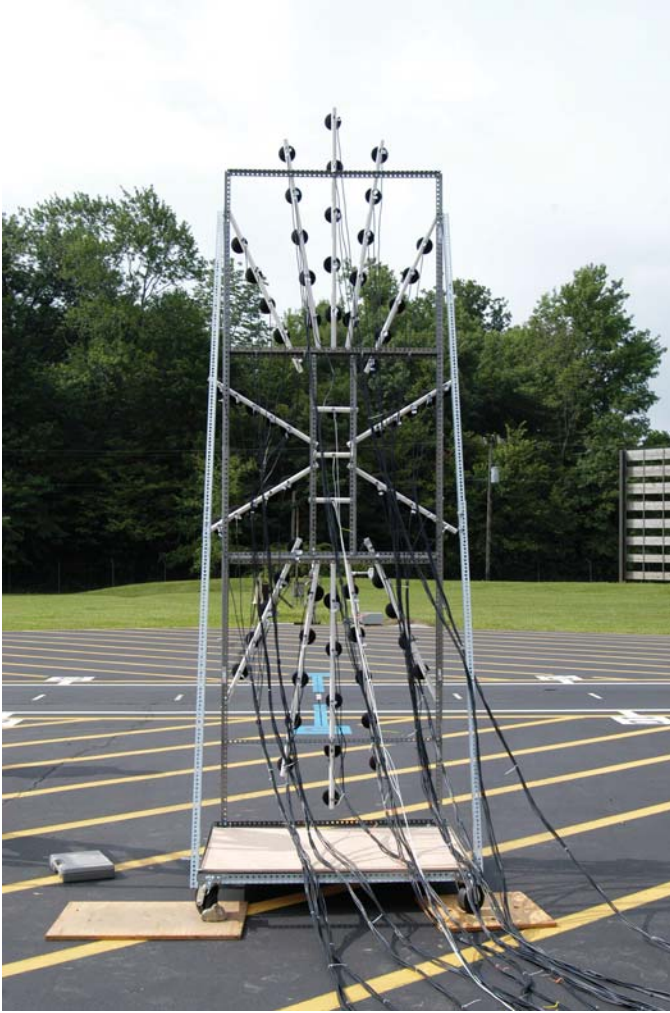
Figure 13. Microphone array at low-speed track.

Figure 14. Omni-directional speaker in front of microphone array at low-speed track.

speed sound pad designed for conducting standard truck passby noise-emission measurements. At this site, the trucks drive on a single lane with sealed, dense-graded asphalt pavement and a maximum speed limit of 35 mph (56 km/h). The microphone array was placed on the asphalt diamond measurement pad, parallel to the direction of truck travel, at a distance of 20 ft (6 m) from the edge of the driving lane, as shown in Figure 13. Each measurement channel of the system was calibrated using a Brüel & Kjær Type 4231 acoustic calibrator.

Initially a series of stationary loudspeaker tests were performed, using a Mackie Model SRM450 loudspeaker and a CESVA Model BP012 omni-directional dodecahedron loudspeaker. Sound from a pink noise generator was played through the speakers at a high volume. The speakers were used for initial evaluation of the fully assembled system as known "point" sources placed at several on- and off-axis locations with different distances and heights in front of the array. One example of such a test setup is shown in Figure 14.

After the stationary on-the-ground loudspeaker tests were completed, the CESVA loudspeaker was placed on a truck.

The speaker was secured to the rear frame of an International® 4400 medium utility truck (with no flatbed; 2002 model year). The truck was powered with an International® DT466 250 hp engine and was equipped with an automatic transmission, a single horizontal under-frame muffler and a horizontal tailpipe. The truck was equipped with four Goodyear G124 low-profile tires on the single drive (rear) axle and two Goodyear G159 tires on the steer (front) axle. The truck with mounted omni-directional loudspeaker is shown in Figure 15.

To evaluate the array/beamforming system performance, a number of tests were performed with the truck stationary and moving both with and without the speaker (pink noise signal) turned on. These tests were intended to determine the array's ability to identify the truck noise sources (e.g., engine, tires, and exhaust) in comparison with the loudspeaker, as the truck passed by the array at a constant speed. Several speeds,

Figure 15. The 4400 truck with omni-directional speaker.

Table 2. Tests of the 4400 truck with speaker at the low-speed track.

Speed (mph)	rpm	Gear	Speaker
0 (stationary)	idle	Neutral	Off/On
0 (stationary)	2000	Neutral	Off/On
18	1500	2nd	Off/On
25	2000	2nd	Off/On
31	2500	2nd	Off/On
27	Cruise	4th	Off

Table 3. Tests of the 9200i truck at the low-speed track.

Speed (mph)	rpm	Gear	Notes
0	Idle	Neutral	
0	650	Neutral	Stationary
0	1200	Neutral	
0	1800	Neutral	
15	1200	6th	Constant rpm, varied gear
25	1200	7th	
30	1200	8th	
13	650	7th	Constant gear, varied rpm
20	1200	7th	
31	1850	7th	
29	Coast down	Neutral	
29	Cruise	7th	
Acceleration	700	7th	

revolutions per minute, and gear settings used for the truck runs are summarized in Table 2.

The next truck tested at the low-speed track was an International® 9200i Eagle truck (2006 model year). This is a heavy-duty truck used for long hauls. It was powered with a Cummins ISX 450 hp engine and had a single horizontal muffler and a vertical tailpipe, which was mounted to the rear passenger side of the cab. The truck tractor with no trailer was used, equipped with eight Goodyear G372 tires on tandem drive (rear) axles and two Goodyear G395 tires on the steer (front) axle. The truck was also equipped with aero skirts under the cabin. The truck is shown in Figure 16. The truck tests, performed with no loudspeaker, are summarized in Table 3.

The testing then continued with the third truck, an International® 5900 PAYSTAR™ (2004 model year), which is a "severe service" truck designed to have other equipment mounted on the frame, such as a concrete-mixer drum and associated equipment, and to be used with very heavy payloads. It was powered with a Cummins ISX 565 hp engine. For these tests, the truck had dual vertical mufflers and tailpipes mounted to the back sides of the cab. Only the truck tractor was driven, with approximately 7000 lbs of weight added on the rear section of the tractor frame. There were eight Goodyear G167 tires on tandem drive (rear) axles and two Goodyear G287 tires on the steer (front) axle. In this case again, a loudspeaker was not

used in the testing. The truck is shown in Figure 17. The truck test conditions are listed in Table 4.

The measurement data collected during the testing at IT's low-speed track were preliminarily reviewed in the laboratory the following week and determined suitable for full post-processing and analysis. The key results of the analysis are presented and discussed in Section 3.5. The microphone array and data acquisition system performed as expected and required no major adjustments for the next stage of the proof-of-concept testing at IT's high-speed endurance track.

3.4.2 High-Speed Tests

For high-speed testing, the microphone array and data acquisition system were transported to IT's endurance track. It consists of a 1 mi (0.6 km) long multiple-lane loop designed for conducting long-term truck testing with a maximum speed limit of 50 mph (80 km/h). The microphone array was placed in the sealed asphalt area along the middle part of the track, at

Figure 16. The 9200i truck at the low-speed track.

Figure 17. The 5900 truck in front of microphone array at the low-speed track.

Table 4. Tests of the 5900 truck at the low-speed track.

Speed (mph)	rpm	Gear	Notes
0	650	Neutral	
0	1500	Neutral	Stationary
0	2000	Neutral	
14	1500	4th	
25	1500	5th	Constant rpm, varied gear
28	1500	6th	
10	650	5th	
20	1500	5th	Constant gear, varied rpm
26	2000	5th	
30	Coast down	Neutral	
30	Cruise	7th–8th	
From 14	From 1500	4th	Acceleration

a distance of 20 ft (6 m) from the edge of the nearest driving lane of unsealed, dense-graded asphalt. First, the stationary CESVA omni-directional speaker tests were performed at this location for initial check-out and additional array performance validation. After that, the truck passby tests were carried out in 3 days. The trucks (all by International®) tested at the high-speed endurance track are listed in Table 5 (not in the order of testing).

The International® 4400 truck was the same as the one tested before at the low-speed track. The other trucks tested at the high-speed track were not tested at the low-speed track. The 9200i truck with a 450 hp engine, shown in Figure 18, had front and rear Goodyear G395 tires and a short vertical tailpipe, unlike the truck of the same type tested at the low-speed track (compare with Figure 16). This 9200i truck also was not equipped with aero skirts covering a fuel tank and a horizontal part of the exhaust pipe under the cabin.

To test a truck with no muffler, the exhaust system of another 9200i Eagle truck (with 370 hp engine) was modified by replacing its vertical muffler with a pipe, as seen in Figure 19. This truck was also equipped with an aerodynamic wind fairing over the cabin.

The International® 5900i tractor truck was tested at the high-speed track in three different configurations: (1) bobtail with eight Michelin XZE tires on the drive axles; (2) bobtail with eight Goodyear G164 RTD aggressive tread, high-traction (noisy) tires on the drive axles; and (3) loaded trailer with the same aggressive tread tires on the drive axles. Figures 20 and 21 show the truck without and with the trailer, respectively. Unlike the truck of this type (5900 PAYSTAR) tested at the low-speed track, the 5900i tested at the high-speed track was equipped with a more powerful engine, but had a single muffler and a tailpipe.

Tables 6 through 11 summarize the tests performed for each truck at the high-speed track. The tables present the test conditions of the trucks, including the speed, engine rpm, and gear. Also shown in the tables is the overall A-weighted sound level (L_A) measured with a single microphone at the distances of 25 and 50 ft (7.5 and 15 m) from the track for each truck run, as described in Section 3.4.3. For the stationary tests, L_A is the measured time-averaged sound level; for the passby tests, L_A is the maximum sound level measured during the single truck run. No tests were performed at this track with a loudspeaker mounted on a truck.

3.4.3 Passby and Intensity Measurements

In addition to the array measurements of the test trucks for the stationary and passby truck conditions, conventional single-microphone and sound intensity measurements were conducted. These measurements are described in this section.

To complement the beamforming results, single-microphone sound pressure level measurements were performed at distances of 25 ft (7.5 m) and 50 ft (15 m) from the centerline of vehicle travel. These microphones were set on a line perpendicular to the direction of travel offset 5 ft 8 in. (1.7 m) from the center of the array, as shown in Figure 22. The microphones were adjusted to a height of 5 ft (1.5 m) above the pavement. The microphones were 0.5 in. (12.5 mm) Larson-Davis (LD) Model 2541 fitted onto 0.5 in. (12.5 mm) LD Model PRM900C microphone preamplifiers. The signals from these microphones were fed into an LD 3000 two-channel real-time

Table 5. Trucks tested at the high-speed track.

Truck Type (model year)	Engine Type	Front/Rear Tires (no.)	Exhaust Configuration
4400 (2002)	International DT466 250 hp	G159 (2) G124 (4)	Single horizontal muffler & horizontal tailpipe
9200i (2006)	Cummins ISX 450 hp	G395 (2) G395 (8)	Single horizontal muffler & short vertical tailpipe
9200i Eagle (2004)	Cummins ISM 370 hp	G395 (2) G372 (8)	Single modified vertical tailpipe with no muffler
5900i (2006)	Cummins ISX 600 hp	G286 (2) Michelin XZE (8)	Single vertical muffler & vertical tailpipe
5900i w/o and with loaded trailer (2006)	Cummins ISX 600 hp	G286 (2) G164 RTD (8)	Single vertical muffler & vertical tailpipe

Figure 18. The 9200i truck with short vertical tailpipe at the high-speed track.

Figure 20. The 5900i truck with no trailer at the high-speed track.

analyzer. The signals were also recorded on a Sony TCD D-100 two-channel DAT recorder for data backup and any further data reduction required later.

For the stationary tests of either the trucks or the loudspeaker, linear time averages of the sound pressure levels were obtained for a 15 s time period. These were analyzed in one-third octave frequency bands from 20 to 20,000 Hz. The average overall A-weighted sound levels measured for the stationary conditions on the high-speed track were given previously in Tables 6 through 11 for both the 25 and 50 ft microphone positions. For the passby truck tests, one-third octave band spectra were captured every 0.100 s with a 0.125 s exponential (fast response) averaging time applied to the signals for a period of 10 s. These data were then used to examine the overall A-weighted time history of the passby event, as well as the one-third octave band spectrum at the time of maximum overall A-weighted level during the passby. The maximum overall

A-weighted sound levels measured for the truck passby conditions on the high-speed track were also given in Tables 6 through 11.

Note that the 25 and 50 ft measurements in Tables 6 through 11 are generally consistent with inverse square law, but there are some variations. Near-field effects associated with source size may be a factor in the variations. This phenomenon is particularly likely for the data in Table 8, where the modified exhaust resulted in a strong exhaust source significantly above the engine source. Near-field effects are a concern for passby measurements with a single microphone. They are not, however, an issue for beamforming measurements which are intended to discriminate among a distribution of sources.

For each of the test trucks under no-load stationary conditions, sound intensity averaged over areas to the side of the

Figure 19. The 9200i Eagle truck with drag fairing and no muffler at the high-speed track.

Figure 21. The 5900i truck with trailer at the high-speed track.

Table 6. Tests of the 4400 truck at the high-speed track.

Speed (mph)	rpm	Gear	Notes	L$_A$ (dBA) at 25 ft	50 ft
0	740 (idle)	Neutral		69.1	62.7
0	1150	Neutral	Stationary	72.4	65.7
0	1400	Neutral		73.7	66.6
0	2100	Neutral		79.3	72.6
35	2100	Drive	Automatic	80.4	74.3
50	1400	Drive	transmission	83.6	77.6
35	2100	3rd	Constant rpm,	80.3	74.7
50	2100	4th	varied gear	84.3	78.0
From 50	*	Throttle off	Coast down	80.9	73.3
From 10 to 15	1500 to 2450	2nd	Acceleration	81.9	76.2
From 22 to 31	1800 to 2450	2nd	Acceleration	83.7	78.7

* Not recorded

Table 7. Tests of the 9200i truck at the high-speed track.

Speed (mph)	rpm	Gear	Notes	L$_A$ (dBA) at 25 ft	50 ft
0	Idle	Neutral		**	**
0	1100	Neutral		74.6	68.2
0	1400	Neutral	Stationary	78.7	72.2
0	1500	Neutral		78.6	71.7
0	1800	Neutral		81.1	74.1
35	1400	8th		77.8	72.3
46	1800	8th		84.2	77.9
50	1500	9th		83.0	77.5
50	1100	10th		82.6	76.5
35	2100	3rd	Constant rpm,	**	**
50	2100	4th	varied gear	**	**
From 50	*	9th	Coast down	81.4	74.7
From 50	*	9th	Compression brake	83.6	77.3
46	From 900 to 1800	8th	Per SAE J366	84.5	78.5

* Not recorded
**Missing data

trucks was measured. The sound intensity probe used for this purpose consisted of two 0.5 in. (12.5 mm) phase-matched condenser microphones spaced 0.625 in. (16 mm) apart in a side-by-side configuration. The microphones were a G.R.A.S. 40AI intensity microphone pair fitted to LD Model PRM900C 0.5 in. (12.5 mm) preamplifiers. Signals from these micro-phones were input to a LD 3000 two-channel analyzer for immediate sound intensity measurement in one-third octave bands. To determine the average sound intensity for an area in the plane parallel to the side of a vehicle, the probe was manu-ally swept over specific subareas, as shown in Figures 23 and 24, several times as linear averaging was performed over a period

Table 8. Tests of the 9200i Eagle truck (modified exhaust, no muffler) at the high-speed track.

Speed (mph)	rpm	Gear	Notes	L$_A$ (dBA) at 25 ft	50 ft
0	Idle	Neutral		68.6	63.5
0	1500	Neutral	Stationary	77.6	72.8
0	1600	Neutral		79.6	74.9
0	1900	Neutral		81.7	76.7
35	1900	7th		85.2	79.9
35	1500	8th		82.6	76.7
45	1900	8th		89.2	84.3
50	1600	9th		89.6	82.1
From 50	*	*	Coast down	80.0	75.6
From 50	1400	9th	Compression brake	96.2	90.9
*	*	*	Low-speed acceleration	89.2	85.9

* Not recorded

Table 9. Tests of the 5900i truck (standard tires) at the high-speed track.

Speed (mph)	rpm	Gear	Notes	L$_A$ (dBA) at 25 ft	L$_A$ (dBA) at 50 ft
0	Idle	Neutral		66.5	60.3
0	1400	Neutral	Stationary	76.2	68.7
0	1800	Neutral		79.9	74.7
0	2000	Neutral		81.1	74.2
35	1800	6th		81.0	75.3
35	1400	7th		79.6	73.8
50	2000	7th		84.3	78.5
50	1400	8th		84.7	78.9
From 50	*	*	Coast down	81.8	76.2
From 50	1400	8th	Compression brake	83.3	77.6

* Not recorded

Table 10. Tests of the 5900i truck (aggressive tread rear tires) at the high-speed track.

Speed (mph)	rpm	Gear	Notes	L$_A$ (dBA) at 25 ft	L$_A$ (dBA) at 50 ft
35	1800	6th		81.4	76.1
35	1400	7th		79.3	73.7
50	2000	7th		85.5	79.9
50	1400	8th		83.5	77.8
From 50	*	Neutral	Coast down	81.8	77.1
From 50	1400	8th	Compression brake	83.4	78.2
13 to 16	From 1300	4th	Per SAE J366	80.5	75.2

* Not recorded

Table 11. Tests of the 5900i truck (aggressive tread rear tires) with trailer at the high-speed track.

Speed (mph)	rpm	Gear	Notes	L$_A$ (dBA) at 25 ft	L$_A$ (dBA) at 50 ft
35	1800	6th		82.7	77.2
35	1400	7th		82.2	76.7
50	2000	7th		88.0	82.8
50	1400	8th		87.2	82.4
From 50	*	Neutral	Coast down	86.9	81.4
From 50	*	Neutral	Compression brake	87.4	81.3
50	1400	8th - Full throttle		87.9	82.4
35	1400	8th - Full throttle		84.2	78.5

* Not recorded
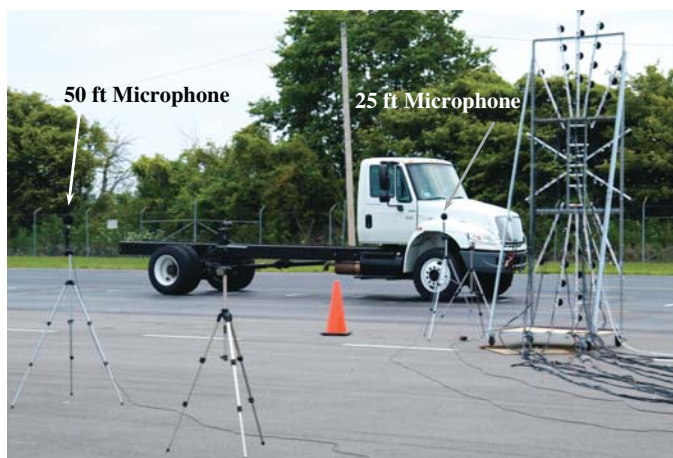
Figure 22. Positioning of passby measurement microphones.
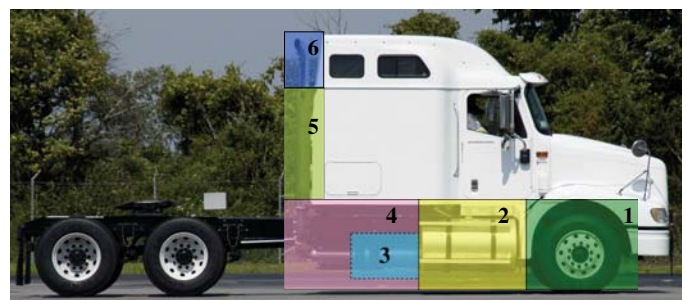
Figure 23. Sound intensity scan areas for the 9200i truck.

Figure 24. Sound intensity scan of muffler (subarea 3) for the 9200i truck.

Figure 26. Sound intensity scan areas for the 4400 truck with loudspeaker.

of 40 s. Once the average intensity was determined for each subarea, the sound power radiated through each surface was calculated. These calculations were then summed to determine the total sound power radiated on the side of the truck facing the array. In this manner, the contribution of each subarea to the total sound power radiated to the side of the truck was evaluated.

This methodology was initially applied to the 4400 truck when tested at the low-speed track with the loudspeaker installed. The results for the truck alone are shown in Figure 25

for the areas indicated in Figure 26. From these data, it is apparent that the subareas corresponding to the hood and upper cab produce lower levels of sound power, and the sound intensity is negative at the lower frequencies. The latter is an indication that in these subareas the sound energy flows in the opposite direction (toward the structure rather than from it) because of the presence of the other, more powerful sound source(s) in the vicinity. As a result, for subsequent trucks the hood and upper cab subareas were excluded from the analysis. For the 4400 truck, the sound power contribution was also determined for the loudspeaker, and its relationship to the total for the truck only is given in Figure 27.

The sound power breakdown for the stock 9200i truck for the subareas of Figure 23 is shown in Figure 28. For this truck the contributions from the muffler and exhaust outlet are quite
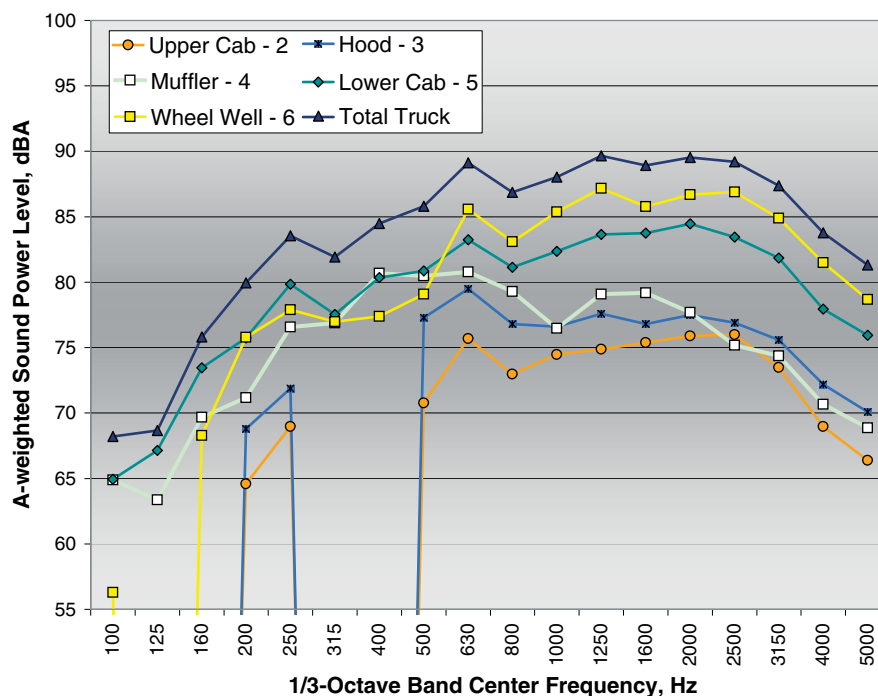
Figure 25. Sound power levels for subareas and total of the 4400 truck at 2000 rpm.
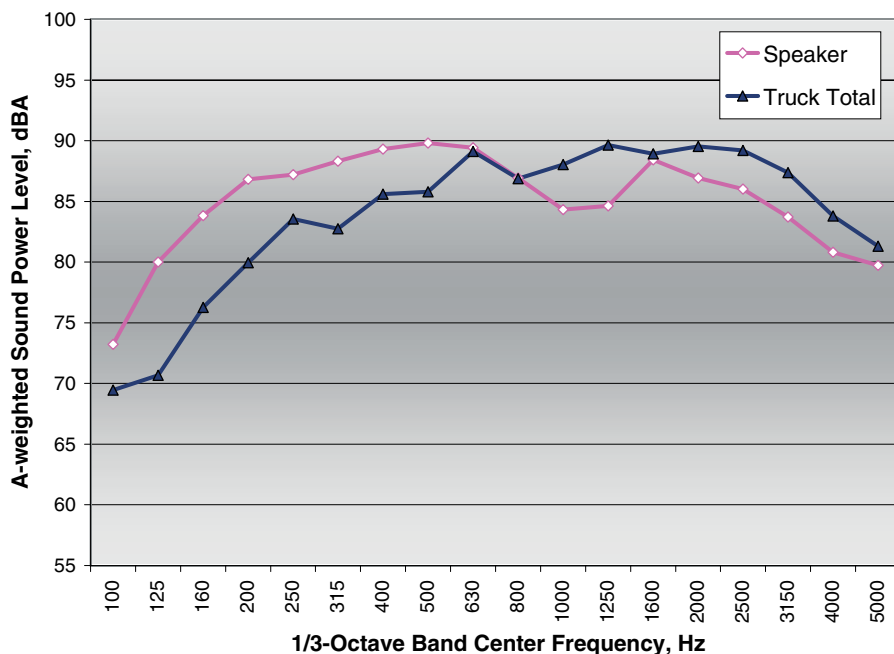
Figure 27. Sound power levels of the 4400 truck and loudspeaker.

low compared to the sound power coming from underneath the truck and through the wheel well. Only at very low frequencies of 100 to 160 Hz is there a significant contribution of the exhaust outlet.

For the 5900i truck, trends similar to the stock 9200i truck are seen in Figures 29 and 30, except that there is somewhat

more contribution from the muffler. For the case of the 9200i Eagle truck with the modified "straight-through" exhaust (no muffler), a significantly different contribution of subareas can be seen in Figures 31 and 32. In this case, radiation from the exhaust pipe still remains low; however, sound radiation from the exhaust outlet subarea dominates the total radiation
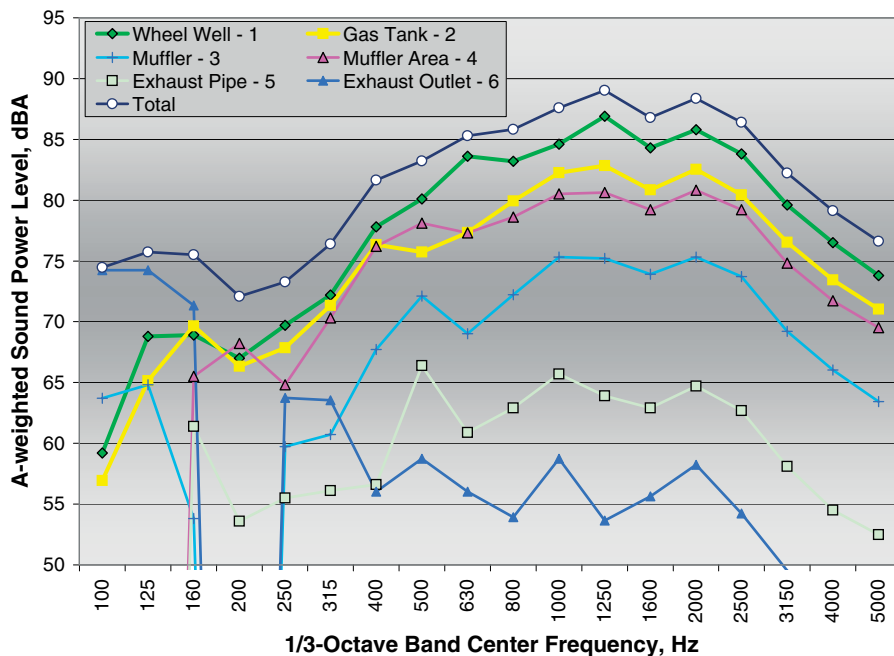
Figure 28. Sound power levels for subareas and total of the 9200i truck at 1800 rpm.

Figure 29. Sound intensity scan areas for the 5900i truck.

Figure 31. Sound intensity scans areas for the 9200i Eagle truck with straight-through exhaust (no muffler).

between 160 and 500 Hz, with the sound levels 6 to 15 dB greater than any of the other subareas. Even at the higher frequencies, the contribution of the exhaust outlet remains high.

Upon completion of testing at IT's high-speed track, the measurement data collected was post-processed and analyzed in the laboratory. The key results of the analysis are presented and discussed in Section 3.5. Again, the microphone array and data acquisition system performed as expected and required no major adjustments. From experimenting with the number of

array microphones, however, the study team determined that increasing the number of microphones to 73 or 77, by adding units at and near the center of the array, was beneficial for the array's beamforming performance and resulting noise source mapping. Also, assembling the array in the field, which involved handling multiple cable connections between the microphones and PXI unit, was found to be labor intensive and time consuming. These aspects of the first field experience were addressed prior to subsequent application of the array for the roadside truck noise measurements.
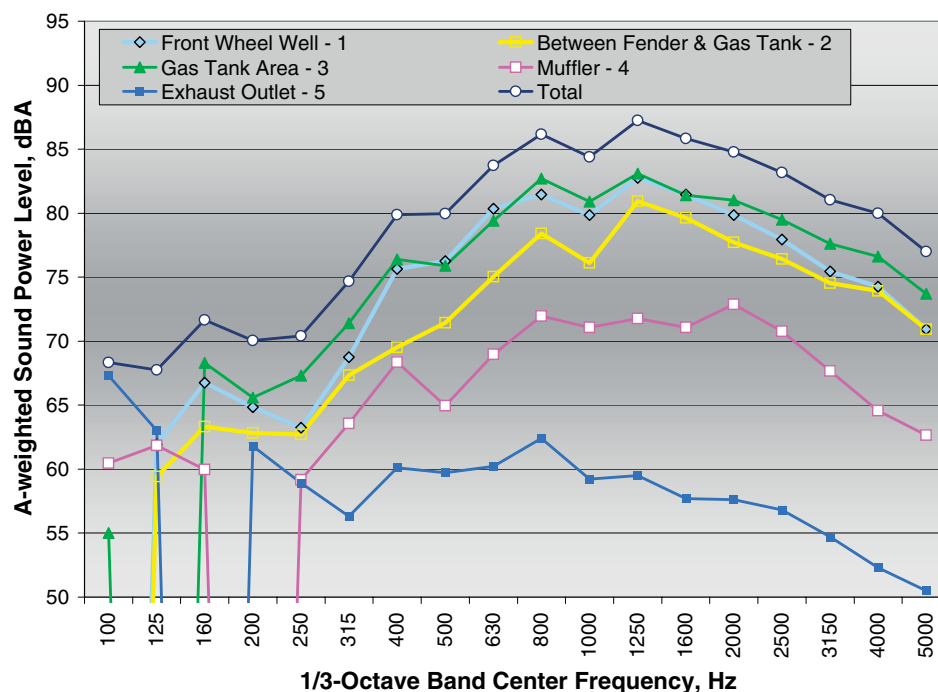
Figure 30. Sound power levels for subareas and total of the 5900i truck at 1400 rpm.
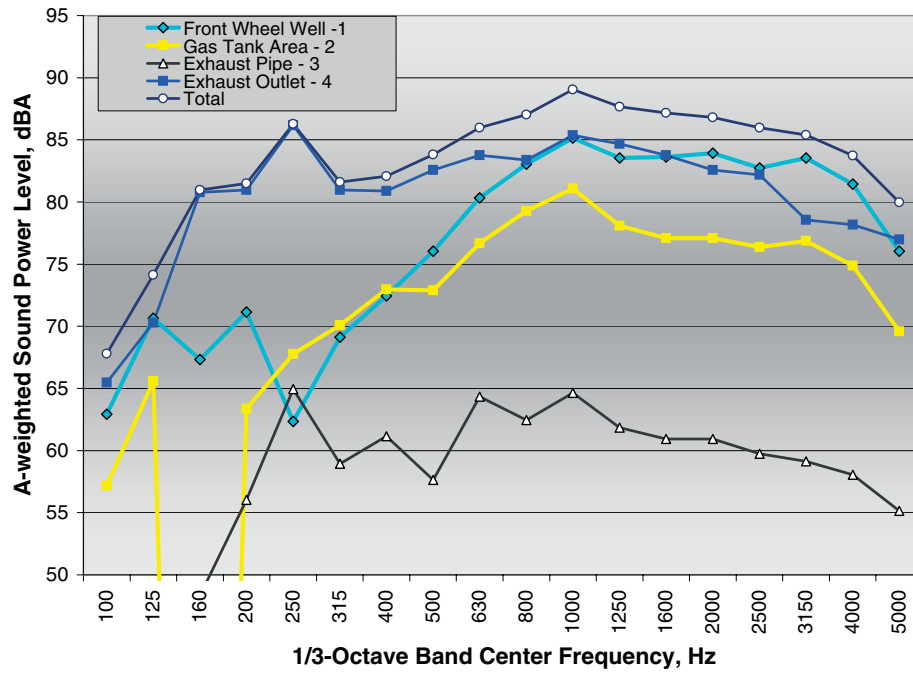
Figure 32. Sound power levels for subareas and total of the 9200i Eagle truck with straight-through exhaust (no muffler) at 1500 rpm.

3.5 Proof-of-Concept Test Results

This section discusses the proof-of-concept test results in four categories:

- Beamformer calibrations with the omni-directional (spherical) source, in which in-situ frequency response and steering characteristics of the array are established;
- Benchmark localization measurements with a moving truck with and without the spherical source on board, in which the array's ability to discriminate among multiple sources is verified and the rudiments of developing temporal histories during passby are established;
- Comparisons with the intensity measurements made on stationary trucks, in which the array's ability to localize the principal (i.e., largest magnitude) source on the truck and identify the lesser sources is established; and
- Example results from low- and high-speed track passbys, in which localization and characteristics of individual noise sources for the tested moving trucks are evaluated.

3.5.1 Beamformer Calibrations with Spherical Source

The beamformer characteristics of the array were calculated for comparison to the test results using a theoretical model of the received signals at each array element with a simple source above ground with ground reflection, for which the ground reflection coefficient was assumed to be between 0.7 and 1.0. Figure 33 shows a side-view diagram of the array, spherical sound source and its image in the ground half space, direct acoustic propagation path, and two example ray traces for the reflected path that were used in the analytical model. Figure 34 is an illustration of the coordinate axis orientations of the source and array planes. The latter figure also labels the
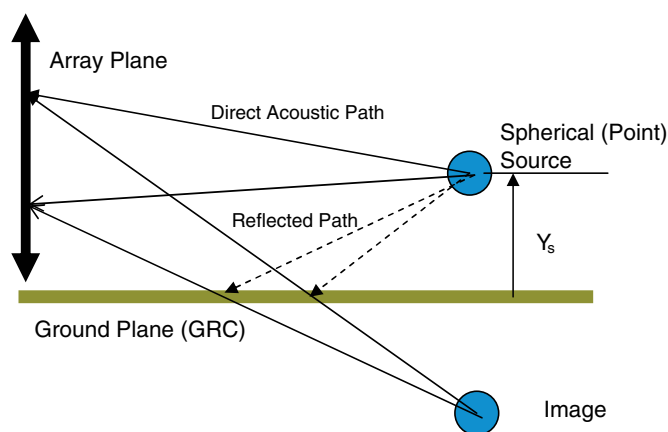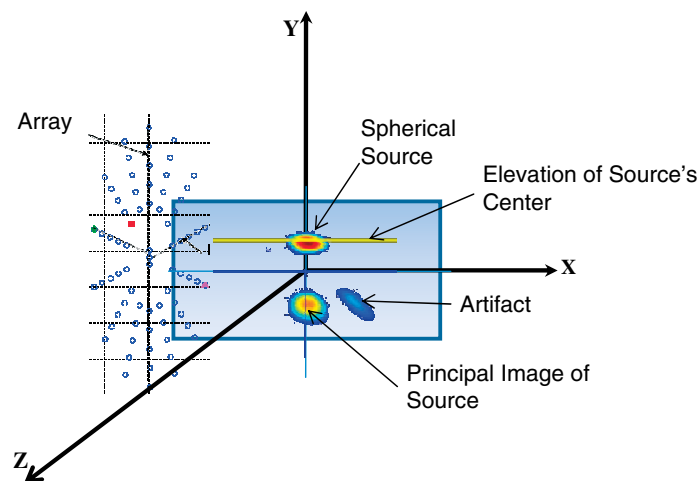
Figure 34. Array and typical image orientation for spherical source emission.

characteristics to be found in the images that will be discussed in this section.

Without going into details yet, note that the ground plane is at $y = 0$ and the array is positioned above it. The physical sources are all also above ground, with all reflected image sources below the ground plane. These characteristics are shown in Figure 34. All images of a single acoustic source will therefore show a single "hot spot" above ground with its mirror image below ground, as illustrated. Grating lobe effects in the array, a coherent (localized) background source, or a non-specular reflection may contribute an artifact at low level, also as illustrated.

Figures 35 through 38 show corresponding calculated and measured images of the spherical source at a series of frequencies that serve to define the spatial resolution of the measurement array. In these figures and all other source images presented in this section, numbers in the color bar legend indicate approximately equivalent one-third octave band sound levels in decibels. At 922 Hz, for example, Figure 35 shows elliptical spots whose major and minor axes are complementary to those of the array. The vertical (−6 dB) width of the spot is about 0.38 m (1.2 ft), while the horizontal width is about 0.67 m (2.2 ft) at a range of 5.8 m (19 ft) which corresponds approximately to the side of the truck or the closer wheel track and an elevation of 1.98 m (6.5 ft). Figures 36 and 37 show examples at lower and higher frequencies, respectively, for the same source at this range and elevation. The two low frequencies define the lower limit of the array performance. The two high frequencies define the upper limit of the array performance. These figures show that the array performs adequately between approximately 250 and 2000 Hz.

Figure 38 shows good focusing at a longer range of 7.62 m (25.2 ft), which corresponds to the center of the passby lane.

Figure 33. Side view of spherical source and its image in the ground half space.

Figure 35. Images of (a) measured and (b) calculated signals for spherical source emission at 922 Hz [source elevation 1.98 m (6.5 ft), array stand-off at road side 5.8 m (19 ft)].
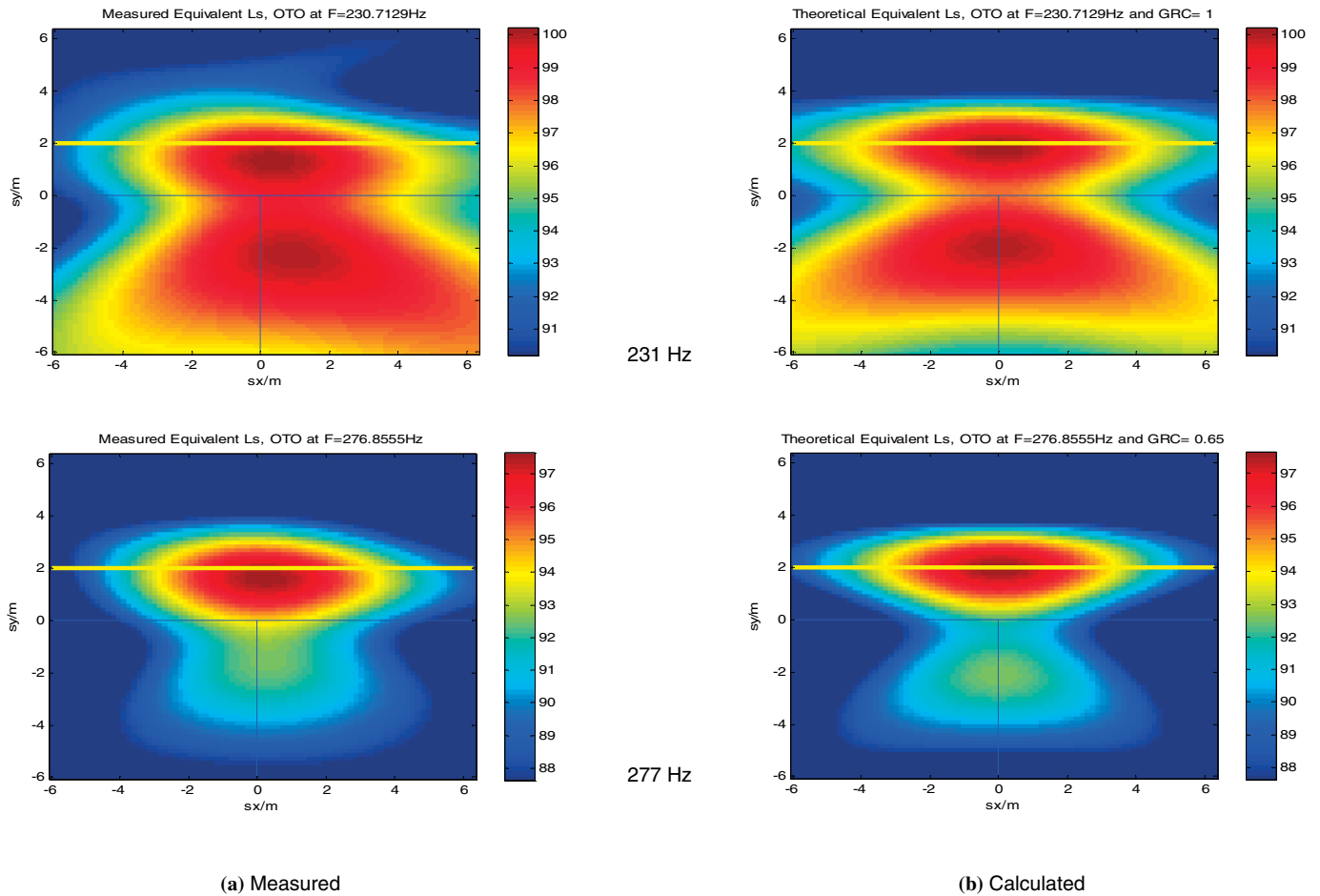
Figure 36. Images of (a) measured and (b) calculated signals at two low frequencies.

1707 Hz

2123 Hz

(a) Measured
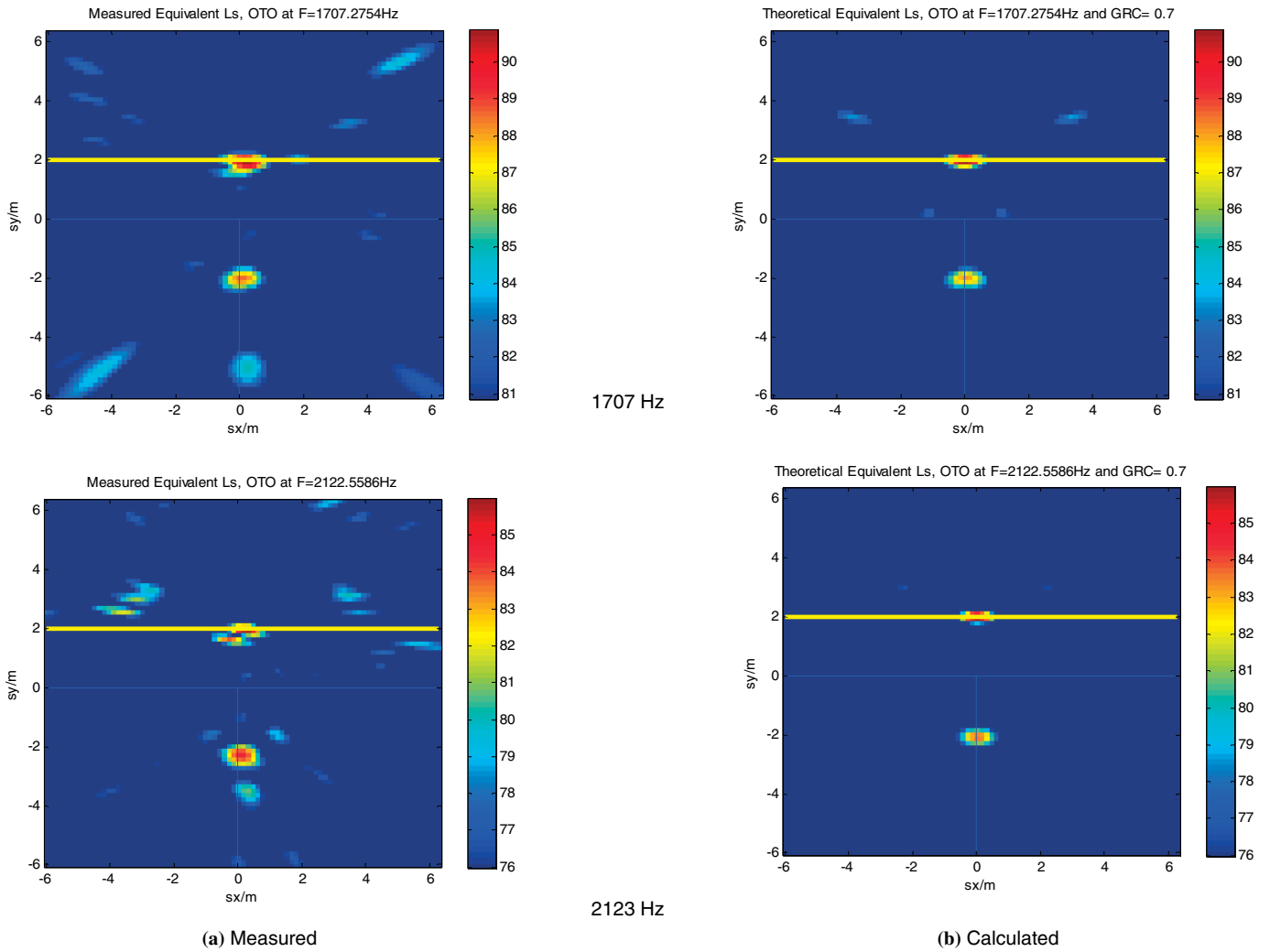
(b) Calculated

Figure 37. Images of (a) measured and (b) calculated signals at two high frequencies.

(a) Measured
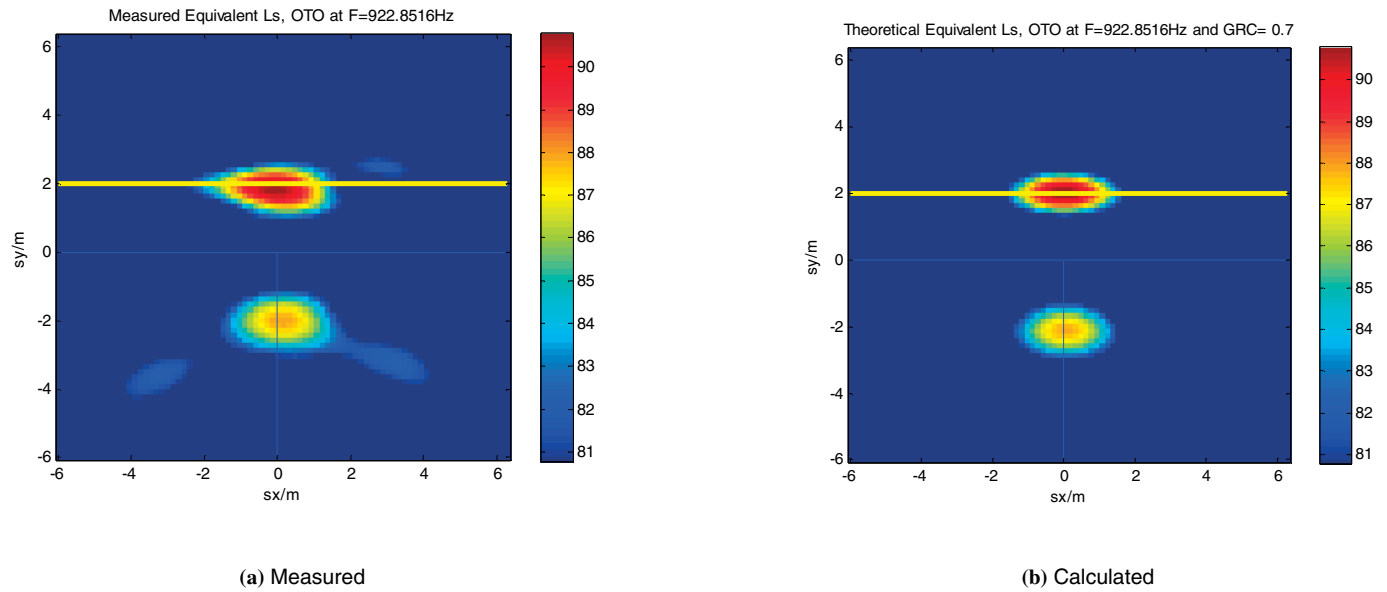
(b) Calculated

Figure 38. Images of (a) measured and (b) calculated signals for spherical source emission at 922 Hz [source elevation 1.98 m (6.5 ft), array stand-off at road side 7.62 m (25 ft)].

Figure 39 allows assessment of the array's actual measured resolution performance compared with the predicted design performance. The measured values for the −6 dB major and minor axes coordinates of the spots at each frequency are shown as points, while the calculated values are shown as lines. This figure illustrates that the acoustic focusing performance of the array is substantially as predicted.

The array's ability to steer is illustrated in Figures 40 and 41. The steering at elevation of 1.24 m (4 ft) and an offset of 7.62 m (25.2 ft) is shown in Figure 40 looking ahead and at 21.8 degrees to the right [x_s = 3.05 m (10 ft)]. Similarly, Figure 41 shows, for an elevation of 1.98 m (6.5 ft), the array's ability to steer 45 degrees off axis [see lower images for x_s = 5.8 m (19 ft) at an offset of 5.8 m (19 ft)]. These illustrations show that, for a spherical source, the array reliably images an omni-directional source at steering angles up to 45 degrees off axis, although at this angle, compared with 21.8 degrees (upper images), there is a slight parallax. As seen in the lower image of Figure 41(a), the source is localized about 1.5 m (5.9 ft) closer than actually located, with the maximum emission measured at a horizontal cross range of x_s = 4.3 m (14.1 ft) rather than the actual x_s = 5.8 m (19 ft). This discrepancy does not occur at 21.8 degrees. Also, note that the measured spot sound levels (84 to 91 dB) are within approximately ±3 dB of one another in all of these images at 922 Hz.

Because the purpose of these measurements was to test localization, not to calibrate array levels, no attempt was made to precisely set the source to the same sound level for each of these measurements. This allowed the sound levels for all runs to be set to a nominal setting, which resulted in certain measurement variability. Thus, in summary and within measurement repeatability, the array steering provided accurate localization and amplitude measurement to within a few deci-

bels at steering angles approaching 45 degrees. In other words, when scanning the region of −6 to +6 m (−20 to +20 ft) in cross range and −6 to +6 m (−20 to +20 ft) in elevation at a stand-off of 6 m (20 ft) from the track, the array will localize and accurately define the magnitude of a stationary source. However, as the following subsection will discuss, truck noise sources are more complex, and that complexity is apparent in the images. Finally, note that with the spherical source at a range of 20.2 m (66 ft) the array still performs well, as shown in Figure 42.

3.5.2 Benchmark Measurements of Spherical Source on Moving Truck with Competing Truck Noise

As a further test of the array steering, with the additional measurement complexity of the moving source and competing truck sources, the omni-directional loudspeaker was strapped to the bed of the 4400 truck on the low-speed track, as was shown in Figure 15. Figure 43 mimics Figure 34 but with the coordinate system and array overlaying an appropriately scaled photograph of a truck (in this case, the 9200i truck) stationed at the closest point of approach (CPA). As with the calibration source, $y = 0$ corresponds to actual ground.

Figure 44 shows the image of the 4400 truck stationary and idling with the spherical source mounted on the truck's bed and activated. The speaker spot and its ground reflection can be seen clearly, as well as engine noise escaping through the wheel well and also by ground reflection. Note that in this case the engine noise reflection image appears about 0.5 m (1.6 ft) below the ground plane.

Figure 45 shows the image of the truck moving to the right at 25 mph (40 km/h), still with the speaker activated. The spherical source and its reflected image are just as clearly represented,
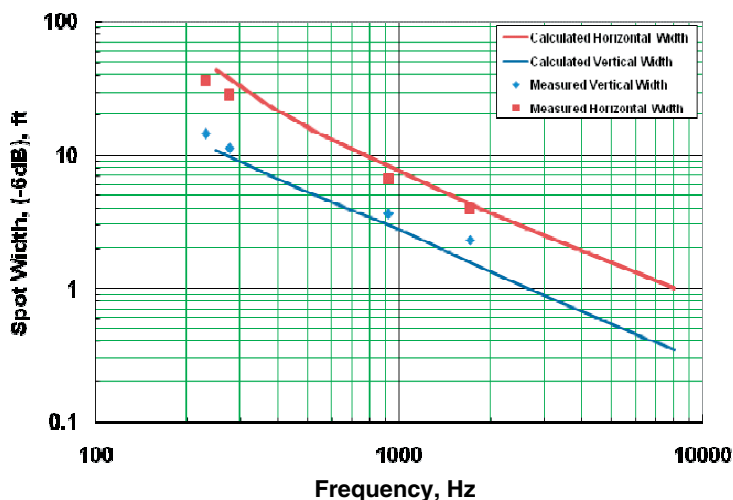
Figure 39. Measured and calculated total spot width (−6 dB) at broad side for elliptical array at 6 m range.

$x_s = 0$

$x_s = 3.05$ m

(a) Measured

(b) Calculated

Figure 40. Images of (a) measured and (b) calculated signals for spherical source emission at 922 Hz for two cross-range source locations $x_s = 0$ and $x_s = 3.05$ m [source elevation 1.24 m (4 ft), offset 7.62 m (25 ft)].

but now with a little horizontal smearing as the result of the truck motion over the measurement time. The engine noise seems to have shifted in its directionality, now being propagated via ground reflection, for which the reflection image appears to be again at approximately −0.5 m (−1.6 ft). Details of the time resolution governances during passby will be discussed in Section 3.5.4.1, as these can affect the noted smearing. In Figure 46, the truck is now passing to the left at 25 mph (40 km/h) with the speaker deactivated. Now no source appears on the truck's bed, yet engine noise is still apparent, although with a new propagation path. The comparison of Figures 45 and 46 is a simple illustration of a reoccurring facet of the truck sound: variability with

engine/fan operating condition and right-left asymmetry in the source distribution and propagation paths.

3.5.3 Benchmark Parallel Array-Based and Acoustic Intensity Measurements for Stationary Trucks

Three trucks with different engine equipment line-ups were examined with both acoustic intensity measurements and array-based measurements in order to develop a fundamental recognition base for defining the truck sources using the array. In the following paragraphs, the relative intensity levels and

x_s=3.05 m, z_s=7.62 m (21.8 deg.)

x_s=5.8 m, z_s=5.8 m (45 deg.)

(a) Measured   **(b)** Calculated

Figure 41. Images of (a) measured and (b) calculated signals for spherical source emission at 922 Hz for two cross-range source locations [source elevation 1.98 m (6.5 ft)].

(a) Measured   **(b)** Calculated

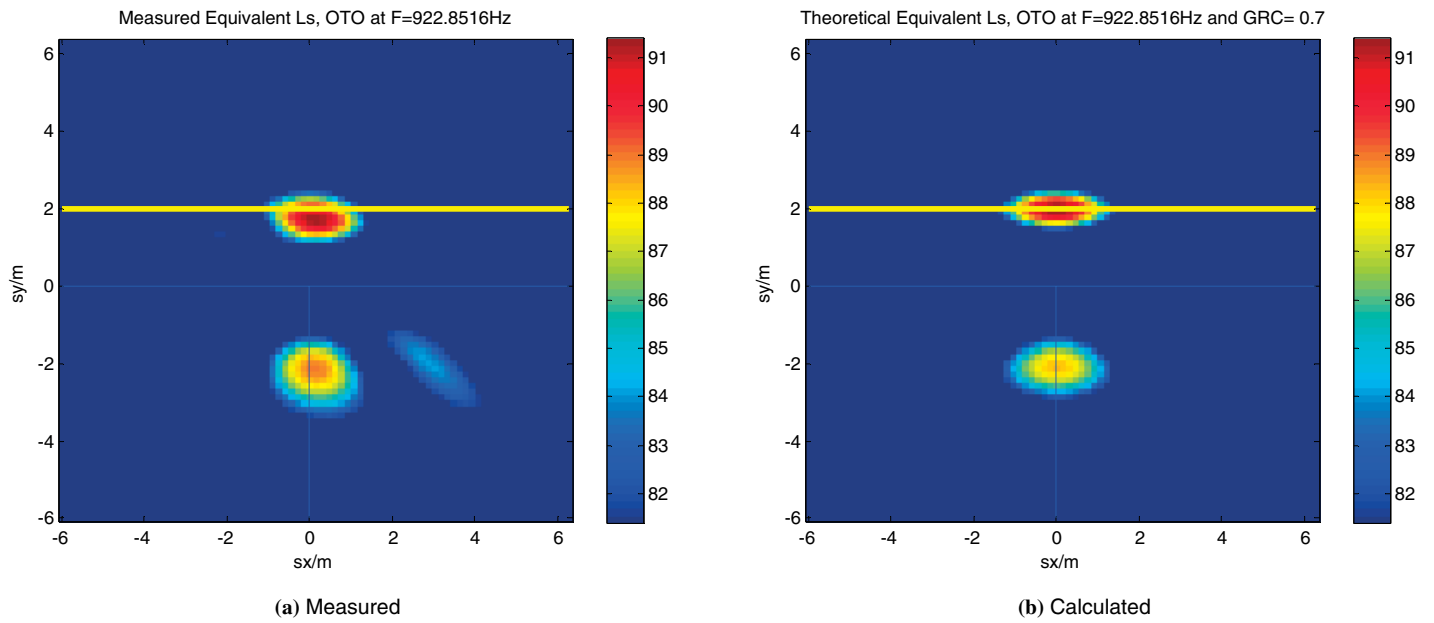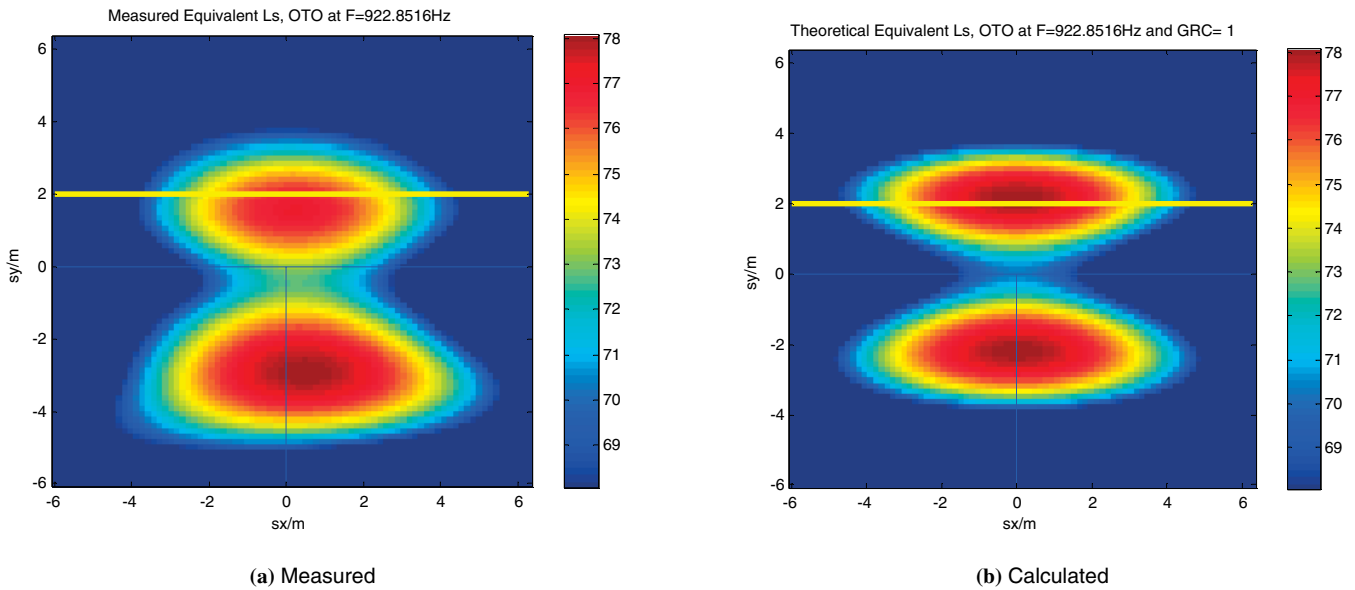*Figure 42. Images of (a) measured and (b) calculated signals for spherical source emission at 922 Hz for 20.2 m (66 ft) array stand-off at road side [source elevation 1.98 m (6.5 ft)].*
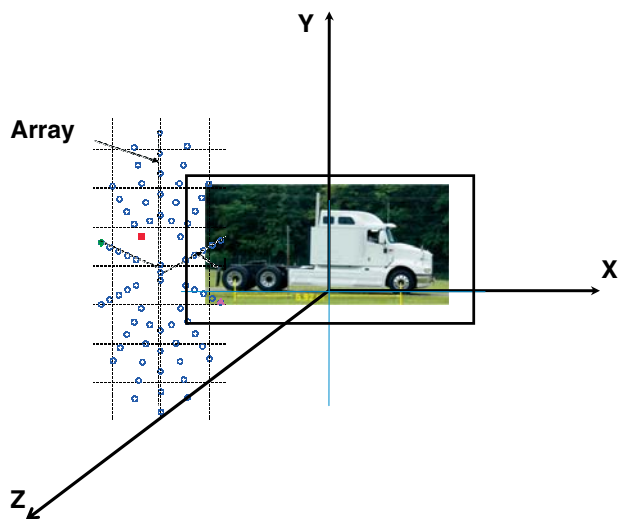
Figure 43. Illustration of the array and truck coordinate orientations during passby event at the instant of CPA.

relative array-based acoustic levels are compared to establish the credibility of the array in rank-ordering the truck sound sources. Note that in all cases to be discussed, intensity levels are in one-third octave frequency bands, while the source images are generally in substantially narrower bandwidths: about 64 Hz constant bandwidth is used with the levels adjusted to provide approximate one-third octave band equivalent sound levels. The array-based and intensity meas-

urements are essentially different and yield identical results only under the ideal conditions of a single-path plane incident wave and a single source. As implemented here, the intensity measurement is made over a plane and provides the average acoustic power which passes across that plane. The planar array captures sound pressures of all arriving ray bundles from the distribution of sources in front of it and, by implementing inter-element phase delays, "localizes" the regions where the rays appear to converge. These regions are called the "sources." Actual directivity patterns of the sources and the existence of multiple acoustic paths (e.g., ground reflection) could cause discrepancies.

Figure 47 shows images at four frequencies for the stationary 4400 truck with the engine set to 2000 rpm, cooling fan running and the spherical source activated. At 922 Hz, as noted previously, the engine compartment sound transmitted through the wheel well, lower cab, and by ground reflection is nearly of equal magnitude to that generated by the spherical source. The spherical source dominates all truck sources at 231 Hz and 600 Hz. At 1937 Hz, the contributions to the sound are from the spherical source and from beneath the cab, but the side lobe effects start to contaminate the source map. These observations agree with Figure 27 in showing complete dominance of the sound by the spherical source below 630 Hz and by the engine noise contributions within 10 dB of the spherical source levels at frequencies above 1000 Hz. Table 12 summarizes these results. The sound power levels (PWL) relative to 10^{-12} W
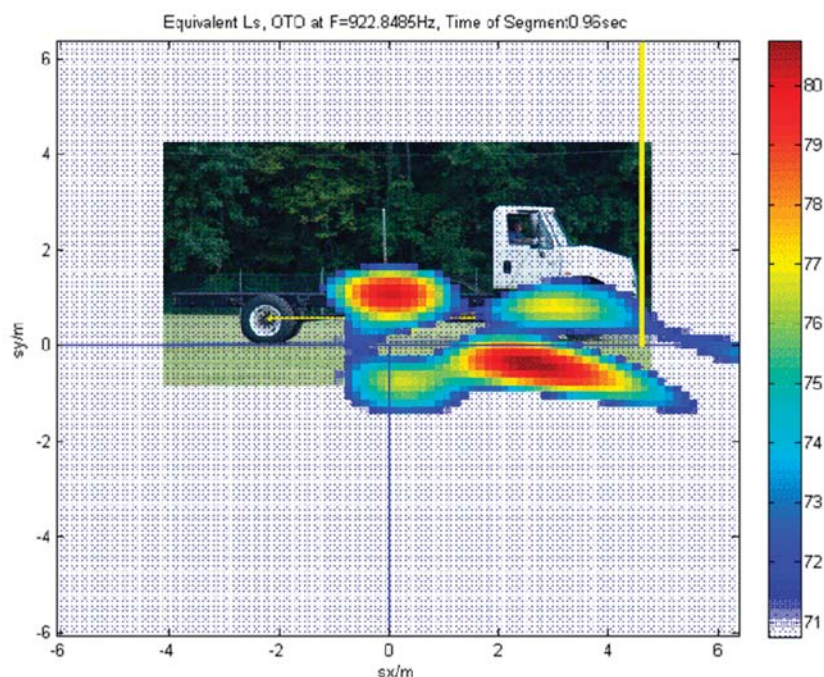
Figure 44. Image at 922 Hz of the 4400 truck idling stationary with engine at 2000 rpm and spherical source activated.
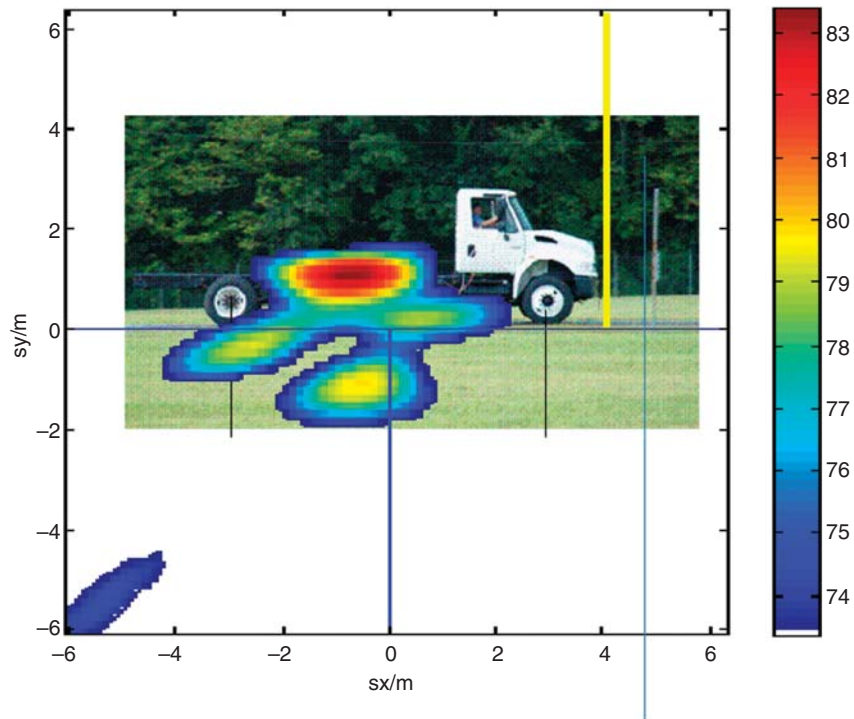
Figure 45. Image at 922 Hz of the 4400 truck traveling to the right at 25 mph with engine at 2000 rpm and spherical source activated.
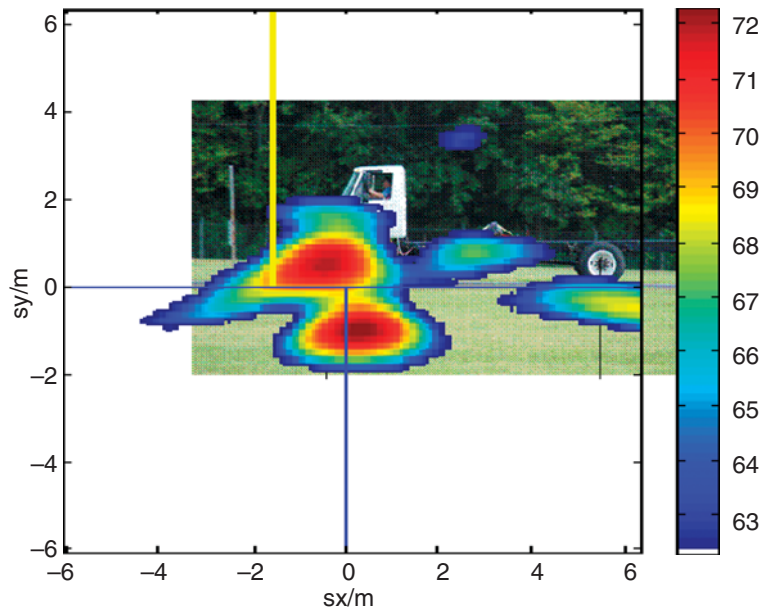
Figure 46. Image at 982 Hz of the 4400 truck traveling to the left at 25 mph (40 km/h) with engine at 2000 rpm and deactivated spherical source.

f = 231 Hz

f = 600 Hz

f = 922 Hz

f = 1937 Hz
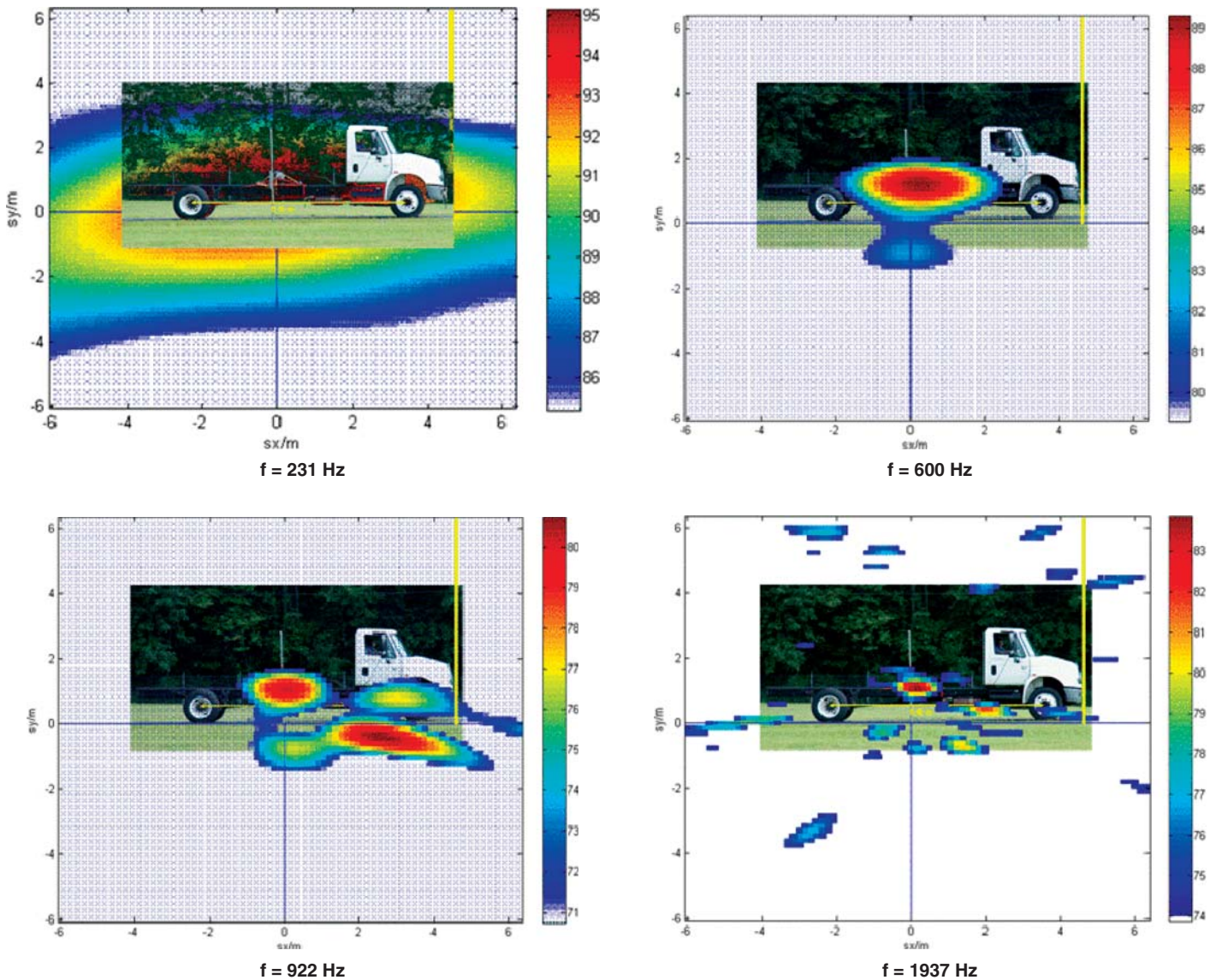
Figure 47. A series of images for source distribution of the 4400 truck stationary opposite the array with engine at 2000 rpm and spherical source activated.

Table 12. Image sound pressure levels and intensity levels (dB) for the stationary 4400 truck with engine at 2000 rpm and spherical source.

Frequency (Hz)		Spherical Source		Wheel Well		Lower Cab	
Image	Intensity	Image	Intensity	Image	Intensity	Image	Intensity
231	250	95	96	<86	87	<86	86
600	630	89	91	<80	87	<80	85
922	1000	80	84	81	85	76	83
1430	1251 to 1600	79	85	77	85	76	83
1938	2000	84	85	77	85	82	83

40

are presented in the table at the one-third octave band center frequencies.

The array-measured image sound levels are presented as equivalent one-third octave band levels using the relationship

$$L_s = 10\log_{10}\left(G(f)\cdot 0.233f / p_0^2\right) \qquad (1)$$

where $G(f)$ is the 1 Hz spectrum level, p_0 is the reference pressure of 20 μPa, $0.233f$ is the bandwidth of a one-third octave band at frequency f, and the frequencies are selected to be within the one-third octave frequency bands of the compared intensity levels. The relative levels L_s and PWL should be equivalent under the ideal conditions noted above, and for the spherical source they essentially are very close. With only one exception,

the PWL and L_s are within 4 dB in their absolute values for the spherical source. The relative rankings of the levels by both measurement techniques, from the spherical source to truck sources, are generally consistent. Note that in these images, the color scale range is 10 dB in order to avoid the appearance of array side lobes which would contaminate the image. The array side lobes (normalized to a main response of unity) are calculated to be approximately a fraction (0.2 to 0.25) of the main lobe (roughly −14 to −12 dB), as shown in Figure 3(c).

For the stationary 9200 truck, the images show significant low-frequency energy being emitted from above the cab, as seen in Figure 48. No spherical source was installed on this truck. Its vertical exhaust muffler was replaced with a pipe ("straight-through" exhaust) before the measurement, and this
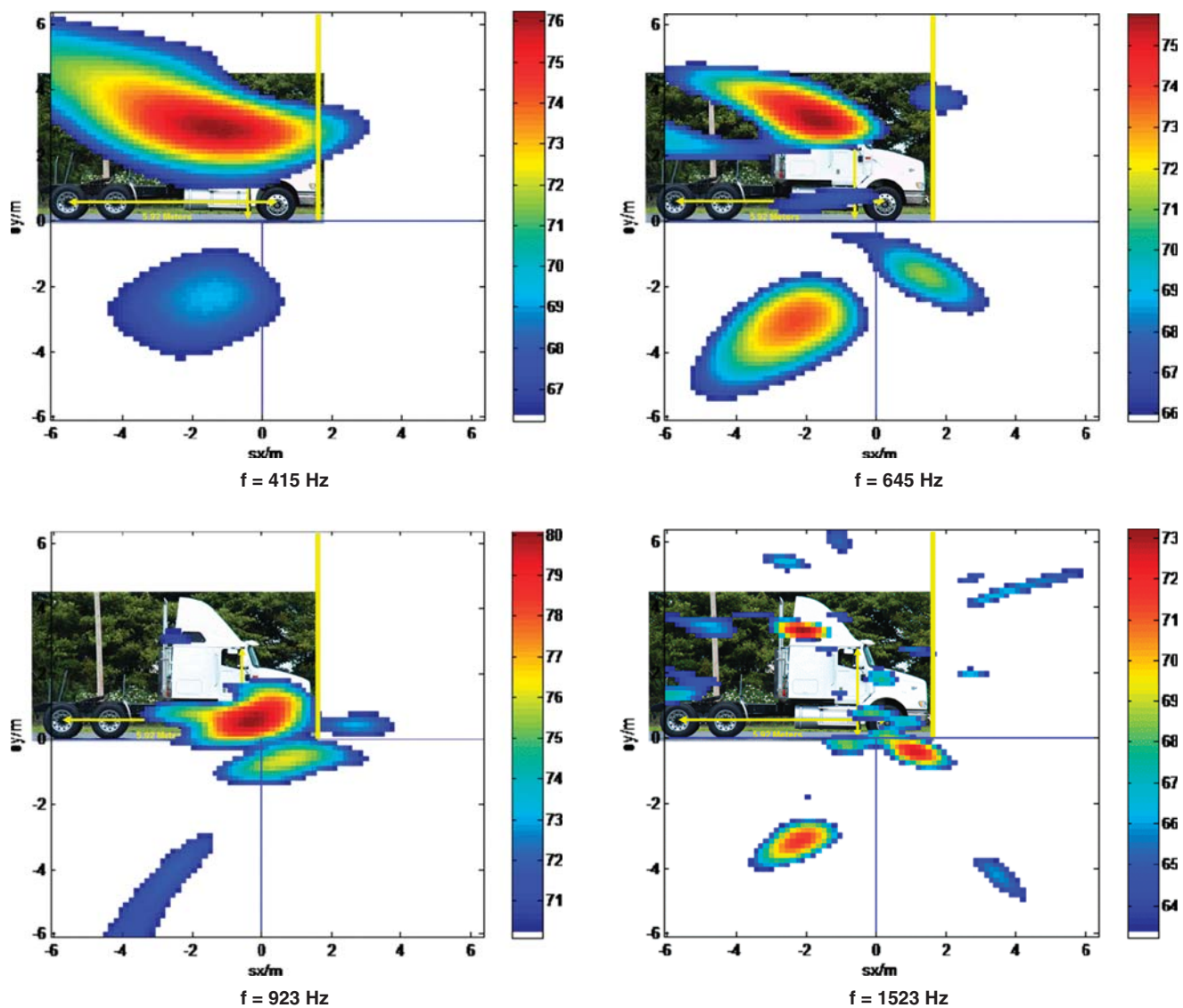
Figure 48. A series of images for source distribution of the 9200i Eagle truck with "straight-through" exhaust (no muffler) and engine at 1500 rpm, stationary opposite the array.

modification made the exhaust noise prevalent at low frequencies. At these frequencies, the location of the source is clearly directly above the cab, not at the exhaust pipe opening. The aerodynamic fairing was open at the back facing the exhaust pipe, which likely excited acoustic volume resonances in the fairing cavity thus amplifying the sound and shifting the source to the fairing. This will be discussed further when the results of the passby for this truck are examined. Noise by the various paths from the engine compartment appears dominant at 923 Hz. Direct radiation from the exhaust, rather than from the exhaust-excited hollow wind fairing appears equally important to the engine noise through ground reflection at 1523 Hz. Note that in the images, the ground-reflected engine noise sources again appear about 0.5 m (1.6 ft) below ground, similar to the location seen with the 4400 truck. The sound power levels presented for this truck in Figure 32 generally corroborate these results by showing dominant exhaust noise at frequencies below 800 Hz. Above this frequency, exhaust and wheel-well noises are generally of comparable order. Table 13 compares the sound levels discussed for this truck, with the notation "(ref)" in the cases where the levels at the array are by ground reflection.

Finally, the 5900 truck with the engine set to 1,400 rpm and the cooling fan running provides a relatively demanding comparison because no single source is dominant. Rather, sound emanates from the engine compartment via multiple paths that are all of relatively similar importance. Figure 49 shows these resolved direct and reflected-path sources. Here again, the locations of ground-reflected sources appear 0.5 to 1 m (1.6 to 3.3 ft) below ground. This location indicates that, in general, engine compartment sources via ground reflection appear at positions -1 m $< y < -0.5$ m (-3.3 ft $< y < -1.6$ ft) depending on truck and frequency: the higher the frequency, the closer the reflected sources to the ground surface. This general observation may provide an important distinction between engine and tire noise sources because the latter should occur at the road surface and appear in the zone within approximately -0.5 m $< y < +0.5$ m (-1.6 ft $< y < +1.6$ ft). Figure 30, which resulted from the sound intensity measurements described in Section 3.4.3, shows that the wheel well, gas tank area (below the cab door), and the region between the gas tank and the wheel well all contribute as pathways for engine sound. The array was unable to discriminate among these paths except at 1799 Hz, because these pathway "sources" are generally rather distributed and the array horizontal beam is too broad (the beam width is greater than 6 ft (1.8 m) at -6 dB below 1000 Hz, see Figure 39) except at high frequencies. Table 14 quantifies these comparisons with reasonable agreement in the image sound level and nearly equal relative ranking of "sources" by the sound intensity measurements.

Further studies in this area might suggest some potential source- or path-targeting treatments.

3.5.4 Example Results from Low- and High-Speed Track Passbys

3.5.4.1 Analysis Technique for Low- and High-Speed Track Passbys

For passby measurements, the arrangements such as the example photographed in Figure 22 were used, with photocells placed on either side or both sides of the array to mark the instant of the front bumper passing a known point in the passby track. Figure 50 illustrates the geometric details, where L_1 and L_2 denote optional locations of the photocells relative to the array for determining truck position. Different locations were experimentally examined and used on the low- and high-speed tracks, although positions were fixed in each case. The cell that indicated approach (i.e., to the left with a rightward approach), used at the high-speed track, was found to give the best timing. The length L_1 for the first cell was 5 ft (1.5 m) and the length L_2 for the second cell was about 20 ft (6 m), as used at the high-speed track. The first cell was always used to mark bumper position in the approaching truck, which was desired as close to the array center as possible without interfering with the microphones. The second cell was used primarily to infer the average speed of truck passby during maneuvers such as braking

Table 13. Image sound pressure levels and intensity levels (dB) for the stationary 9200i truck with engine at 1500 rpm, without muffler.

Frequency (Hz)		Exhaust		Wheel Well		Lower Cab	
Image	Intensity	Image	Intensity	Image	Intensity	Image	Intensity
415	400	76	81	<66	73	<66	73
645	630	76	84	72 (ref)	80	67	77
922	1000	72	85	80	85	76	81
1523	1600	73	84	72 (ref)	84	69 (ref)	77
1938	2000	69	84	71	83	62	77

f = 461 Hz

f = 830 Hz

f = 1245 Hz

f = 1799 Hz
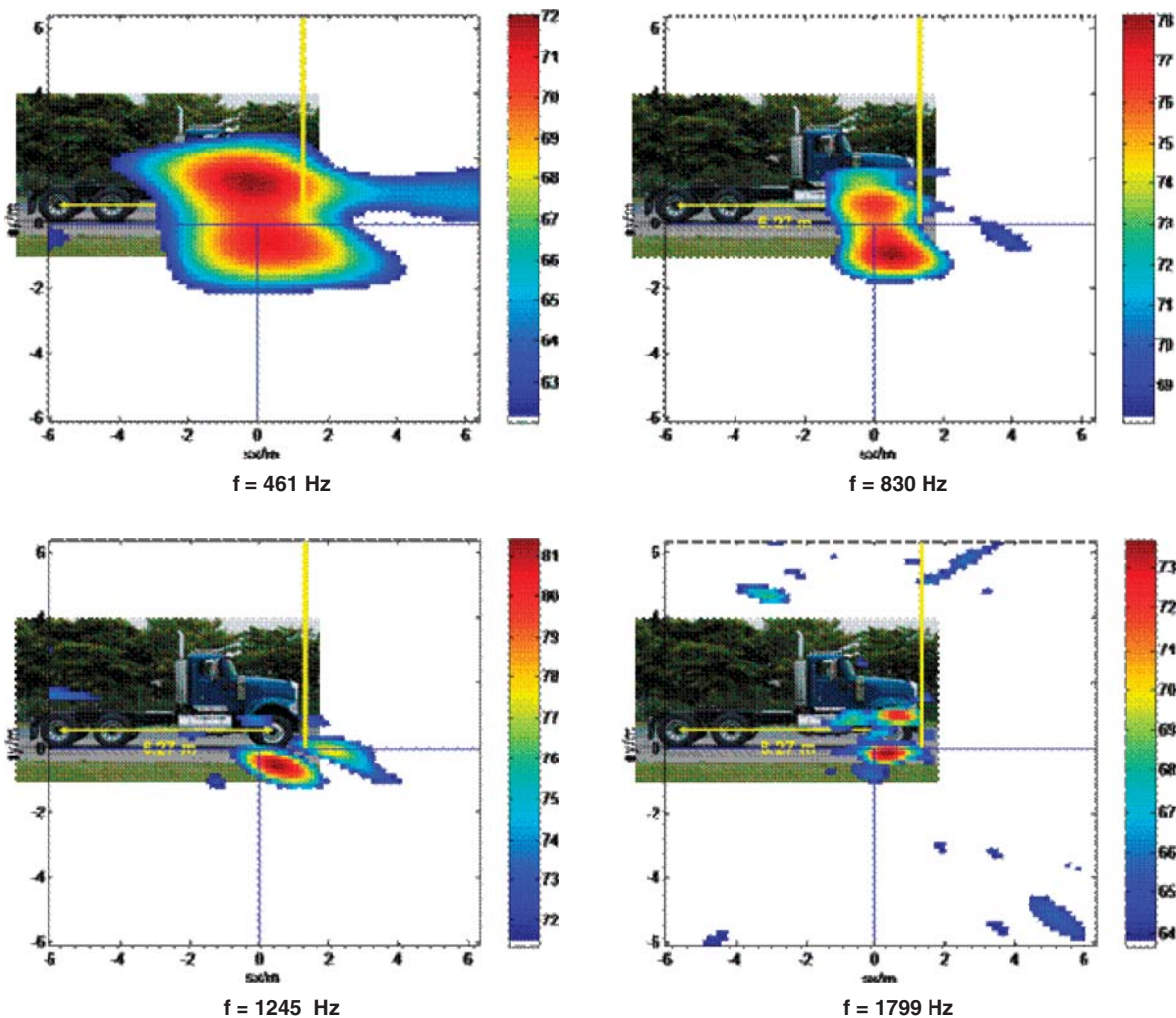
Figure 49. A series of images for source distribution of the 5900i truck stationary opposite the array with engine at 1400 rpm.

and acceleration. It was also used to confirm timing and position. To ensure capturing a complete cab plus trailer length between cells, the second cell was placed further down track relative to the array center than the first. The photocell signal provided a step function as the passing

Table 14. Image sound pressure levels and intensity levels (dB) for the stationary 5900i truck with engine at 1400 rpm.

Frequency (Hz)		Wheel Well		Gas Tank Region/ Lower Cab	
Image	Intensity	Image	Intensity	Image	Intensity
461	500	72	76	*	76
830	800	78	81	*	82
1245	1250	81	83	74	83
1799	2000	74	80	69	81

* Included in wheel well

truck interrupted the light ray, which provided an immediate projection of the truck length onto the time record as shown in Figures 50 and 51. This feature is useful in interpreting the images.

The collected data runs were longer than needed and, to conserve computer memory, the samples were truncated once the passby photocell signal was examined. Typical truncation limits are shown in Figure 51, in which the first and last seconds of data are discarded (shaded areas). In this case, the time to the CPA is 1.25 s after eliminating the first second of the record as indicated by the instant the bumper crosses the photocell signal. The retained data window shown in this example is 3 s; typically, 2 to 3 s were retained, depending on the speed and length of the truck. With the retained data, the truck can be tracked as it approaches and recedes. The increasing and decreasing sound level is due to range (distance) change, as illustrated in Figure 52 for the same run. In this case, for the

Figure 50. Diagram of a typical passby geometry.

3 s retained, the range started at about 15 m (49 ft), closed to 6 m (20 ft) at the CPA, and then opened to 19 m (62 ft). As part of the data analysis, the range from the array center to the front bumper is calculated as reference at each sample time.

Because the acoustic sources on the truck are distributed along the wheel base and otherwise are not known a priori, the range correction approximated to the bumper as a reference. Thus, for any actual source position the actual range correction could be larger or smaller than calculated. An example of corrected and uncorrected sound pressure autospectra for one microphone in the array is shown in Figure 53. The two-dimensional displays of autospectra for a representative sensor in the array are shown in color bar in 1 Hz bands relative to 1 Pa for the passby of Figures 51 and 52. The record is broken into 14 segments of time (the last 13 are plotted) with the range calculated for each. The autospectrum at the top of the figure is uncorrected for range and shows a maximum level at about

1.65 s into the run. At any frequency, the sound level varies by about 15 dB through the run. When range-corrected in the manner described previously, the resulting corrected spectrum, shown at the bottom of the figure, demonstrates less variability. There is over-correction at the beginning and end of the record, however, owing to the uncertainty in the actual range and to the possibility that the tails of the record near 0 and 3 s are contaminated with some background noise. There is a hint of contamination in approximately the first 1.2 s of the overall run, where the rise with time is less steep than later in the run. Of course, once the sources have been localized, it is straightforward to recalculate the range correction to obtain a more precise pressure level history. This iterative step has not been taken because this demonstration was made in conjunction with standard passby measurement procedure that provides absolute A-weighted sound level and the array provides a relative breakout of the contributions with only approximate overall level.
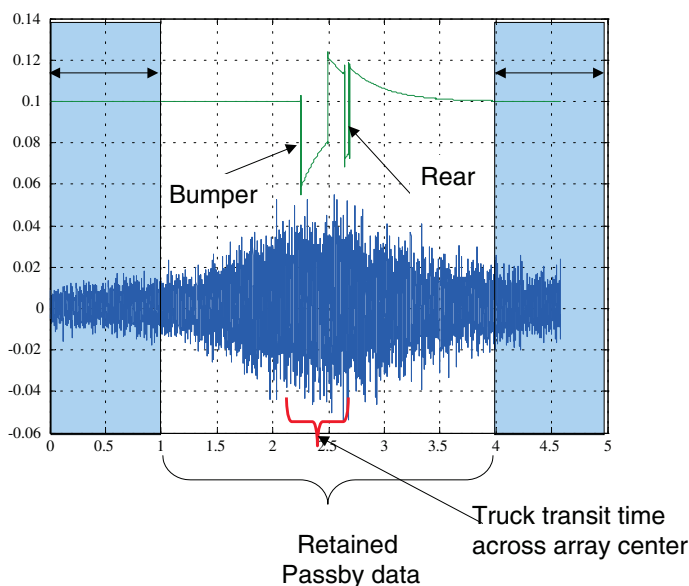
Figure 51. Example of a passby signal record.
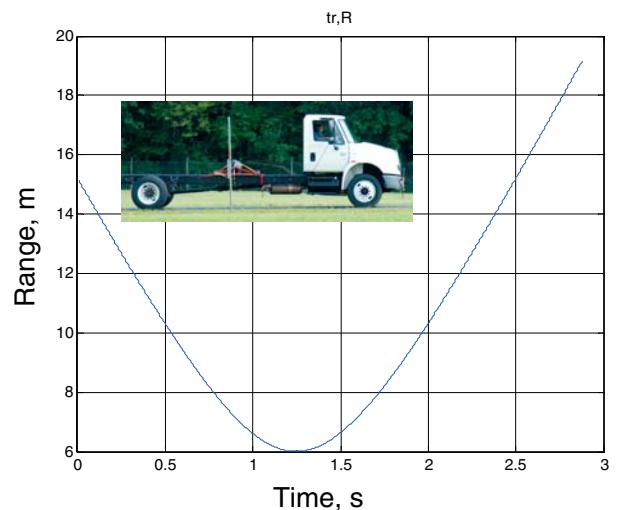
Figure 52. Range from array center to front bumper reference as a function of time during passby.
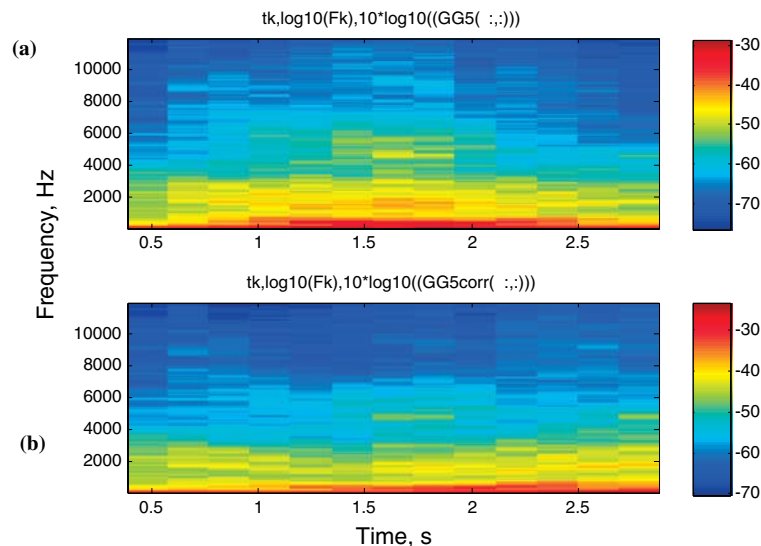
Figure 53. Two-dimensional displays of autospectra for a representative sensor in the array: (a) uncorrected; (b) range-corrected.

The procedure for analyzing the passby starts with determining the resolution at various times during the record. To develop a temporal gradient with multiple segments of adequate statistical sampling and frequency resolution, a balance must be made among the number of Fast Fourier Transform (FFT) frequencies (nfft), the number of ensembles (noens), and the number of time segments along the record (nofiles). Thus, if the total sample size is N (in the example case, 3 s taken at 6000 samples per second), then

$$N = \text{nfft} \cdot \text{noens} \cdot \text{nofiles} \qquad (2)$$

In the majority of cases examined during passby, typical values of these parameters are nfft = 128, noens = 10 to 15, nofiles = 15 to 20 for total sample sizes N up to about 20,000. Fewer nofiles allows a greater number of ensembles or greater frequency resolution, but it gives a much longer time segment that averages over too much of a passby. Too high a value of nfft provides a narrower bandwidth and associated spectral variability. As a practical matter, given the trade-off between some spectral smoothing and some time resolution desired, the above-noted parameter values gave the best results.

3.5.4.2 Passby Evaluations of the 5900i Truck: Localization of Engine Compartment and Tire Noise

Passby measurements with the 5900i truck at 50 mph (80 km/h) show the ability of the array to discriminate among various propagation paths of engine noise and tire noise. Figure 54 shows truck noise images at 868 Hz for a passby speed of 50 mph with the engine at 1400 and 2000 rpm at an instant

opposite to the vertical array axis "A." A few "spot" areas are indicated in the images. The areas designated "F" are located at the front of the truck, just behind the front wheel and below the ground plane. The source levels associated with these spots differ by roughly 6 dB. The spot labeled "T" in the 1400 rpm run is located near the road surface plane and appears to be due to the rear tires. The streaked spots labeled "D" lie below the ground plane between the front and rear wheels and appear to be within 1 dB for the two runs. These sources could be exhaust or drive-train noise. As noted previously, sound generated in the engine compartment and elsewhere on the truck, when reflected off the ground, appear to the array as sources below ground by 0.5 to 1 m (1.6 to 3.3 ft). Comparison of the lower image in Figure 54 with the images in Figure 49 for this truck stationary—with no tire or drive-train noise and the engine operating at 1400 rpm—shows that, for similar frequencies, the levels just behind the front wheel are about 75 to 77 dB in each case. During passby at 50 mph (80 km/h), however, the other sources dominate over the engine noise. At 2000 rpm, the engine noise now competes with the other sources, having increased to about 83 or 84 dB. This increase is consistent with the observation of sources associated with this forward wheel-well acoustic propagation path.

Images at other frequencies for the engine speed of 1400 rpm are shown in Figure 55, which illustrates the localization of sources at the front and rear tires. As noted previously in the discussion of the array calibrations (e.g., Figure 40), the array will successfully localize sources while steering off axis, but the projection of the sound field onto the microphone plane further elongates and slightly rotates the appearance of the point spread spot function. Keeping these image features in mind, clear con-
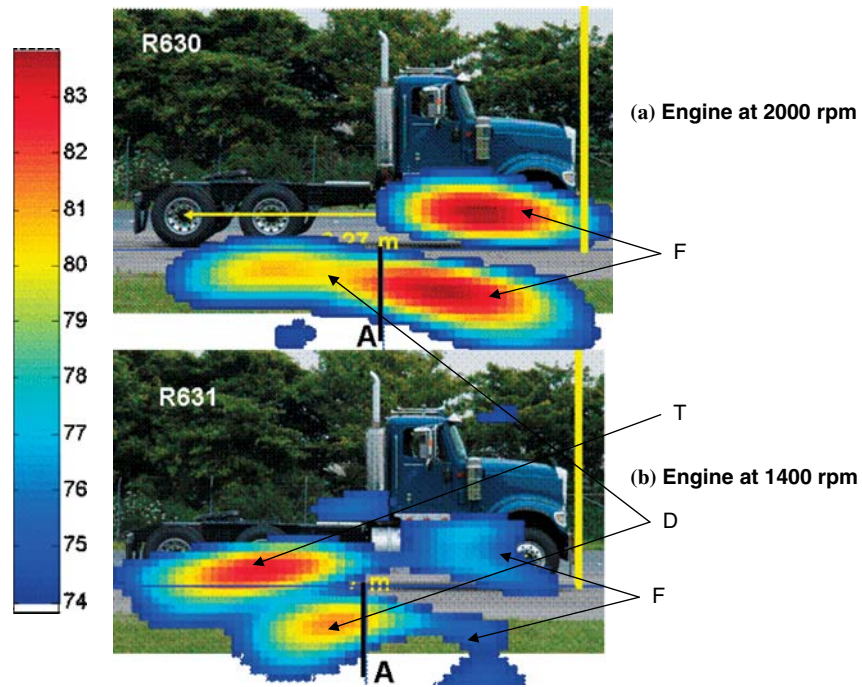
Figure 54. *Source distribution at frequency of 868 Hz of the 5900i truck moving to the right at 50 mph with engine at (a) 2000 rpm and (b) 1400 rpm.*
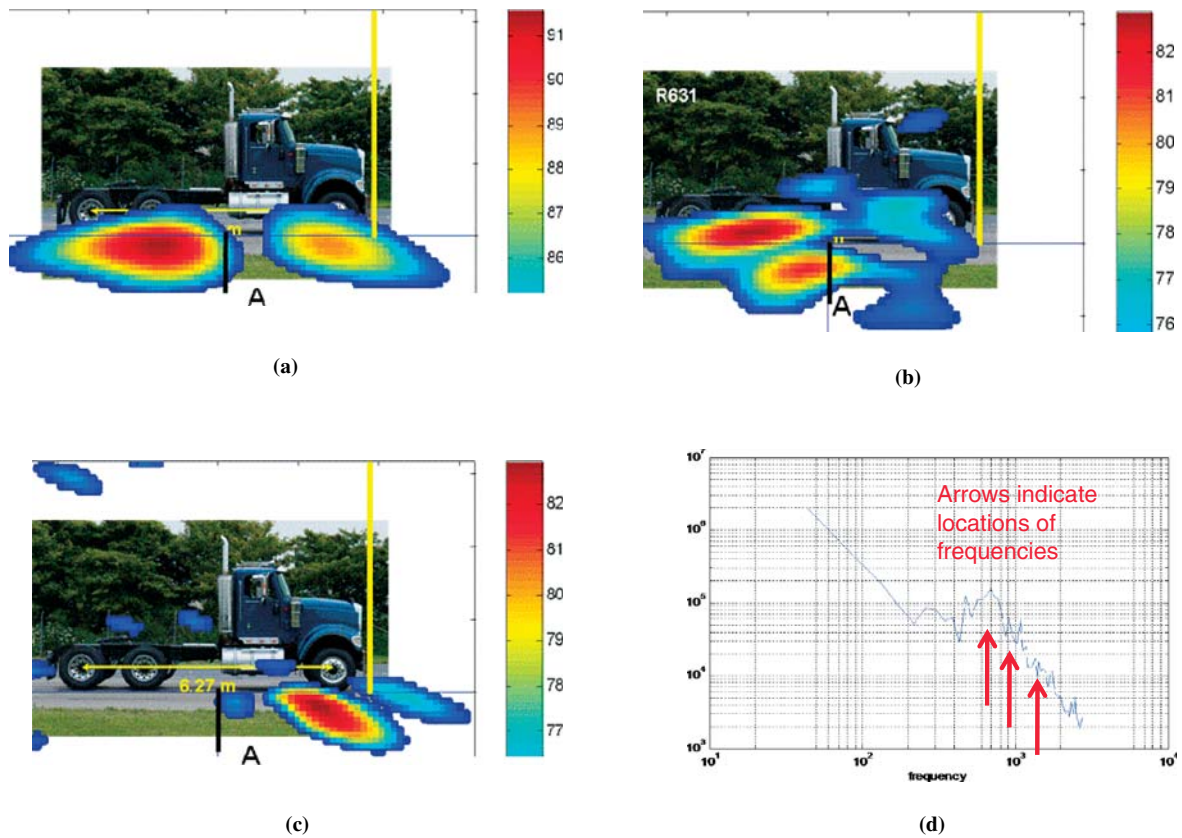
Figure 55. *Source distributions for the 5900i truck moving to the right at 50 mph with engine at 1400 rpm at frequencies: (a) 695 Hz, (b) 868 Hz, and (c) 1346 Hz indicated in (d) the truck noise spectrum.*

R630, 2000 RPM f=868 Hz

R705. 2000. "Noisier Tires" f=870 Hz
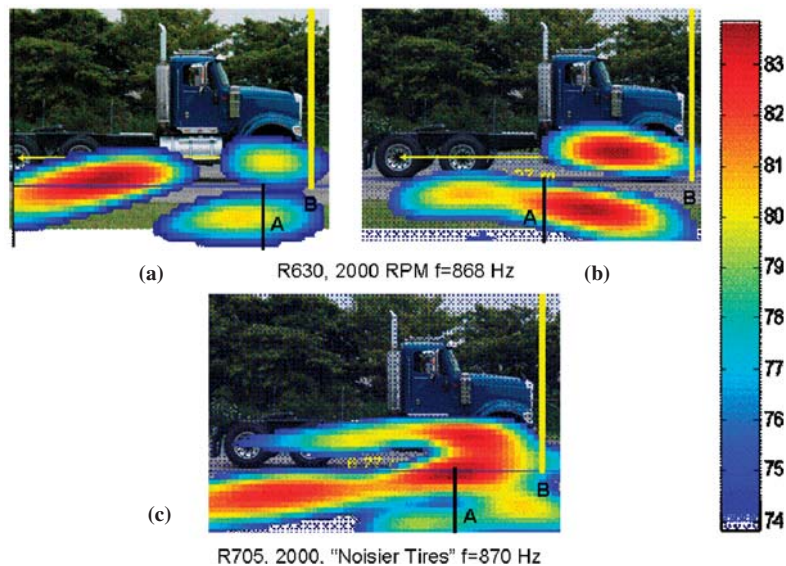
Figure 56. Source distributions for the 5900i truck moving to the right at 50 mph with engine at 2000 rpm.

tributions from the tires are seen at 695 and 1346 Hz; this operating point [lower engine speed and 50 mph (80 km/h) vehicle speed] and these frequencies were selected to minimize the influence of the engine and maximize that of the tire noise.

The directional nature of these sounds is illustrated in Figure 56 for the same truck speed of 50 mph but the engine at higher rpm of 2000. At the top of the figure is a pair of images at 868 Hz from a single passby, but with the truck at two different positions relative to the array. The line labeled "A" in this figure denotes the location on the truck of the array main response axis, so that the tires are directly opposite the array on Figure 56(a) and just to the right of the array on Figure 56(b). Thus, Figure 56(b) shows just behind the front tire, while on Figure 56(a) the perspective is to the side of the tire. These two images lead to the conclusion that the tire noise is directive slightly to the rear, say about 20 degrees off the perpendicular to the truck side-plane. Similarly, in these views, the sound from rear tires appears to be directive forward. The images also suggest rearward directivity of the sound from the engine compartment: see the relative levels of the ground reflection in the upper images of the figure. Figure 56(c) was obtained during a passby for this truck on the following day but with different drive axle tires (G167), which are known to be noisier from other research (*23, 29*). The proof-of-concept testing cannot confirm, however, those results.

3.5.4.3 Passby Evaluations of the 9200i Truck: Localization of Engine Compartment and Exhaust Noise

Figures 16 and 19 show the two body styles of the 9200i series truck that were tested. The style tested at the low-speed track (Figure 16) had a side skirt below the cab and a raised roof at the cab top. The version tested at the high-speed track (Figure 19) had no skirt and an aerodynamic fairing with an open back was set on top of the cab. This truck was tested with a standard vertical muffler installation and with the muffler replaced with a pipe. The data presented in the following paragraphs were collected for the truck speed of 30 to 35 mph with the engine at 1850 to 1900 rpm.

Line plots of autospectra at the time for which the maximum overall sound pressure level was recorded are shown in Figure 57 for each of the three passbys for these truck models. Except for some details in the spectra, the skirted and
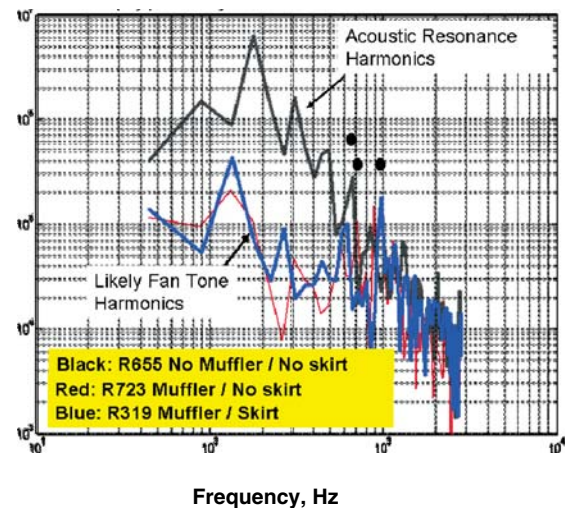
Frequency, Hz

Figure 57. Sound autospectra for different tested models of the 9200i truck at 31 mph with engine at 1850 rpm (dots denote frequencies of images below).

unskirted trucks with a muffler installed provided essentially comparable spectra. With the muffler removed, however, the measured sound pressure levels increased substantially at frequencies below 800 Hz. This frequency range is marked by the occurrence of a series of tones (peaks) at multiples of roughly 90 to 100 Hz: this general periodicity is clear in the sample spectrum shown for the truck with no muffler in Figure 57.

Images of the noise sources of these truck models are presented in Figures 58 through 62 for three frequencies denoted by the dots in Figure 57: 655 to 668 Hz, 709 Hz, and 975 to 980 Hz. These frequencies were selected on the basis of their proximity to the approximately 700 Hz harmonic of the tones. Of note in Figure 58, at 665 to 668 Hz all trucks with a muffler installed, whether traveling to the right [Figure 58(a) and 58(b)] or to the left [Figure 58(c)], have the same characteristic of combined engine and tire noise, with engine noise apparently dominant. This behavior is similar to that in the 975 to 980 Hz range, as shown in Figure 59. Propagation of sound through the wheel well and around the skirt via

ground reflection (in both frequency ranges) appears to generally characterize the natures of the received sound levels. Although the source distributions in rightward [Figures 58(b) and 59(b)] and leftward [Figures 58(c) and 59(c)] travel are both localizable to the lower cab, the detailed source distributions lack symmetry, as discussed previously for the 5900i truck.

With the muffler removed, the expected localization of sound from the region of the exhaust opening is apparent in Figures 60 to 62 for the three frequencies, where the sound source maps for the truck with a muffler are shown on the left side of each figure and labeled (a), and the source maps for the truck without a muffler are on the right and labeled (b). At all three frequencies, the ground reflection of the exhaust noise is perfectly clear. Tire noise at the rear tire is apparent in Figure 60(a) with the sound level of 79 dB, but is only 75 to 76 dB in Figure 61(b). The engine noise or forward tire noise in the two truck runs are at the sound levels of 82 and 79 dB, respectively.

(a)
(b)
(c)
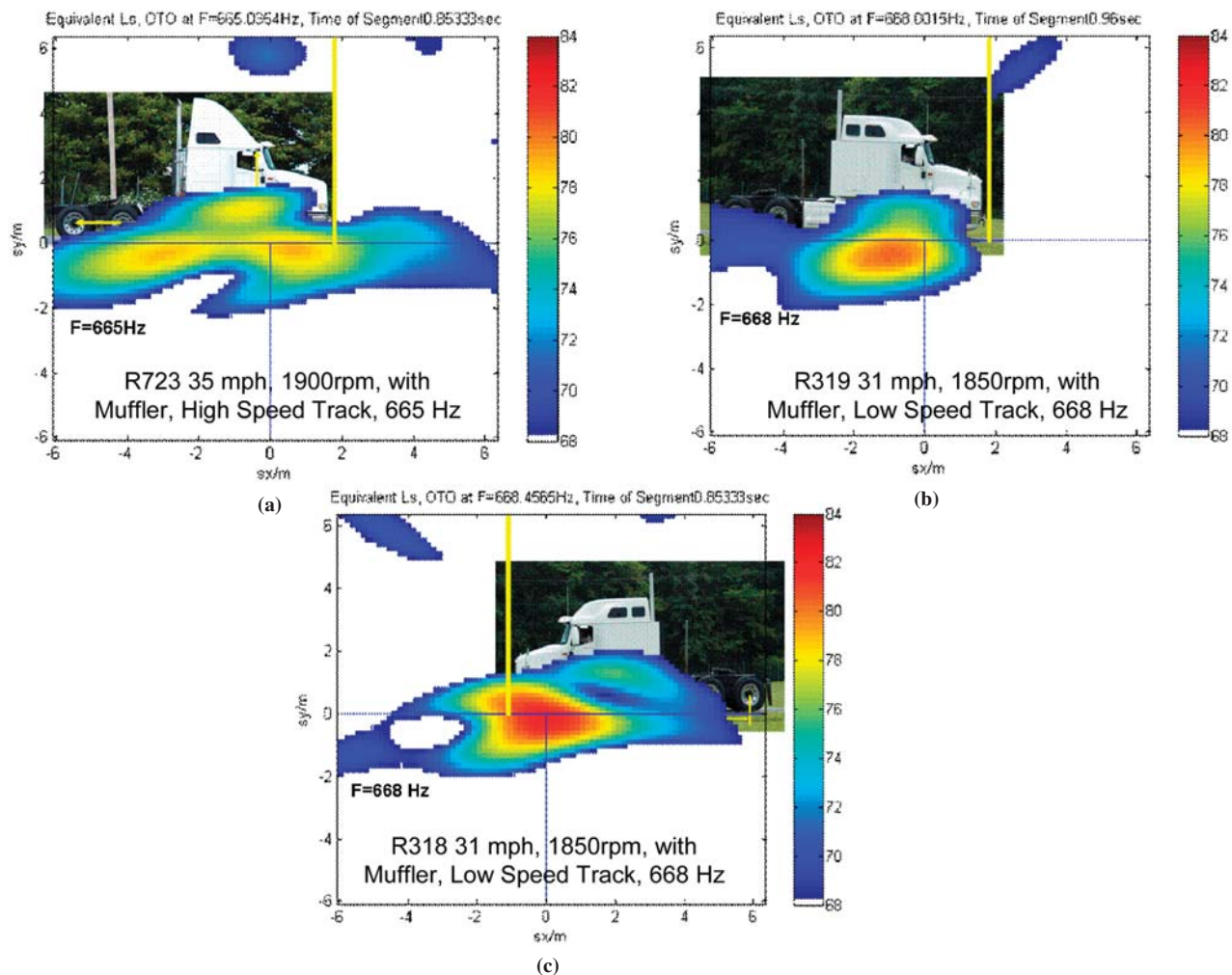
Figure 58. Source distribution at 665 to 668 Hz for various models of the 9200i truck with muffler traveling at 31 to 35 mph.
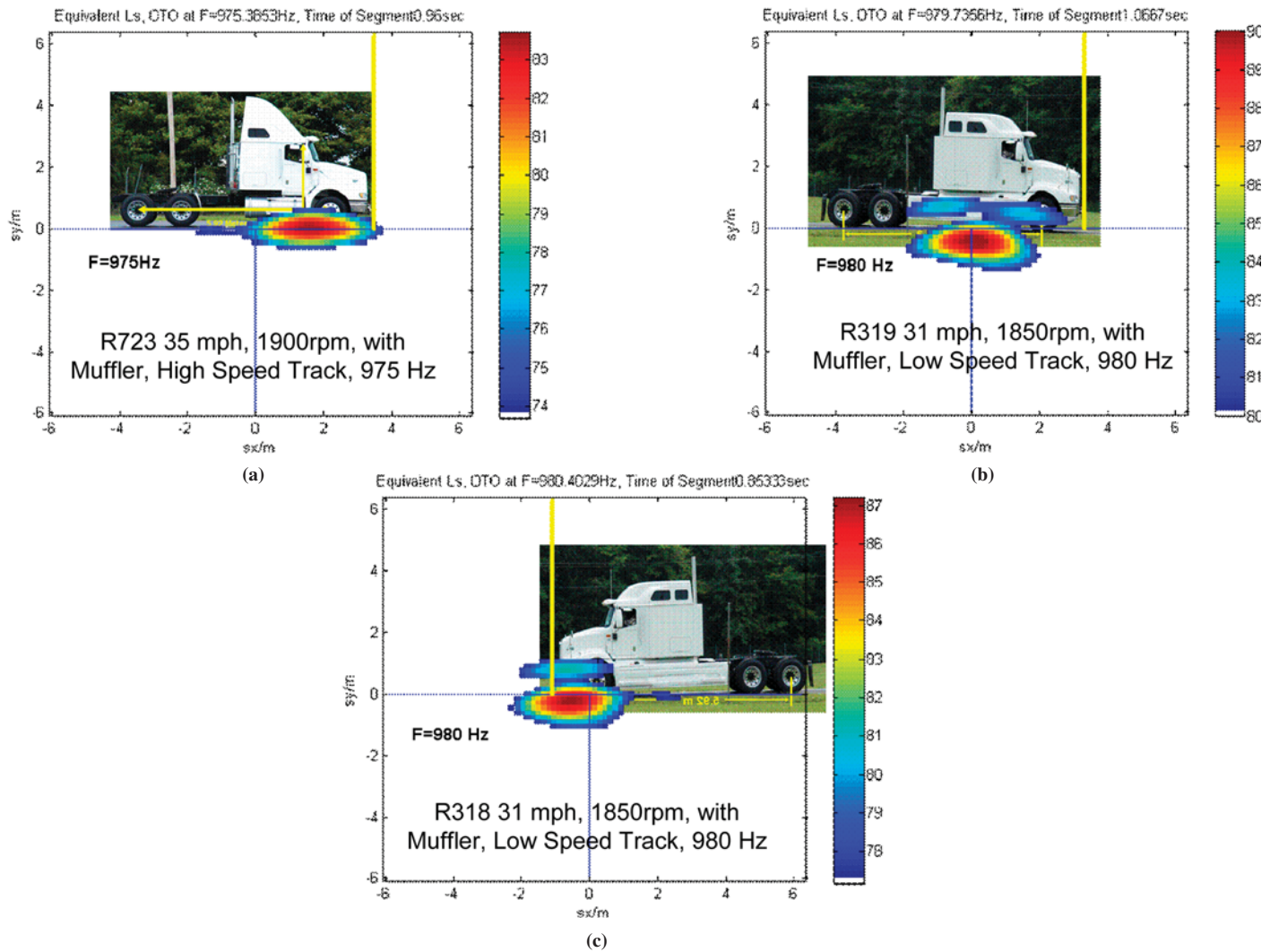
Figure 59. Source distribution at 975 to 980 Hz for various models of the 9200i truck with muffler traveling at 31 to 35 mph.

The main point of these figures, however, is the nature of the exhaust noise. As noted previously, exhaust noise is marked by high tonal content and the source is localized just forward of the stack—above the cab. The sound is conjectured to actually be amplified by the aerodynamic fairing, which acts as a resonator of the noise emitted from the stack. The source is perhaps a series of volume resonances of the hollow fairing cavity excited by a primary exhaust efflux source. The fundamental half-wave resonance of a 6 ft (1.8 m) cavity would be at about 90 Hz, consistent with the observed approximate lowest peak frequency of the exhaust noise autospectrum (Figure 57). The sound from the stationary truck was also noted to have these features, as discussed previously for Figure 48.

Note that the foregoing discussion for this truck is concerned primarily with evaluation of the engine compartment and exhaust noise. In Figures 59 through 62, the color bars indicating the measured sound levels show a range of approximately 10 dB for each image; however, the ranges are of various values

for images (a) and (b) in order to illustrate clearly the differences between these noise sources. As a result, the other sources that remain nearly the same in both compared cases, such as the tire–pavement noise in Figures 60 and 61, appear to be of much different strength if judged simply by the image color rather than by the actual values of the measured sound level.

3.5.4.4 Evaluations of the Truck Acoustic Source Level During Passby as a Function of Vertical Elevation

The acquired acoustic data together with the recording of the exact truck position with time during the passby can be used to generate a map of the sound level as a function of vertical elevation in the truck plane. This map provides a time history of the vertical density of sources at each time increment during the passby. The time history can then be readily interpreted by relative motion as location along the truck. The cal-

R723 35 mph, 1900rpm, with
Muffler, High Speed Track

(a)

R655 35 mph, 1900rpm, NO
Muffler, High Speed Track

(b)
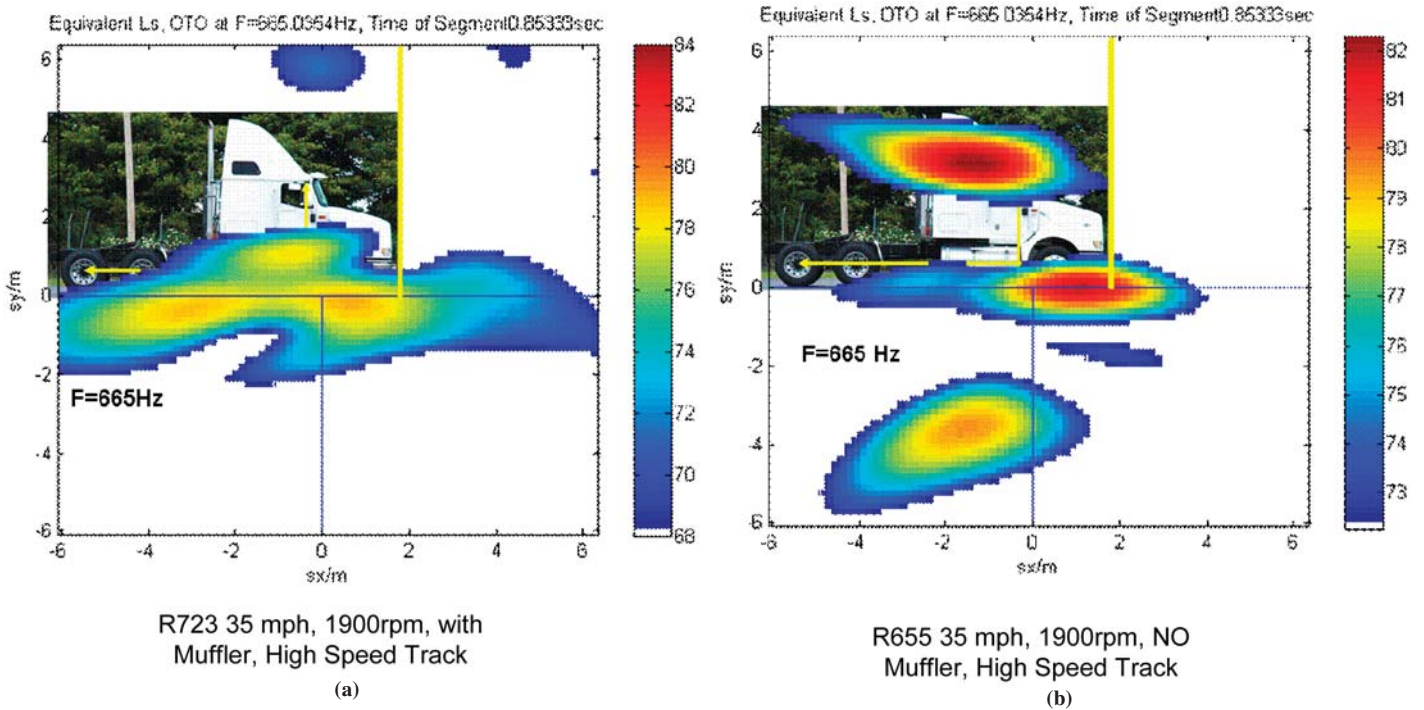
Figure 60. Source distribution at 665 Hz for the 9200i Eagle truck: (a) with muffler and (b) without muffler.

R723 35 mph, 1900rpm, with
Muffler, High Speed Track

(a)

R655 35 mph, 1900rpm, NO
Muffler, High Speed Track

(b)
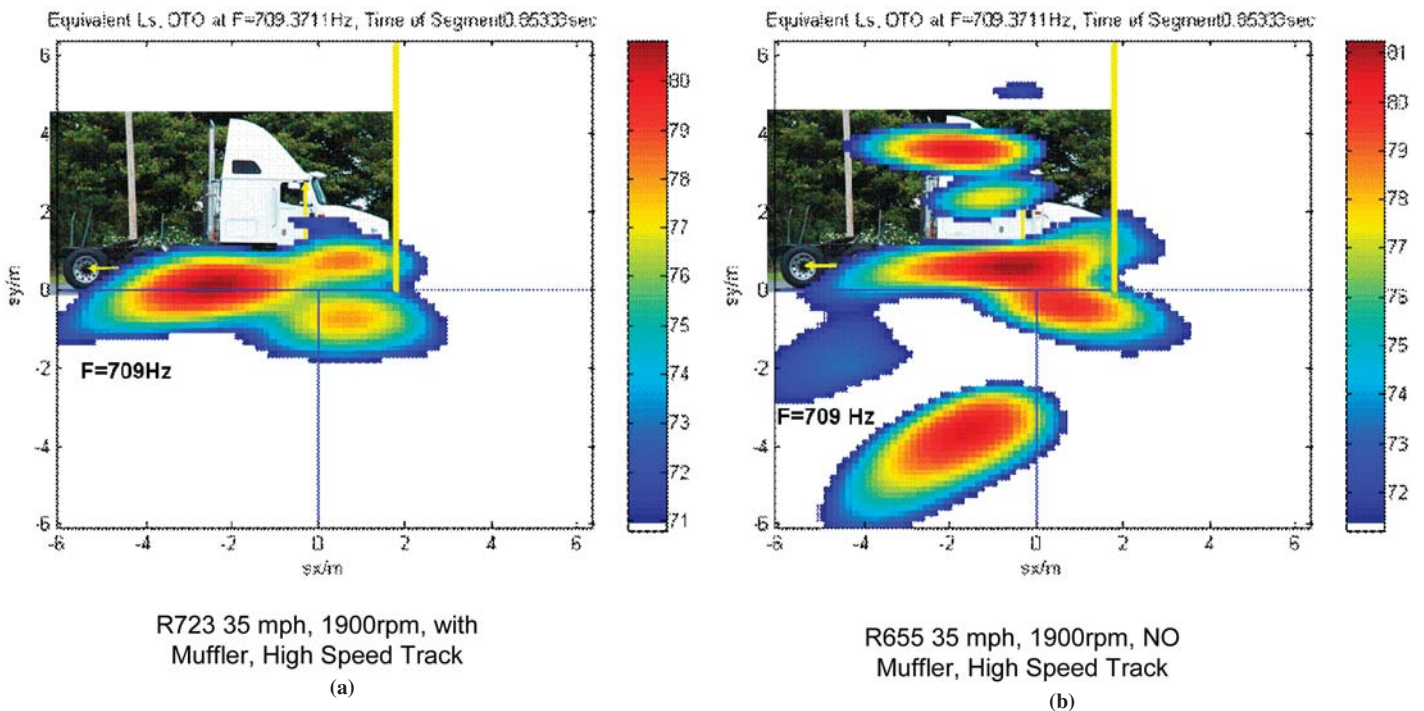
Figure 61. Source distribution at 709 Hz for the 9200i Eagle truck: (a) with muffler and (b) without muffler.

R723 35 mph, 1900rpm, with
Muffler, High Speed Track

(a)

R655 35 mph, 1900rpm, NO
Muffler, High Speed Track

(b)
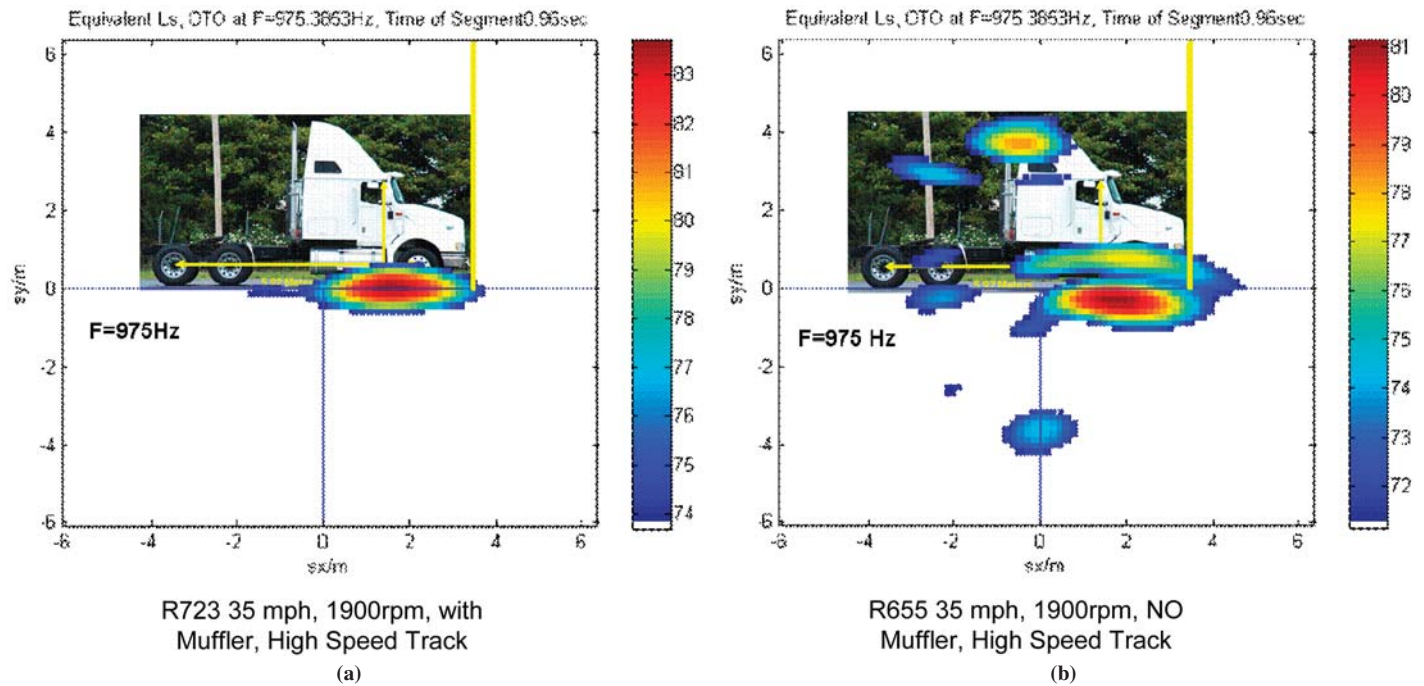
Figure 62. Source distribution at 975 Hz for the 9200i Eagle truck: (a) with muffler and (b) without muffler.

culation can be done for each frequency giving a data set of sound pressure level as a function of time during passby (or location along the truck), elevation in the truck plane, and frequency. This type of processing was fully developed for analysis of roadside measurements. During proof-of-concept testing, preliminary examples were generated for the 4400 truck with and without the onboard spherical source activated. To perform the calculation the array beam was trained to $x = 0$ (the horizontal position dead ahead) and to a series of vertical positions $y = y_{index}$ above the road surface, and acoustic spectra was obtained as a function of time increment during the passby for each elevation. This procedure gives a time–frequency record of all sound arriving at the array center from each of the targeted locations on the truck. The process is repeated for the sequence of values of $y = y_{index}$ up to a maximum that, in this case, was set to about 4 m (13 ft) above the surface of the road. The increment for indexing is about 0.5 m (1.6 ft) and a total of nine vertical positions are used.

Figure 63 shows a time record of the vertical scans for the stationary, idling truck with its spherical source activated. The source was 4 ft (1.2 m) above the road surface. Because the truck is stationary, the source levels at the different elevations are essentially constant except for possible small propagation variability associated with the outdoor acoustic field. These vertical scans show a concentration of source level in the $y = 1$ m (3 ft) pixels with markedly reduced levels in the $y = 2$ m (6.5 ft) (and greater) pixels. The vertical discrimination is smaller for the levels at 1406 Hz than at 937 Hz, given the

beam widths plotted in Figure 39 [i.e., ~3 m (10 ft) and ~2 m (6.5 ft) for the frequencies of 937 Hz and 1406 Hz, respectively]. Also, noting the image plot for this data set in Figure 44, when the array is trained to $y = 0$, the reflection from the road surface is included in the aperture of the array, especially at 900 to 1000 Hz. Thus in Figure 63(a) there is little variation between levels in the pixels at $y = 0$ and 0.5 m (0 and 1.6 ft), while there is noticeable difference in Figure 63(b) for which the total beam width is only 2 m (i.e., ±1 m) [6.5 ft (i.e., ±3.25 ft)]. Given that the truck is stationary, the source level distribution is constant over time and appears as a stripe along the $y = 1$ m (3 ft) pixels.

The frequencies discussed in these figures are slightly different than those discussed in Figures 44 through 46 because a narrower bandwidth was used here for which the FFT gives narrower analysis bands. The vertical scans were used for the roadside measurements to provide vertical distributions of A-weighted one-third octave band levels using summations of narrower bandwidth spectra, so the data presented here are preliminary to that application. By bracketing the 922 Hz point of Figures 45 and 46, say, differences between 922 Hz and 937 Hz for this truck were determined to be negligible.

For the 4400 truck passing to the right at 25 mph (40 km/h) with the onboard source activated, Figure 45 shows an image that localizes the spherical source at a point about 4.6 m (15 ft) behind the bumper. Thus, when the truck is vertically scanned during passby in the manner described previously, the mapping of levels that is shown in Figure 64 is obtained. In this case,
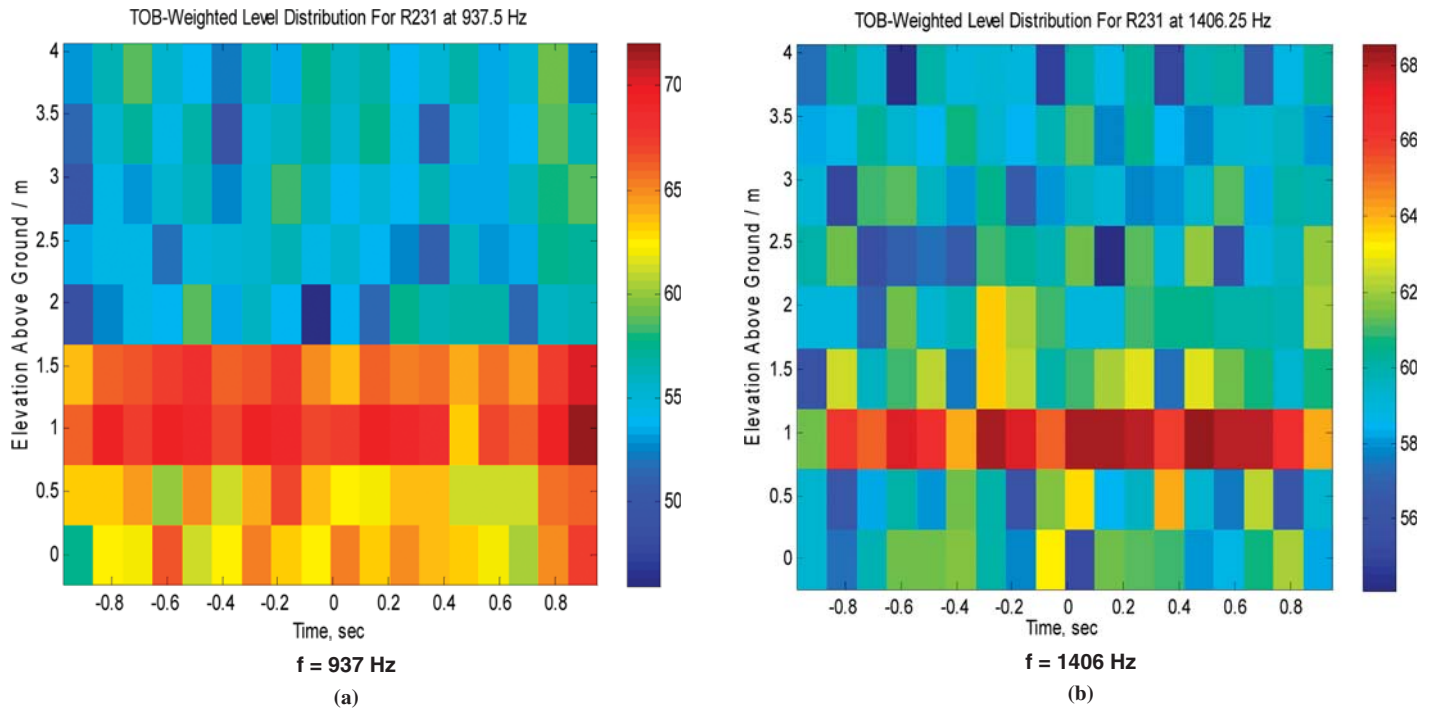
Figure 63. Vertical scan for the 4400 truck stationary, the engine at 2200 rpm, and the spherical source activated at frequency: (a) 937 Hz and (b) 1406 Hz. The time axis is in seconds relative to an arbitrary reference.
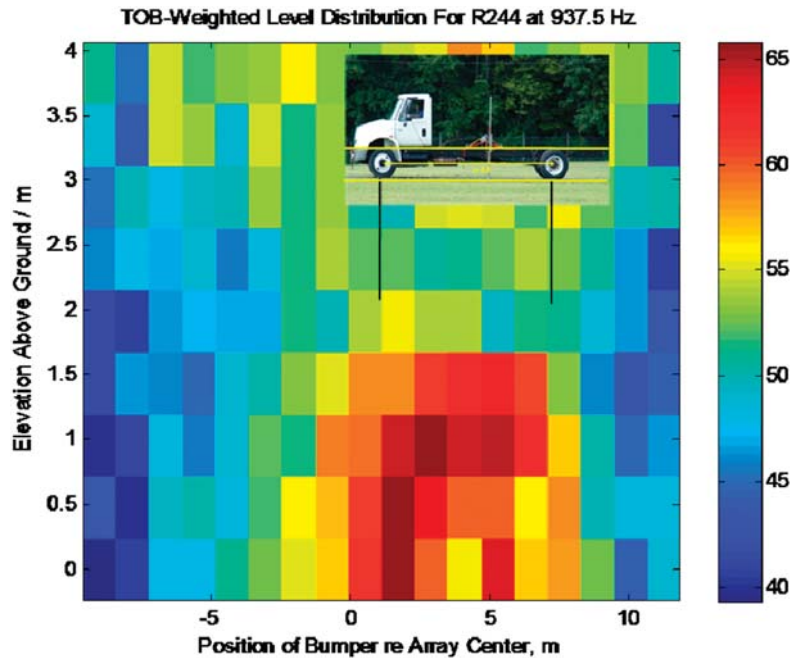
Figure 64. Vertical scan at 937 Hz for the 4400 truck passing to the right with the engine at 2200 rpm and the spherical source activated. The time axis is converted to bumper position relative to the array center. Truck photo is reversed on the horizontal scale with its ~6 m (20 ft) wheel base indicated. Vertical axis of the acoustic scan is expanded with the 1 m mark on the truck indicated with the line.

the time scale has been interpreted for the reader as position along the truck. (The scale has also been reversed, so the image is presented as if the truck were passing to the left.) This is done by taking advantage of the known translational velocity of the truck by which the bumper position is known at all times during the event. Thus as the truck passes, the array scans the truck. The horizontal scale can then be plotted as a horizontal position axis for which the reader has been oriented relative to the truck by the small photograph that has been sized to the horizontal scale of the color chart and positioned to reflect the position on the truck to which the array is "looking" for each horizontal pixel.

Consistent with Figure 45, Figure 64 shows higher levels between 1 and 5 m (3 and 16 ft) behind the front bumper and 1 m (3 ft) above ground. Figure 44 also shows sources in the vicinity of the wheel well and reflection that does not appear in Figure 45, probably due to effects of directivity at the time instant of this image. However, Figure 64 shows a distribution of sound sources in the forward extremity of the truck, because this depiction of the data gives the continuous complete map of the received sound versus time, regardless of directivity. Note that the depiction of the type shown in Figure 45 would show these other sources at another instant.

When the onboard spherical source is deactivated, its contribution disappears from the vertical scan. This phenomenon is illustrated in Figure 65 for which the corresponding image is given in Figure 46. Figure 64 is a combination of the distributions that are shown in Figures 63 and 65. Also, note that the sound source distribution for this low-speed passby is concentrated to the 1 m (3 ft) elevation from the surface of the road.
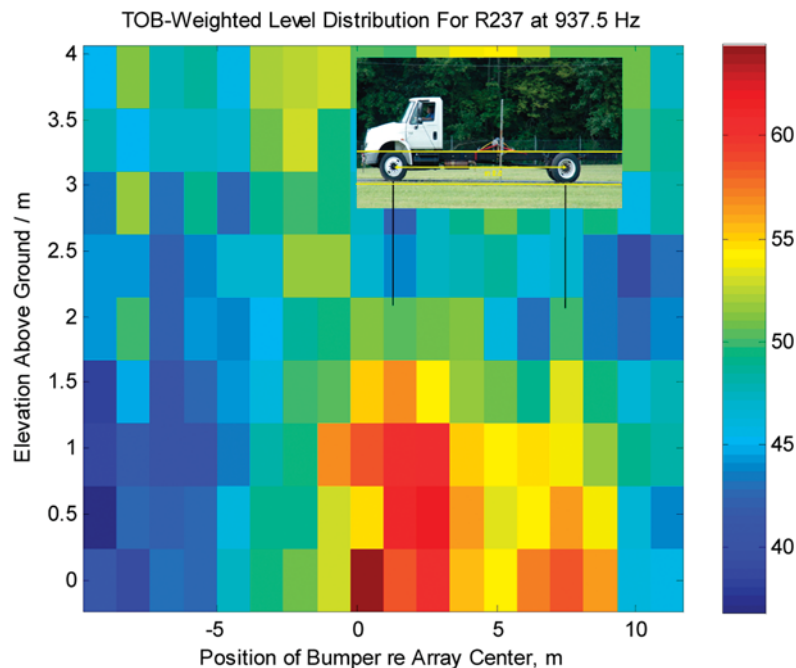
Figure 65. Vertical scan at 937 Hz for the 4400 truck passing to the right with the engine at 2200 rpm and the spherical source deactivated. The time axis is converted to bumper position relative to the array center. The truck photo is reversed on the horizontal scale with its ~6 m (20 ft) wheel base indicated. Vertical axis of the acoustic scan is expanded with the 1 m mark on the truck indicated with the line.

3.6 Roadside Testing

The beamforming noise mapping technique developed in this project and validated through the proof-of-concept testing as described in Sections 3.1 through 3.5 of this chapter was further applied to quantify noise sources for a wide range of trucks under actual road conditions. This second experimental task of the project was accomplished through the roadside truck noise measurements using the developed measurement system on an in-service highway. Four related issues are discussed in the following subsections: (1) microphone array modifications for the roadside testing, (2) modifications to the test data post-processing algorithm, (3) site selection for the roadside testing, and (4) roadside measurement setup. The roadside test results are presented and discussed in Section 3.7.

3.6.1 Microphone Array Modifications

The results of the proof-of-concept testing presented previously confirmed that the microphone array, data acquisition system, and beamforming software developed in the course of the study performed generally as expected and required no major adjustments. Based on the field experience obtained during the testing, certain improvements to the system were implemented prior to the roadside testing of the array to simplify its setup and tear down. A few minor modifications for the microphone array were necessary to speed up assembly of the array and improve handling of multiple microphone cables between the array and data acquisition system in the field.

For the previous proof-of-concept testing, individual 50 ft (15 m) long microphone cables were connected directly between the microphones and data acquisition system, as could be seen in Figure 10. While functional, that setup was laborious for the large number of microphones employed. To make setup more efficient, microphones at each of the three frame sections of the array were pre-wired with a cable junction panel, as shown in Figure 66 for the lower section. When mechanical assembly of the frame sections of the array was complete in the field, three cable bundles similar to professional audio cable snakes, also seen in Figure 66, were connected between the three junction panels and the data acquisition system. For measurements, the total frame and cable connections could now be set up in approximately 30 min compared to several hours previously.

The array dimensions and microphone locations remained unchanged from the design described in Section 3.3.1. Each of the 14 radial spokes had 5 microphones, and 7 additional microphones were mounted vertically in the center, such that the total of 77 microphones was used for the roadside testing. The microphone coordinates in the array are provided in Appendix A.
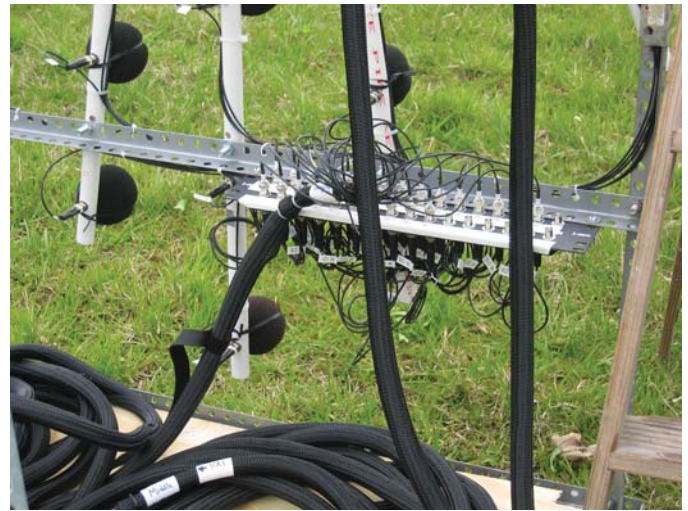
Figure 66. Microphone cable junction box.

3.6.2 Data Post-Processing Algorithm Modifications

The data analysis relies heavily on a time-gated FFT technique that provides a detailed frequency–time decomposition of the truck's sound levels and frequency content during its passby. The sound pressure spectra are measured in 1 Hz frequency bands evenly distributed from 0 Hz to the selected upper limit (generally taken to be 3000 Hz). Numerical efficiency and limitations on the processing time provide a constraint on the number of frequencies analyzed and the number of times for which spectra are calculated. This was discussed in detail in Section 3.5.4. For the earlier proof-of-concept tests, the settings were used that provided a frequency range from 0 to 3000 Hz in 64 steps for each of 15 to 20 time segments. The actual measurement bandwidth used at that time was about 47 Hz (3000/64) at all frequencies, with occasionally broader bandwidths. Once these spectra were obtained, using a simple arithmetic conversion formula the source levels were presented as equivalent A-weighted one-third octave band levels of sound pressure relative to 20 μPa at each indicated frequency. This was done to provide levels that could be compared approximately to classically processed one-third octave band levels, which were also collected during the passbys.

This use of approximate one-third octave band equivalents, though convenient, was not ideal because of its fundamental inability to accurately present one-third octave band levels that contain tones, such as tire tones. Thus, a wrapper code for use in batch-processing and saving the spectral files with frequency intervals much smaller than 47 Hz was developed for the analysis of the roadside recordings. Using a frequency range of 200 to 2500 Hz for the desired one-third octave band spectra, and the need for at least 3 frequency samples in each band, the number of digital frequency samples within the 0 to 3000 Hz

range was increased to 256. This increase brought the interval of frequency analysis down to 11.7 Hz, ensuring the existence of an adequate number of frequency samples in each one-third octave band used for array beamforming. A-weighting factors were then applied to each band sound level. To compensate for the increased sample time of the FFT processing, the number of ensembles for analysis was also reduced from that used earlier.

The additional code development in this second phase also provided the vertical distribution of the sound received at the array, to infer the vertical distribution of apparent sources above and below the road surface. The processing that was developed consisted of applying the array's beamformer algorithm to each truck passby, but with steering limited only to points directly in front of the array and steered to points along a vertical line extending both above and below the surface of the road. These vertical distributions are consistent with the two-dimensional beamformed images, as confirmed by evaluations of distributions with the loudspeaker source.

A network of codes provided a sequence of steps used in resolving the acoustic images of the passby: display the time records of the passby; truncate the record to roughly 2 s; develop the image functions at 11.7 Hz intervals; and calculate A-weighted one-third octave band levels of image values, reference microphone levels, and vertical distributions of source levels.

3.6.3 Test Site Selection

Five candidate sites, all on Maryland highways, were considered for the roadside truck noise measurements:

- I-70 rest stop north of Frederick
- US 15 near the Pennsylvania border, at a southbound rest stop (Mason-Dixon Discovery Center) near Emmitsburg
- US 301 near the Delaware border, at a side spot just south of Wilson Street/Strawberry Lane
- US 301 at MD 405 Price Station Road
- I-895 Harbor Tunnel Throughway in the vicinity of Halethorpe

All of the sites were visited prior to the testing, and their suitability for the measurements was evaluated. The following conditions were considered in this evaluation:

- Sufficient number of random traveling trucks in the range of 15 to 20 vehicles per hour, on average, to provide adequate time separation and discrimination among passbys.
- Sufficient space separation between the opposite directions of travel to minimize overlapping passbys and noise interference from the opposite traffic lanes.
- No road curvatures and no grades in the direction of travel that would cause vehicles to decelerate or accelerate.

- Adequate, accessible, and safe side spot or shoulder location for placing the microphone array at a distance of 20 ft (6 m) from the edge of the nearest driving lane, as well as for parking a minivan with the data acquisition system.
- The setup should be located on a flat surface at the road elevation, with no buildings or other reflective surfaces behind.

Based upon the site review and evaluation, the site on US 301 at MD 405 Price Station Road was selected for the roadside testing as meeting all of the criteria. At this location, the opposite directions of travel on the four-lane highway split forming a wide median with trees, while the northbound lanes remain straight, generally flat, and provide a wide, paved turning lane with a shoulder convenient for the measurement array installation. The road pavement in the vicinity of the site was dense-graded asphaltic concrete (DGAC). The posted speed limit at the site was 55 mph.

3.6.4 Roadside Measurement Setup

The microphone array sections with pre-assembled microphones, the data acquisition system, and other equipment were transported in a minivan to the US 301 site selected for the testing on April 9, 2008. The array was assembled in the field and placed on a shoulder at a distance of 20 ft (6 m) from the edge of the nearest northbound driving lane. The data acquisition system was located in the minivan. The overall measurement setup is shown in Figure 67.

Each measurement channel of the system was calibrated using a Brüel and Kjær Type 4231 acoustic calibrator. To track a vehicle and determine its speed at the test site, the same two photocells that were used for the proof-of-concept testing were again installed on tripods near the microphone array, with their signals fed into the data acquisition system. Still photographs of vehicles passing the array were taken in order to later relate the vehicle geometry to the sound distribution images. The measurement session was recorded with a video camera for later references as necessary. The results of these measurements are presented and discussed in the next section.

Figure 67. Roadside measurement setup.

3.7 Results of Roadside Measurements

For initial check-out of the array performance and calibration of the test site geometry, a short test was performed first using a stationary loudspeaker. After this initial test, the actual truck passbys were measured using the microphone array and data acquisition system. In the following subsections, roadside test results are presented and discussed in three categories: (1) calibration of the test site geometry using imaging tests performed with the loudspeaker source; (2) acoustic image and noise source distribution results of the vehicle passbys; and (3) example of truck source modeling for simulating noise propagation.

3.7.1 Calibration of the Test Site Geometry

A loudspeaker source, Mackie Model SRM450, was used to calibrate the positioning alignment of the array relative to the road surface in the path of the trucks in the near lane of the highway. The source was mounted on a tripod and the assembly was located on the roadway with its center approximately at the expected wheel path of the closest side of the trucks at a height of 4.5 ft (1.4 m) above the road surface. This test was performed during a short break in the traffic, just prior to the commencement of truck measurements. Noise from a pink noise generator was played through the speaker at a high volume for the test. Figure 68 shows acoustic images of the speaker obtained at frequencies of approximately 270, 1000, and 2000 Hz. In these plots, a small offset to the vertical coordinate [about 0.27 m (0.9 ft)] was provided to compensate for misalignment of the array acoustic plane with the road surface and road crowning. This offset is not (and obviously should not be) a function of time or of frequency. Note the presence of the ground-reflected image source with the sound

level slightly less than the direct path image, especially as frequency increases. The reflected image of the source is below ground and is 1 to 2 dB lower in level than the direct image. This suggests a reflection coefficient of 0.8, which is comparable to that apparent in the proof-of-concept measurements earlier in the study. Overall, the measurement system performed as expected and was adequate for conducting the roadside truck measurements.

As noted previously, one of the extensions made to the processing was to provide vertical source distributions. Figures 69 to 71 provide vertical profiles of the sound source distributions at frequencies 250, 1000, and 2000 Hz, respectively. In these figures on the left-hand side is a level distribution of the stationary source over a 1.3 s time interval, which demonstrates the (expected) invariance of the sound profile with time for each frequency. On the right-hand side is a line plot of the A-weighted sound level vertical profile at one of the time increments. Comparison of Figures 68 through 71 illustrates the duality of the source two-dimensional imaging and the vertical distributions in localizing the noise sources.

3.7.2 Image Results of the Vehicle Passbys

Of 100 truck passbys recorded in a single day of data acquisition, passbys for 59 heavy trucks and 4 medium trucks were analyzed and are discussed here for the definition of source levels. Because the objective was to interpret source level images and vertical distributions of the sources, the following requirements were necessary for a passby to be analyzed: the vehicle in the curb lane, significant time–space separation between passby vehicles to allow for distinct one-to-one vehicle–passby identification, a photograph of the vehicle, and nearly constant vehicle speed. The remaining 37 passbys were also acoustically viable as recorded passby data, but they could not be examined in detail because at least one of the required characteristics for
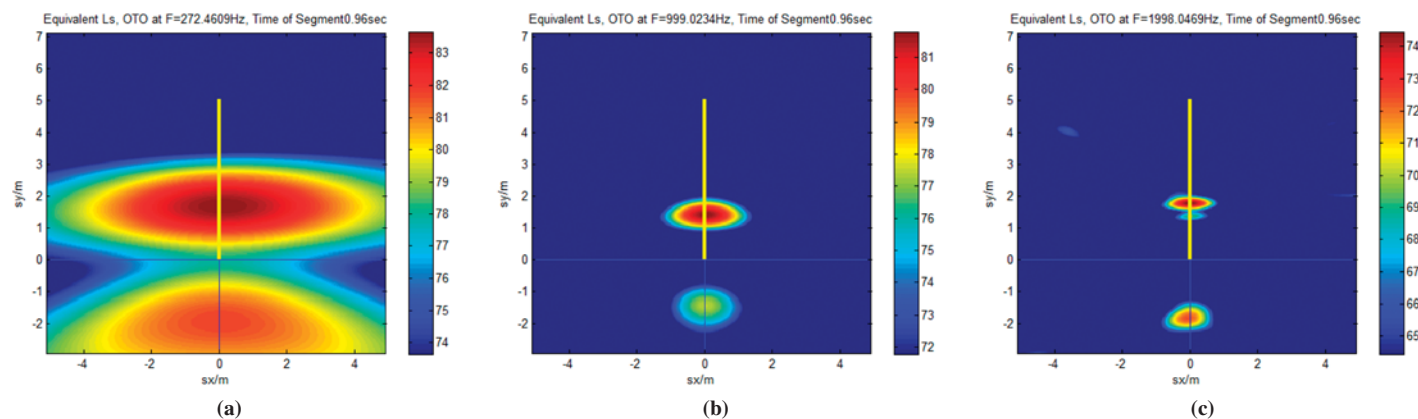
Figure 68. Images of the loudspeaker positioned on the roadway at the test site for frequencies of (a) 270 Hz, (b) 1000 Hz, and (c) 2000 Hz.
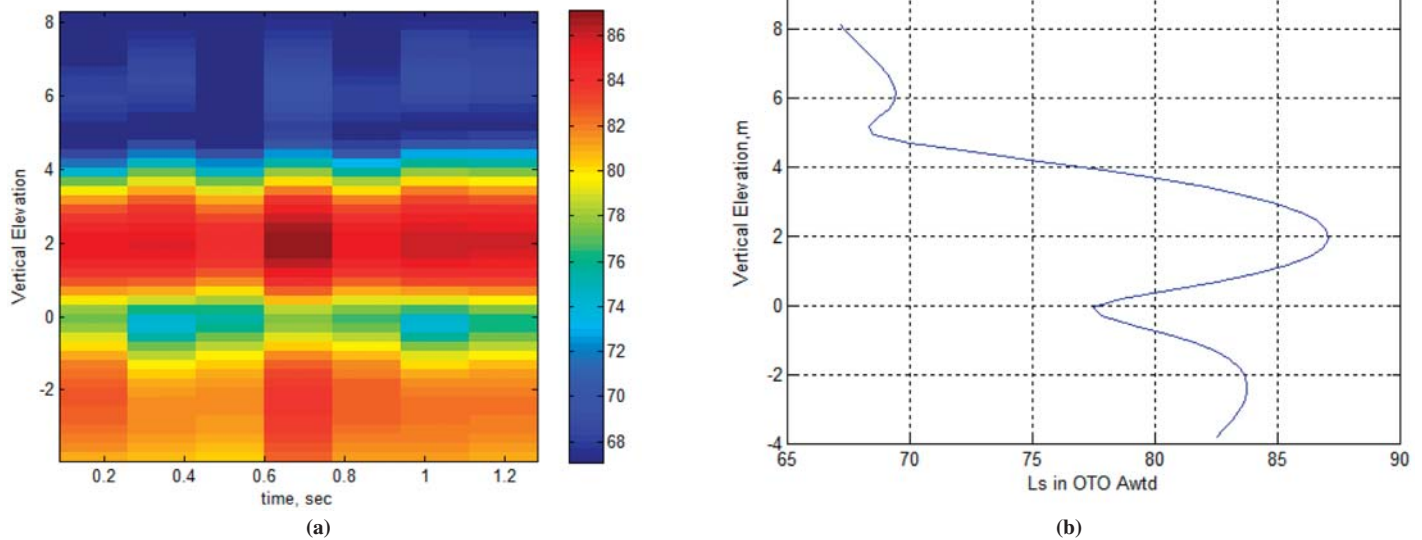
Figure 69. *Calibration source, vertical scan at 250 Hz: (a) time–level distribution; (b) line plot at 0.62 s.*

complete analysis was missing or they were tractors with atypical trailers (boat or car haulers, wide-load modular houses, etc.). Acoustic source maps obtained during truck passbys were then used to provide time histories and spatial distributions of sources and source paths from the engine, exhaust, tires, and certain body components. Individual vehicle speed during passbys varied from 55 to 70 mph (88 to 112 km/h).

The total sets of 59 heavy truck passbys and 4 medium truck passbys (to a much lesser extent) provide ensembles of sound levels by vehicle, one-third octave frequency band, time, and vertical position. These profiles can be used to define maximum levels, mean levels, and sound exposure levels—all across the ensembles of trucks. The roadside setup geometry used for these measurements followed that used for the proof-of-concept tests, with improvements in the timing of the truck position relative to the center of the array in order to reduce positioning error. For this, two photocells were positioned at distances 5 ft (1.5 m) before and 20 ft (6 m) after the array
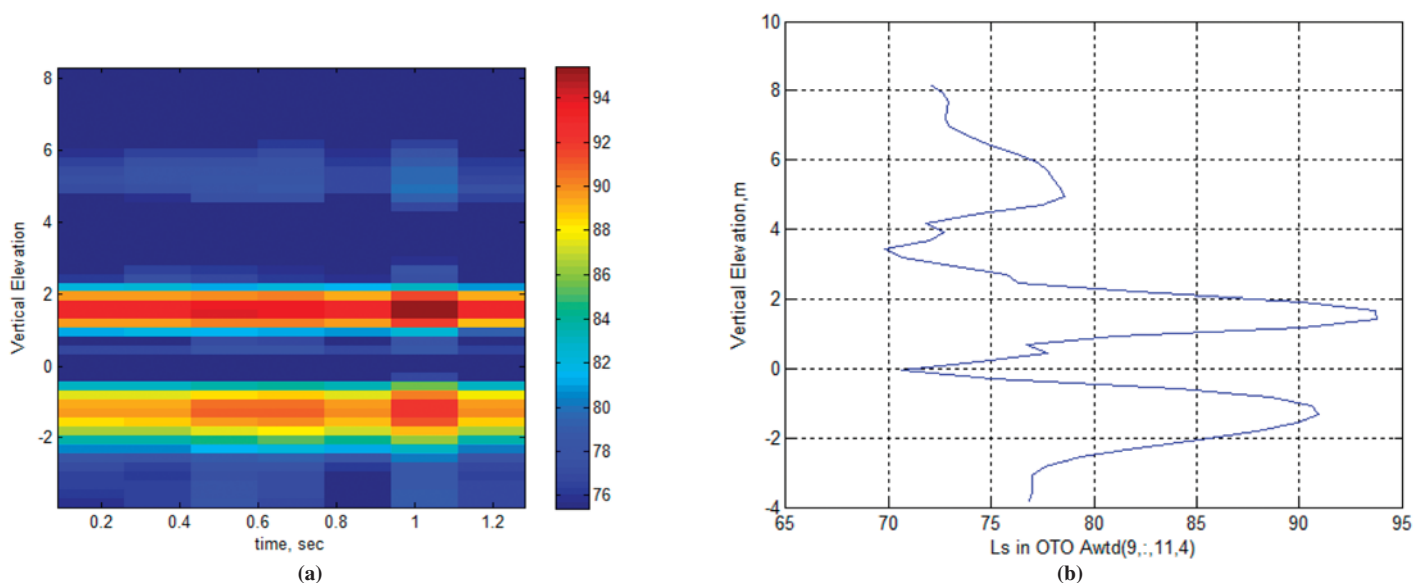
Figure 70. *Calibration source, vertical scan at 1000 Hz: (a) time–level distribution; (b) line plot at 0.62 s.*
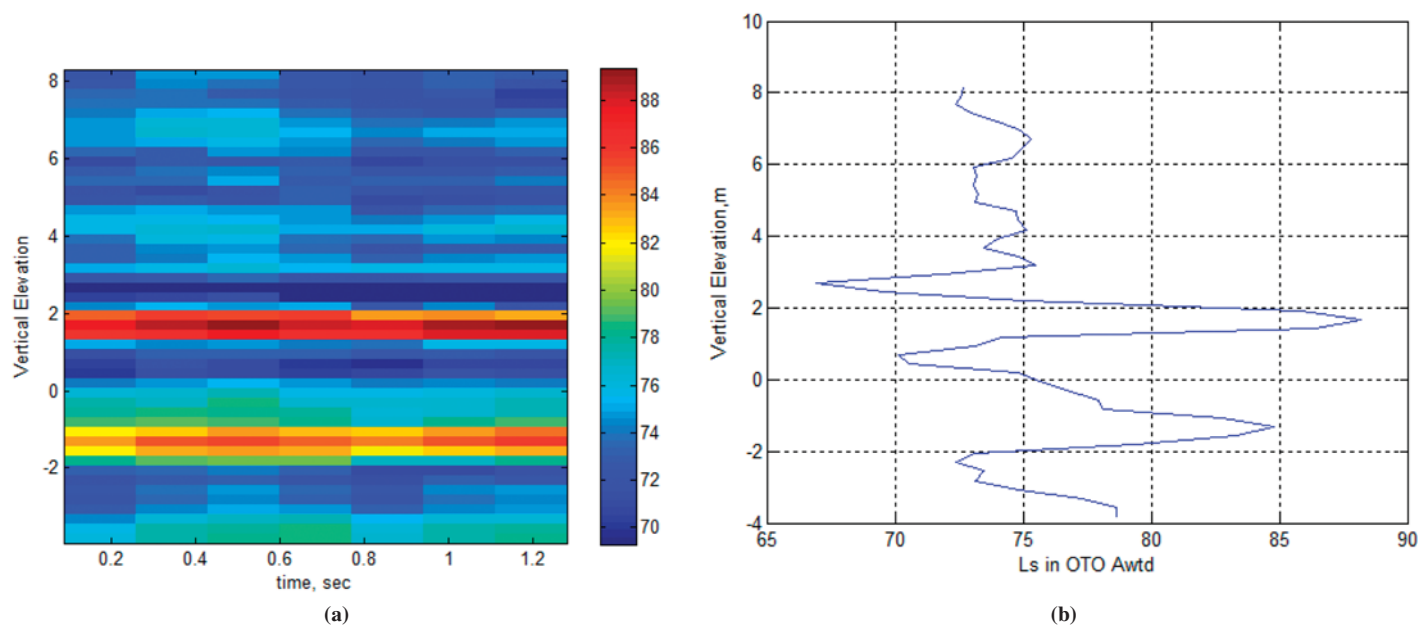
Figure 71. Calibration source, vertical scan at 2000 Hz: (a) time–level distribution; (b) line plot at 0.62 s.

center. The positions of the photocells and array relative to the test track were the same as illustrated in Figures 50 and 51. In the dimensions used at the highway site, the length of the truck as it intermittently cuts the photocell beam is shown by the total length of its signal. Figure 72 shows an example from roadside case 60, which is a heavy truck. The front bumper is again taken for all runs as the reference point on the truck, so that the maximum sound occurs slightly later (typically about 0.06 s for this highway speed limit) than the bumper passage by the array center. The data processing, including the distance correction for equalizing the passby levels and the Doppler shift for frequency correction, is described in Sections 3.5.4.1 and 3.6 and requires these time-accurate truck coordinates. Components of the signal alignment and truncation as relevant to time-synchronizing the time–frequency spectrogram and the photograph of the truck 60 are shown in the figure. The upper traces include the first photocell signal (red), the second photocell signal (green), and the signal from the reference microphone in the array (blue). The truck passing at 58 mph (93 km/h) is positioned so that its bumper is at the first photocell. The size of the truck photograph is determined by the speed and the known spacing between the red cones [7.3 m (24 ft)]. The spectrogram is taken approximately every 0.05 s with the 87 Hz frequency intervals. Clearly seen is the correspondence between instances of high sound levels at multiples of approximately 450 Hz that are due to the tires, although high background levels are also seen below 200 Hz.

Figure 73 shows the distribution of the one-third octave band A-weighted spectra for all 59 heavy trucks. Each spectrum is measured with the single reference microphone stationed at the array distance [20 ft (6 m)] and at height of 1.9 m (6 ft)

above the road grade at the time of the maximum overall A-weighted sound level (OASPL) for each truck. The dotted black lines indicate the statistical maximum and minimum levels, and the bold solid black line indicates the mean level across the selected truck population. Truck 60 is also shown for reference, as it is a typical truck with sound levels near the mean of the population. All of the individual trucks are not identified here, but their levels are all shown to indicate the distribution of levels within the population. More discussion of the distribution will be presented below. Note that a commonly occurring spectral feature is the pair of 500 and 1000 Hz peaks, likely due to tire noise (see also Figure 72).

Figure 74 shows the spectra for the four medium trucks in the data set. Again, the prominent 500 and 1000 Hz peaks are present. These spectra are all measured with the single reference microphone stationed at the array distance [20 ft (6 m)] and at height of 1.9 m (6 ft) above the road grade at the time of maximum level for each truck. Although the population is too small for generalization, the levels are slightly lower than for the heavy truck mean levels.

That the sound from the typical truck is due to tire noise is emphasized in Figure 75, which shows a full set of images for the one-third octave frequency bands from 315 to 2000 Hz obtained for truck 60. Each point spread function is shown in the upper left corner with the same scale as in the main image. Though the number legends for these are unreadable, they act as tic marks that correlate with the main figure. The color bar provides a relative 10 dB scale for which the reference value is approximately the red dot level for truck 60 in Figure 73. Note that the tractor drive-axle tires and the trailer tires are both contributing, but prevail in different frequency bands.

58
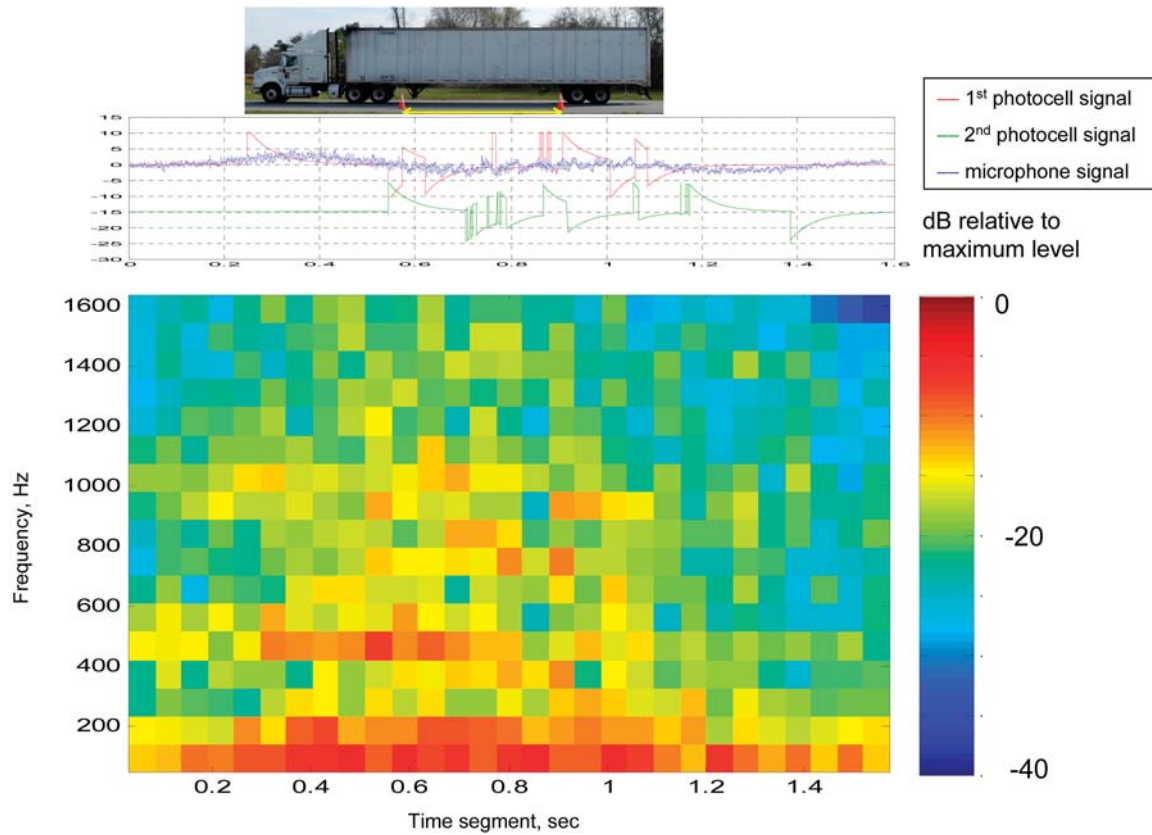
Figure 72. Signal alignment and acoustic spectrogram with the photograph of truck 60.
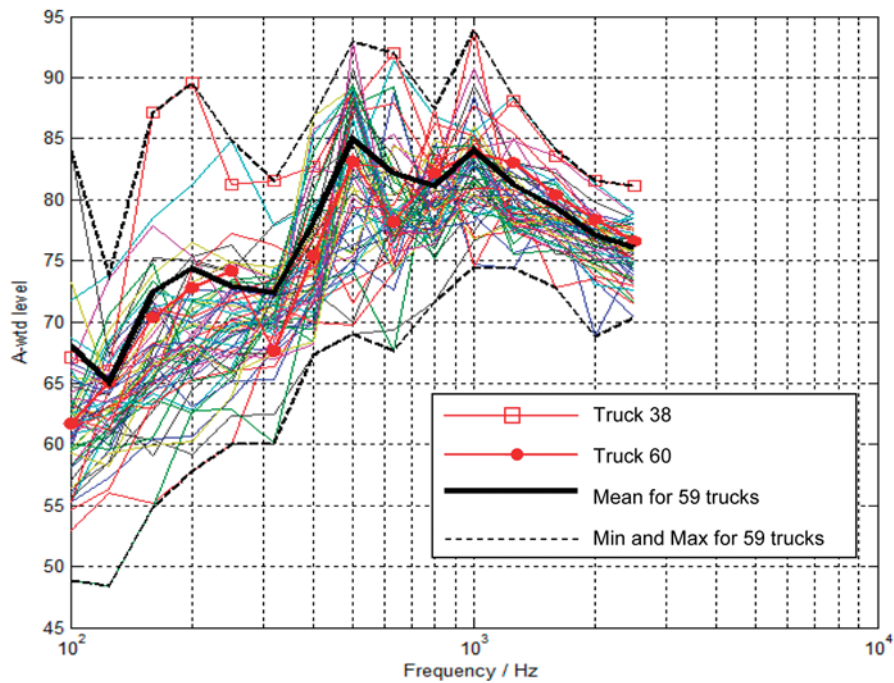
*Figure 73. One-third octave band sound spectra (in dBA)
for 59 heavy trucks.*
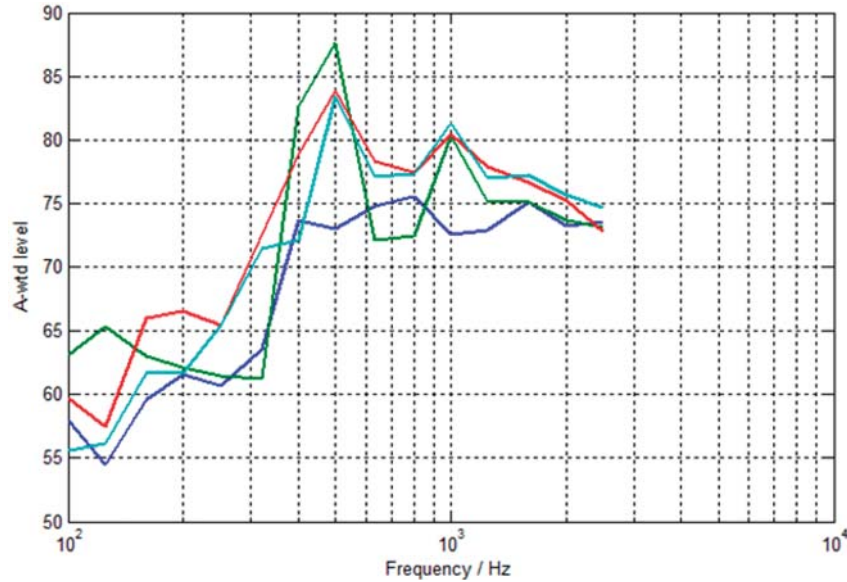
Figure 74. One-third octave band sound spectra (in dBA) for four medium trucks.

This phenomenon suggests that different tire patterns were used on the tractor and trailer of this truck. All nine of these images were made for the same computer settings of the array's spatial scanning, so any biases in sound level equalization for distance correction are the same for all frequencies. Thus, the frequency-to-frequency relative comparisons in this figure are valid.

The vertical distribution of sound sources at the nearest truck's side plane can now be assessed in various ways. One way is to examine the vertical profiles of source sound levels at 6 m (20 ft) reference distance for the mean values of all heavy trucks. Figure 76 shows the source height distributions of the mean A-weighted one-third octave band levels for each band from 100 to 2500 Hz and for the mean OASPL. As discussed in Section 3.6.2, these distributions are obtained by mathematically focusing the array at a sequence of vertical positions above and below the road surface directly in front of the array. The sound levels are determined at the instant of the maximum OASPL passby level at the reference microphone for each truck, and are evaluated by the microphone array at that instant for each truck. The mean levels for each frequency band and steering elevation over all trucks are then evaluated and plotted in the figure.

It is clear from Figure 76 that the vertical distribution for the average truck sound level is dominated by sources between −1 and +1.5 m (−3 and +5 ft). This distribution holds for the frequencies above 315 Hz. Below 200 Hz, although the vertical beam width is larger for the array, the source distribution seems to drift upwards. Comparison with the images of Figure 75 confirms that the tire sound sources are positioned just above the road surface.

Figure 77 shows the measured vertical source distributions for three individual trucks. These distributions compare reasonably well with those obtained in the Caltrans study (*30, 31*). To illustrate this comparison, Figure 78 reproduces Figure 8 from Donavan et al. (*30*). The level distributions are similar in shape, although those in Figure 78 show the maximum levels at or slightly below the road surface, while in Figure 77 the maximum levels occur at or slightly above the road surface. This discrepancy is caused by an uncertainty in calibrating the position of the array's acoustic axis relative to the ground plane. It is expected that the certainty with which the ground plane can be accurately established from either set of data is within about 0.2 m (0.6 ft). Some contributors to this uncertainty include the distance to the actual sources versus the beamforming analysis plane, the size and directivity of the calibration loudspeaker, the frequency-dependent reflection coefficient for the path of reflected sound between the sources and the array, and the precision with which the array can be aligned because the relative tilt angle of the array and the inclination of the road crown could not be measured. This 0.2 m uncertainty is equivalent to effective acoustic inclination error of less than 2 degrees. The resolution of this discrepancy may become the subject of a separate follow-up study.

The statistical distributions of the sound levels measured across the population of heavy trucks are provided in the form of histograms in Figure 79 for the OASPL at the reference microphone and at the 0.4 m (1.3 ft) height for the one-third octave frequency bands centered at 500, 1000, and 2000 Hz. All of these levels were recorded at the time of maximum OASPL for each truck. The data for these histograms and for Figure 73 discussed previously are the same. The breadth of
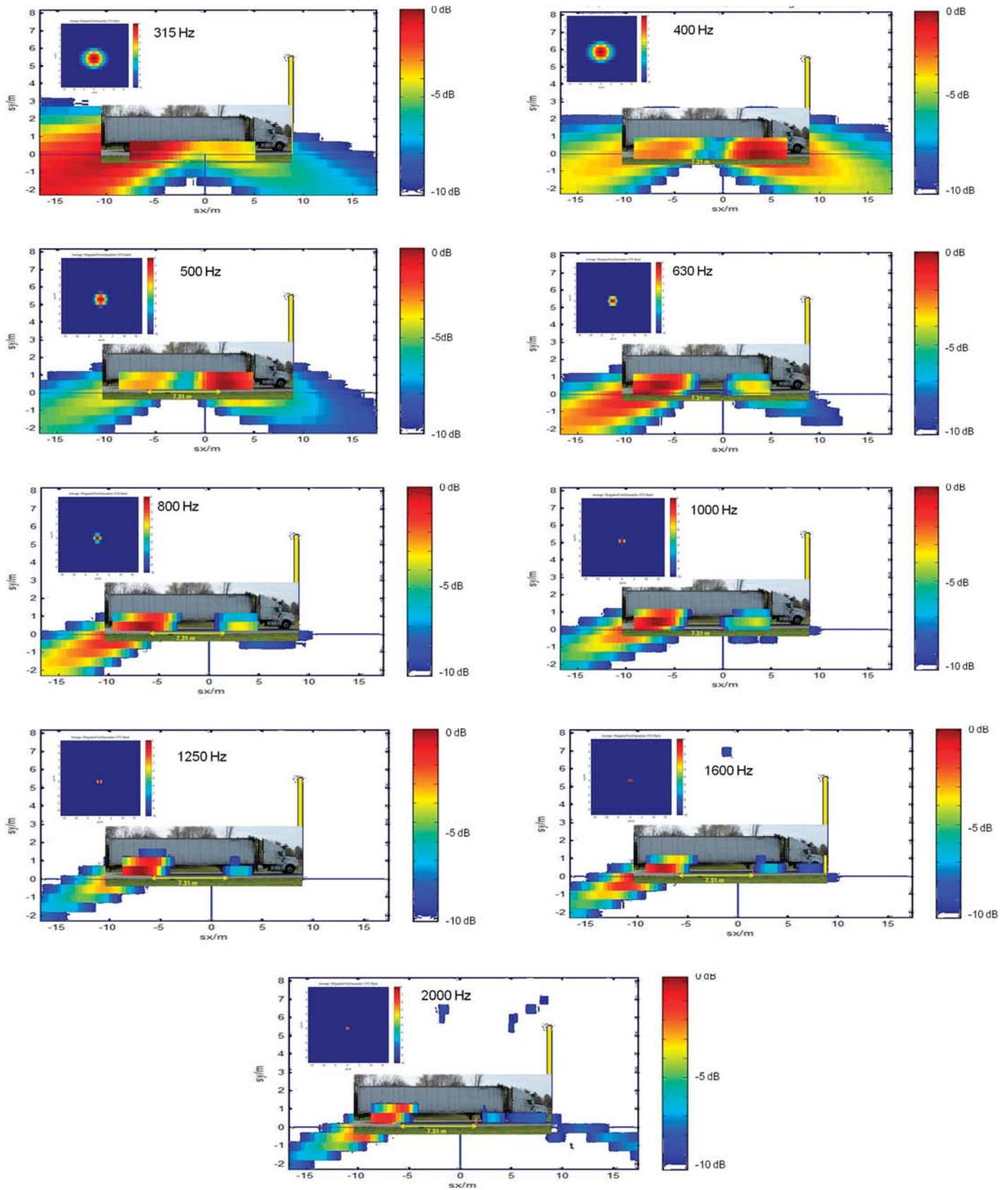
Figure 75. Source image maps of truck 60 for one-third octave frequency bands from 315 through 2000 Hz.
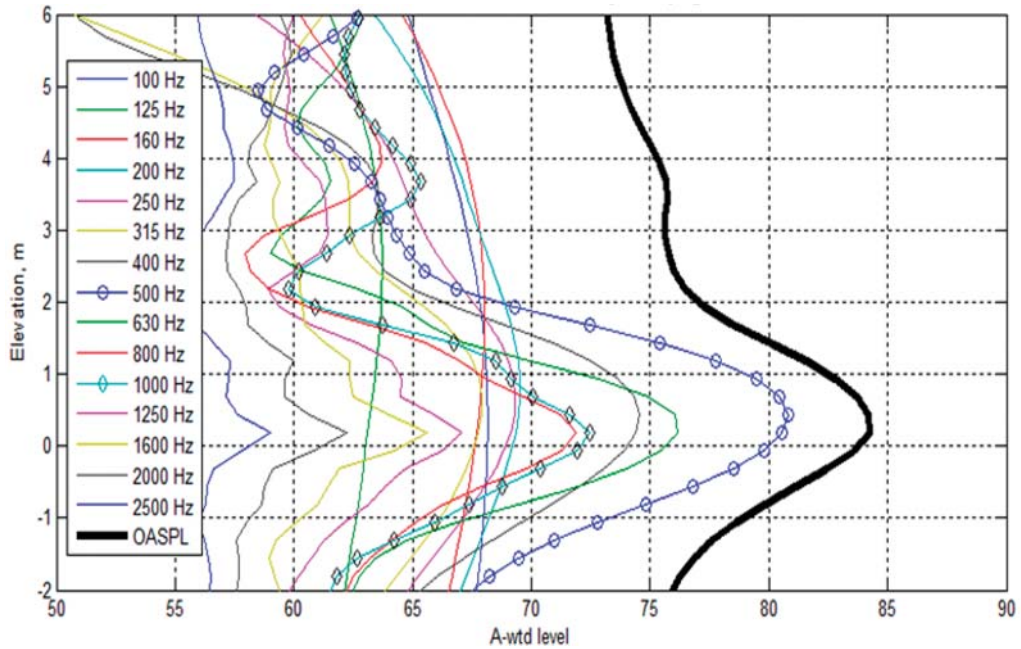
Figure 76. Vertical distributions for mean one-third octave band and overall A-weighted sound levels (in dBA) for 59 heavy trucks.
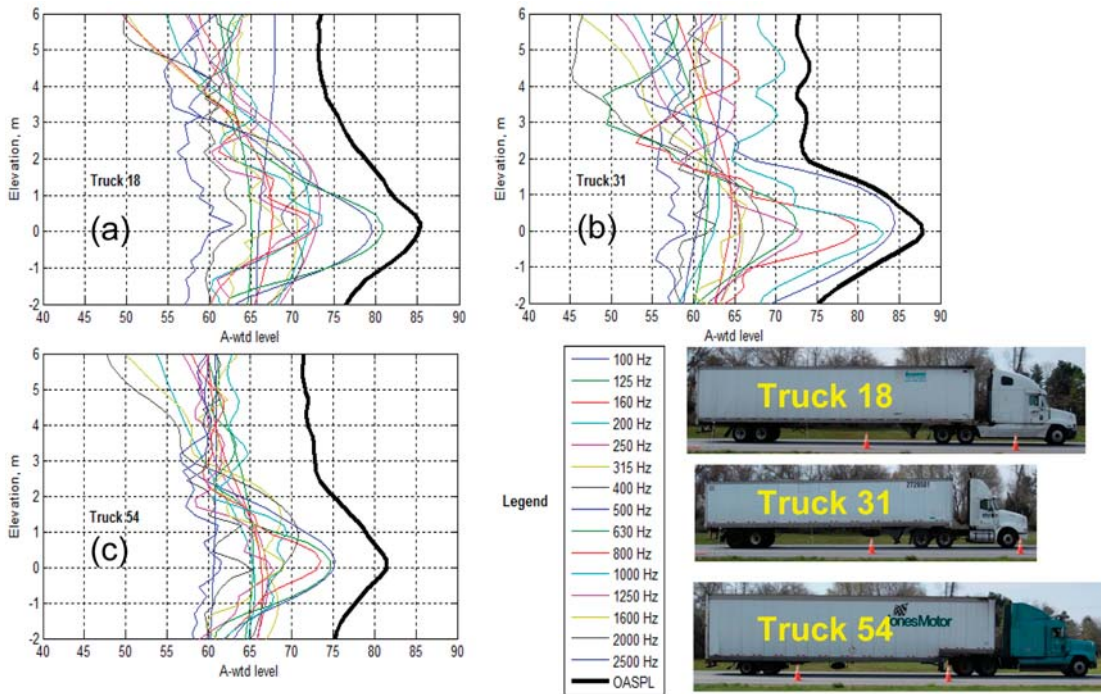
Figure 77. Vertical distributions for one-third octave band and overall A-weighted sound levels (in dBA) for individual heavy trucks (truck images are to the same scale): (a) truck 18, (b) truck 31, and (c) truck 54.
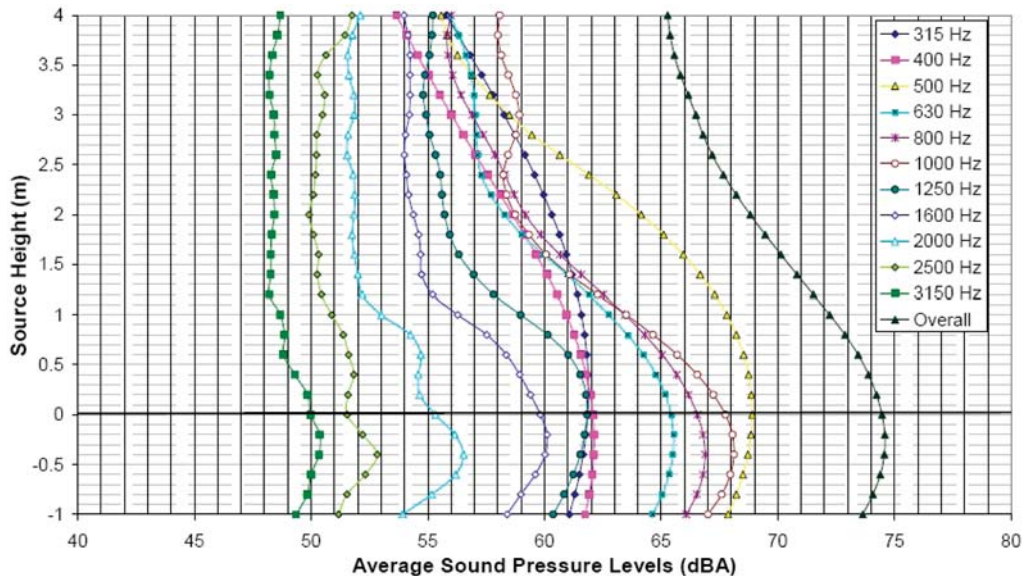
Figure 78. Vertical distributions for one-third octave band and overall A-weighted sound levels for an example truck at the Lakeview site, CA [from Donavan et al. (30, Fig. 8)].
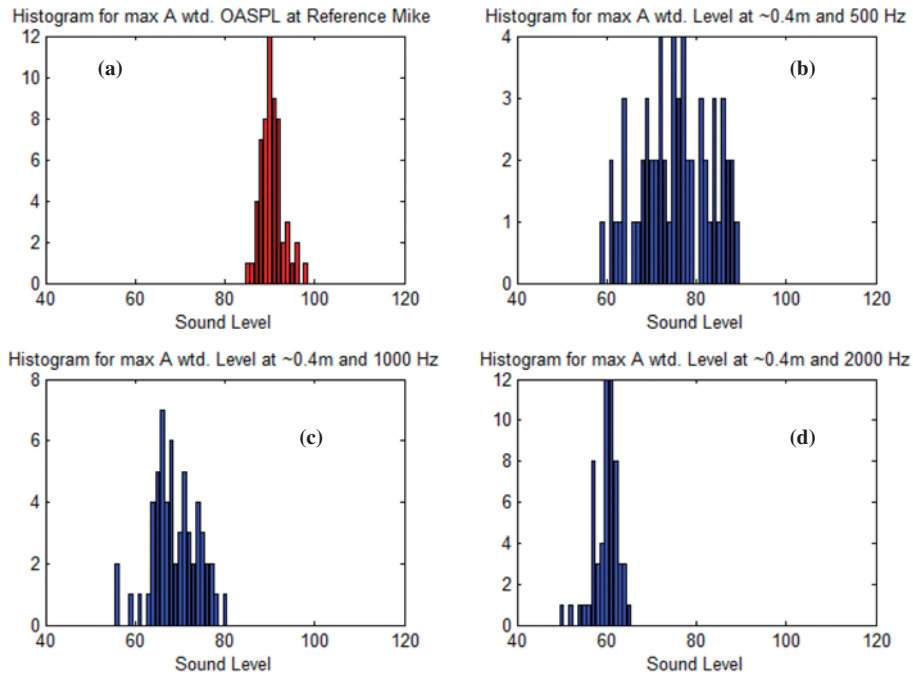
Figure 79. Statistical distributions of the (a) overall sound levels and one-third octave band sound pressure levels (in dBA) at (b) 500 Hz, (c) 1000 Hz, and (d) 2000 Hz for 59 heavy trucks.

the sound level distribution shown in Figure 79 is identical to that shown in Figure 73 at the corresponding frequencies. The larger spread at 500 Hz is due to the variation of levels in this band apparent in both figures.

Other examinations of the vertical distributions of sound sources are also possible. Figure 80 shows the vertical distribution of the highest sound levels among the 59 heavy truck passbys in each one-third octave frequency band and for each elevation. These distributions identify the levels for the noisiest truck at each vertical position. The levels are determined at the instant of the maximum OASPL at the reference microphone for each truck and evaluated by the microphone array at that instant for each truck; then the maximum levels at each frequency and steering elevation for all trucks are evaluated. Note that these distributions are for statistical maxima and do not represent levels from any individual truck sample. A modest increase of approximately 8 dBA can be seen in the near-road sources at 500 Hz due to tire variations. A significant increase in sound levels at elevations of 3 to 4 m (10 to 13 ft) is also noticeable. It is shown later in this section that the latter increase correlates well with the truck source images localized at the vertical exhaust position.

In a similar manner, Figure 81 shows the vertical distribution of the 1 s sound exposure levels (SELs). The levels are determined at the instant of the maximum OASPL at the reference microphone for each truck and evaluated by the microphone array at that instant for each truck. Then the maximum A-weighted SELs are determined for each one-third octave

frequency band and steering elevation for all of the trucks. These distributions also show the expected dominance by sound sources located near the road surface.

Figures 82 through 84 show the same types of vertical distributions for the four medium trucks measured during the roadside testing. Although this small sample does not form a statistically significant population, these results are included here for completeness and to indicate the similar general distributions as obtained for the heavy trucks. For each figure, the sound levels are determined at the instant of the maximum OASPL at the reference microphone for each medium truck and are evaluated by the microphone array at that instant for each truck; then the mean levels, the highest levels, and the maximum 1 s SELs, respectively, are determined for each one-third octave frequency band and steering elevation for all four medium trucks. The absence of sound sources at the 2 to 4 m (6.5 to 13 ft) elevations may be due to a lack of samples in the population, but it also is likely due to the absence of vertical exhaust stacks on these trucks.

As previously noted, the vertical distribution of the sound sources has its highest levels near the surface of the road, which dominate the levels for the average truck. The maximum levels during heavy truck passbys also appear to have significant components at elevations between 2 and 4 m (6.5 to 13 ft). Figure 85 shows the vertical distributions of OASPL for the 59 heavy trucks. In the following paragraphs, a few representative truck passbys are discussed further in more detail. Truck 60 is a typical truck with the sound spectrum near the mean of
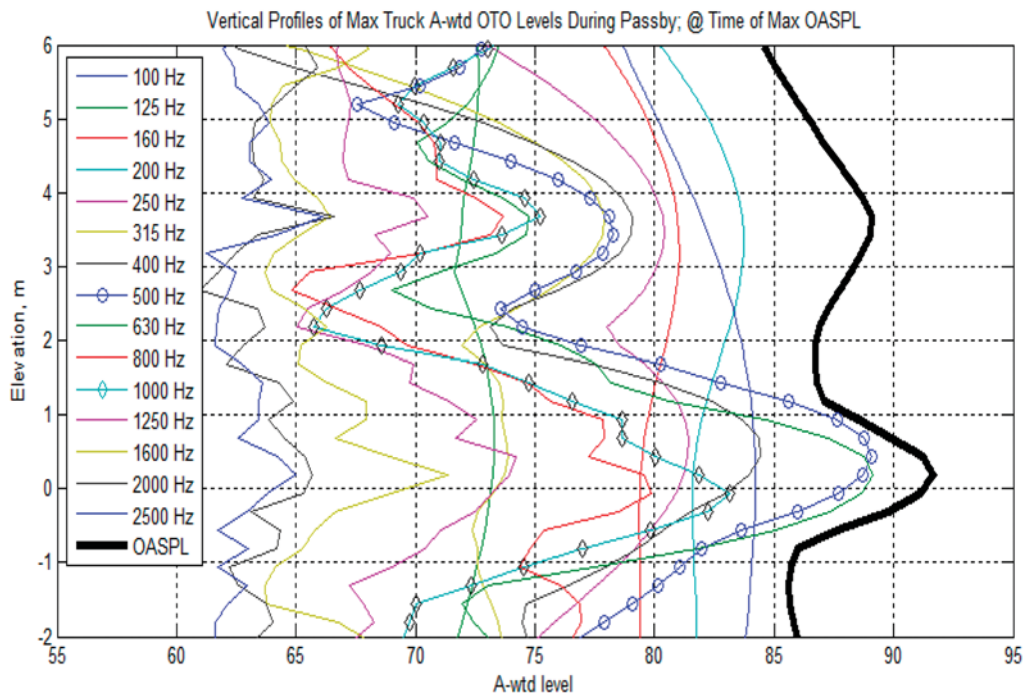
Figure 80. Vertical distributions of highest A-weighted sound levels in one-third octave bands and of overall sound level (in dBA) for 59 heavy trucks.
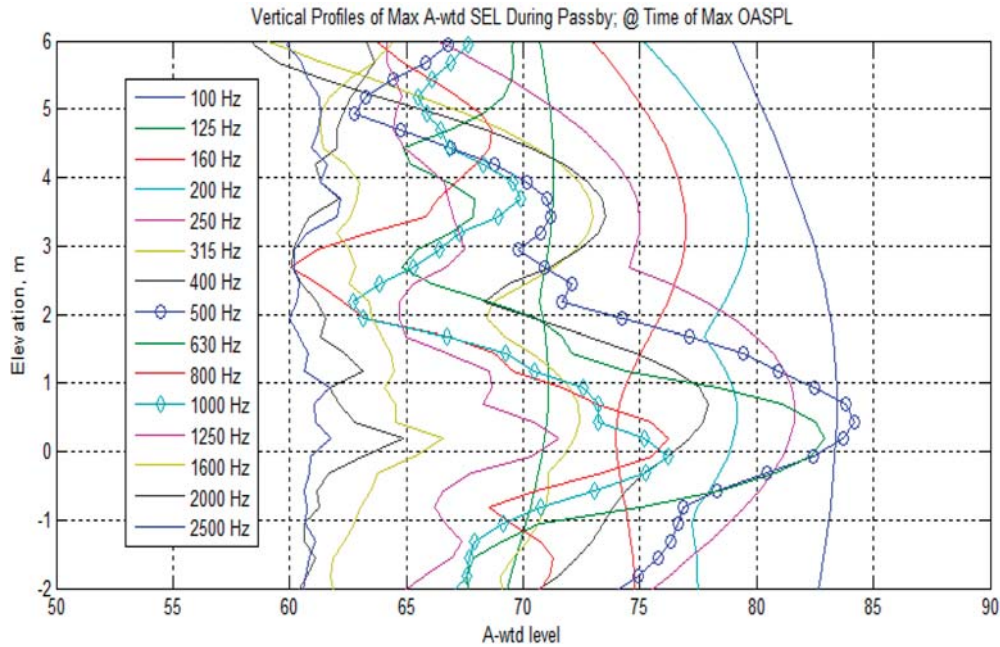
Figure 81. Vertical distributions of maximum 1 s sound exposure levels (in dBA) in one-third octave bands for 59 heavy trucks.

the heavy truck population. Earlier in this section (see discussion of Figure 75), the tires on truck 60 were identified as the primary sound originators. Truck 15 is representative of the maximum sound levels, and the image in Figure 86 for this truck also clearly identifies the tires on the tandem trailers as the source originators.

Trucks 38 and 50 are uniquely relevant to the low-frequency sound levels. Note the identification of the sound spectrum for truck 38 in Figure 73, which dominates the level maxima for the population. Truck 38 is a three-axle dump truck that produced both exhaust tones and tire tones over the frequency range. The bold red line in Figure 85 shows two maxima in the vertical OASPL distribution at the elevations of about 0.4 and 3.6 m for this truck. Figure 87 shows the acoustic images of this truck in various frequency bands. As can be seen in the figure, near the road surface the tire noise
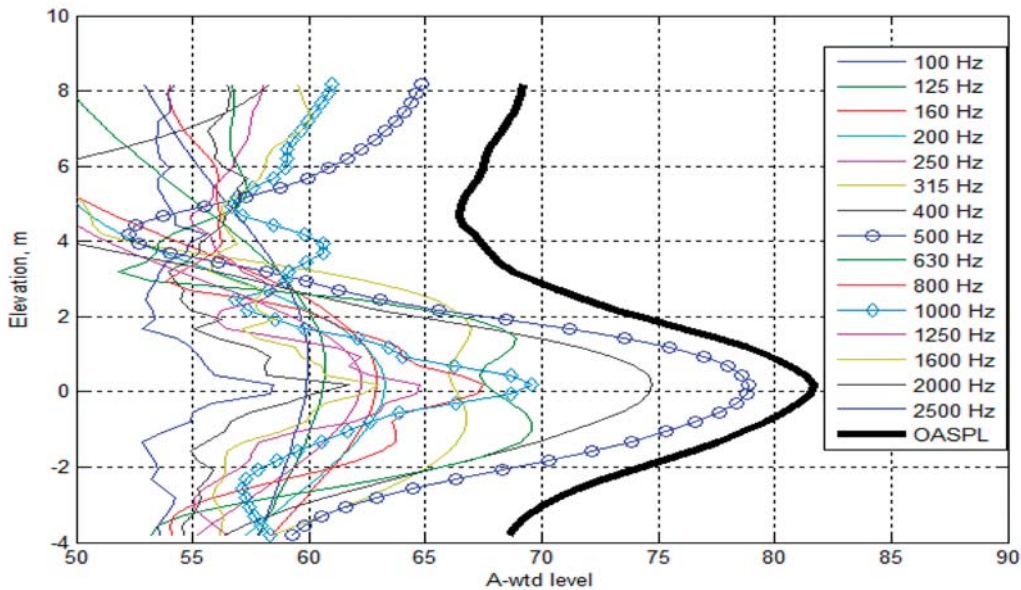
Figure 82. Vertical distributions for mean one-third octave band and overall A-weighted sound levels (in dBA) for four medium trucks.
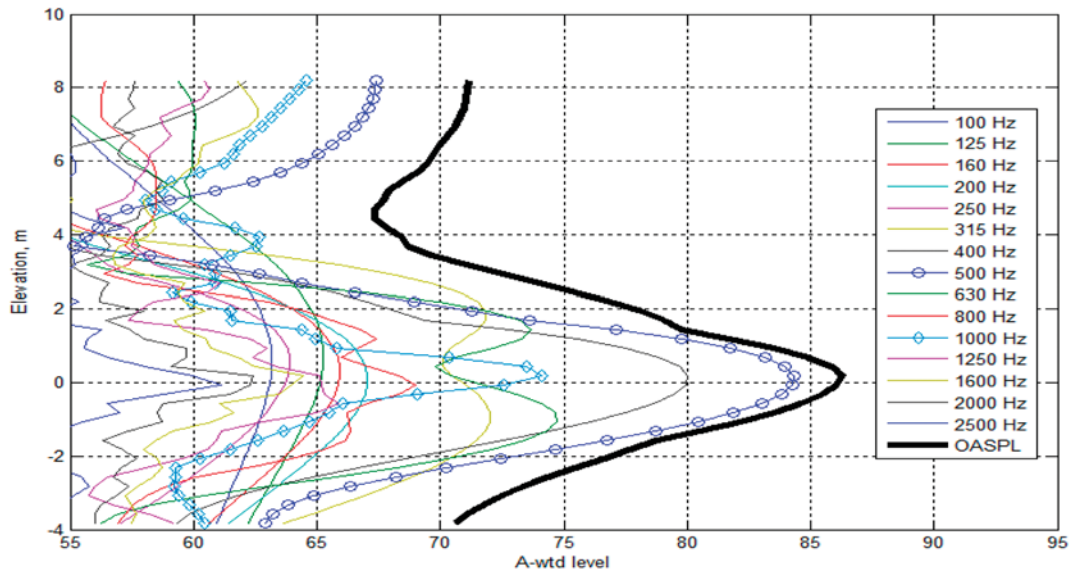
Figure 83. Vertical distributions of highest A-weighted sound levels in one-third octave bands and of overall sound level (in dBA) for four medium trucks.

dominated at higher frequencies (630 and 1250 Hz in this figure), but at lower frequencies (250 Hz) the noise source at the vertical exhaust was predominant for truck 38. Similarly, truck 50 also produced exhaust noise at an elevation of nearly 4 m, as illustrated by the bold magenta line in Figure 85 and the acoustic images of the truck in Figure 88. Similar data analysis for trucks 13 and 57 indicated that the exhaust noise appears to be prominent at frequencies below 500 Hz, and the tire noise near the road surface appears to be prominent at higher frequencies. In all these cases, the exhaust noise determines the source levels at the elevation between 3.5 and 4 m above the road surface. The mean sound levels for the total heavy truck population appear to be minimally influenced by the exhaust noise sources; however, the maximum sound
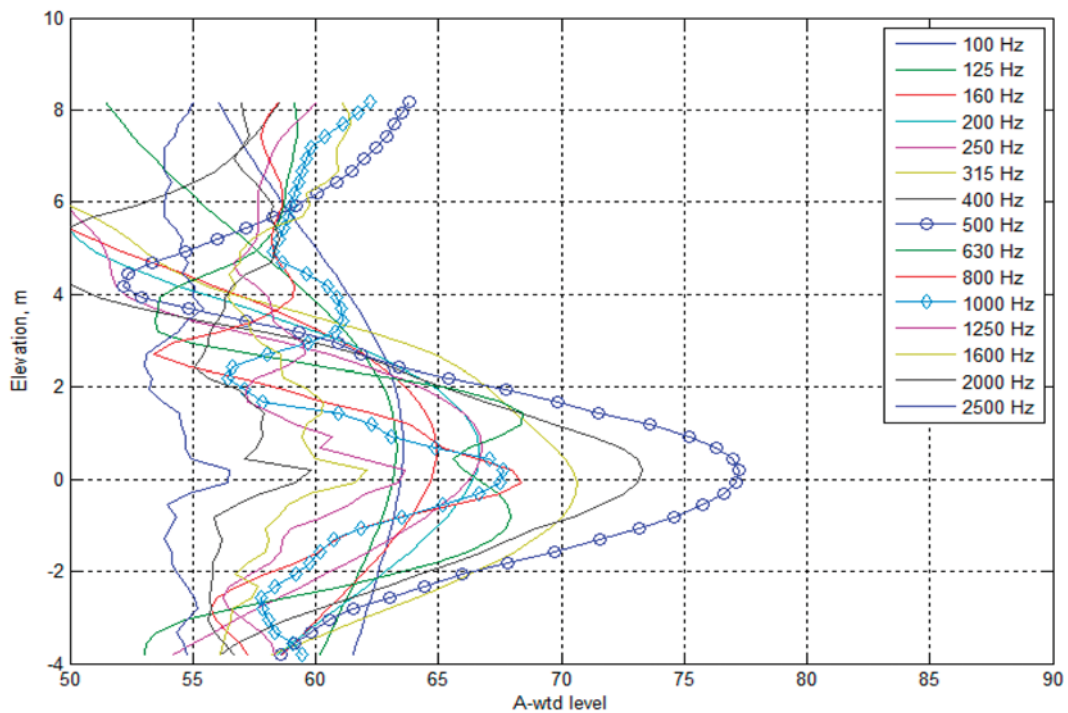
Figure 84. Vertical distributions of maximum 1 s sound exposure levels (in dBA) in one-third octave bands for four medium trucks.
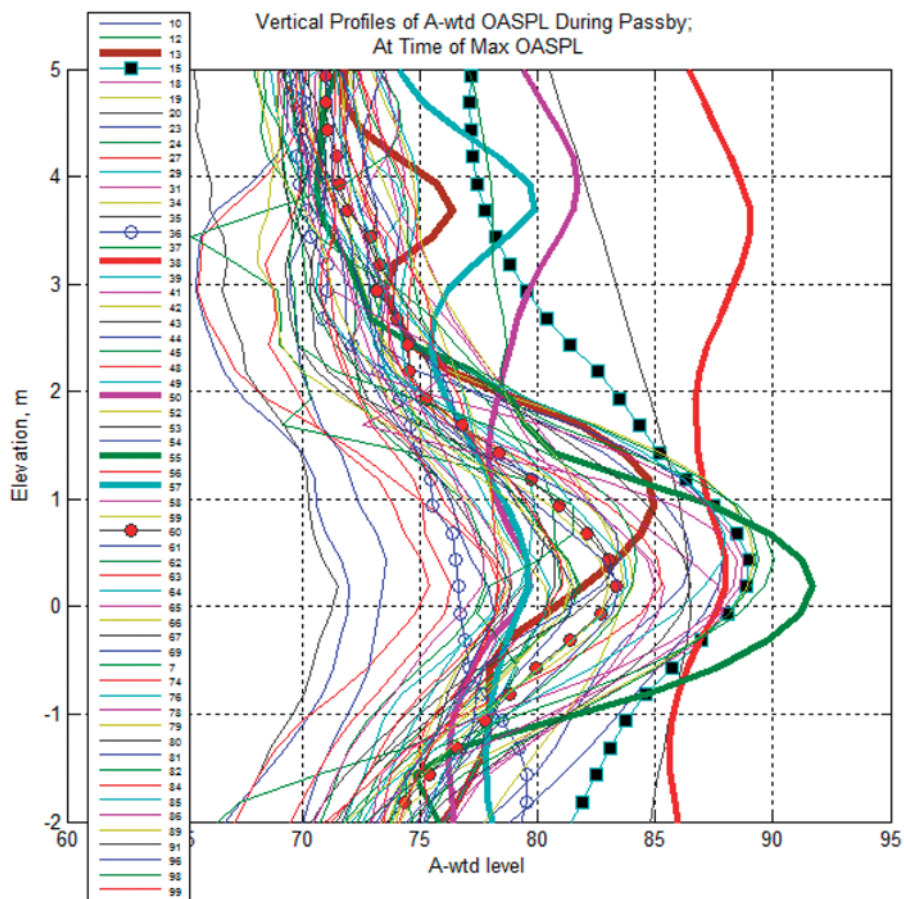
Figure 85. Vertical distributions of overall A-weighted sound levels (in dBA) for heavy trucks. The legend on the left identifies the truck ID numbers.

(a)

(b)
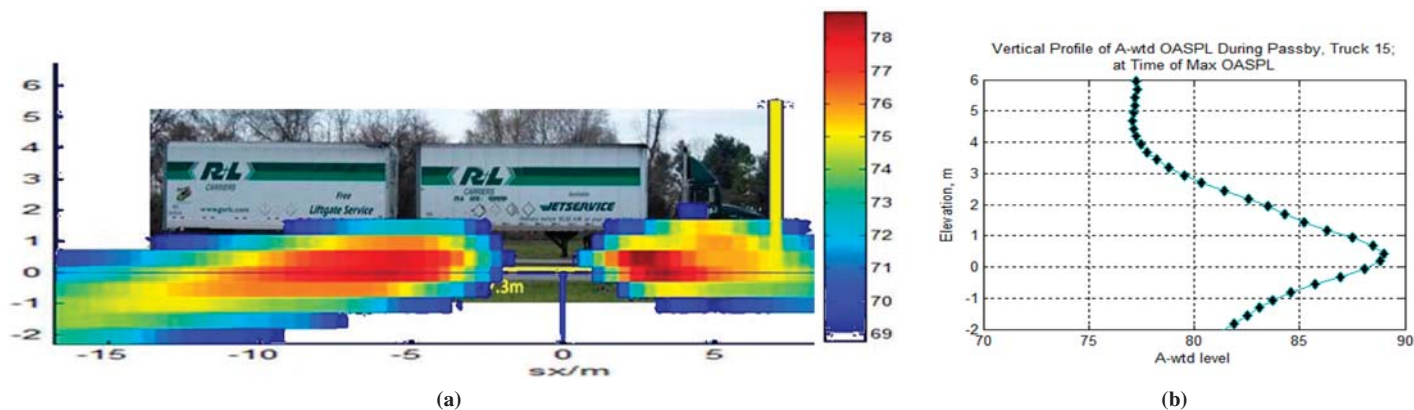
Figure 86. (a) Typical source image and (b) vertical profile of OASPL for truck 15.
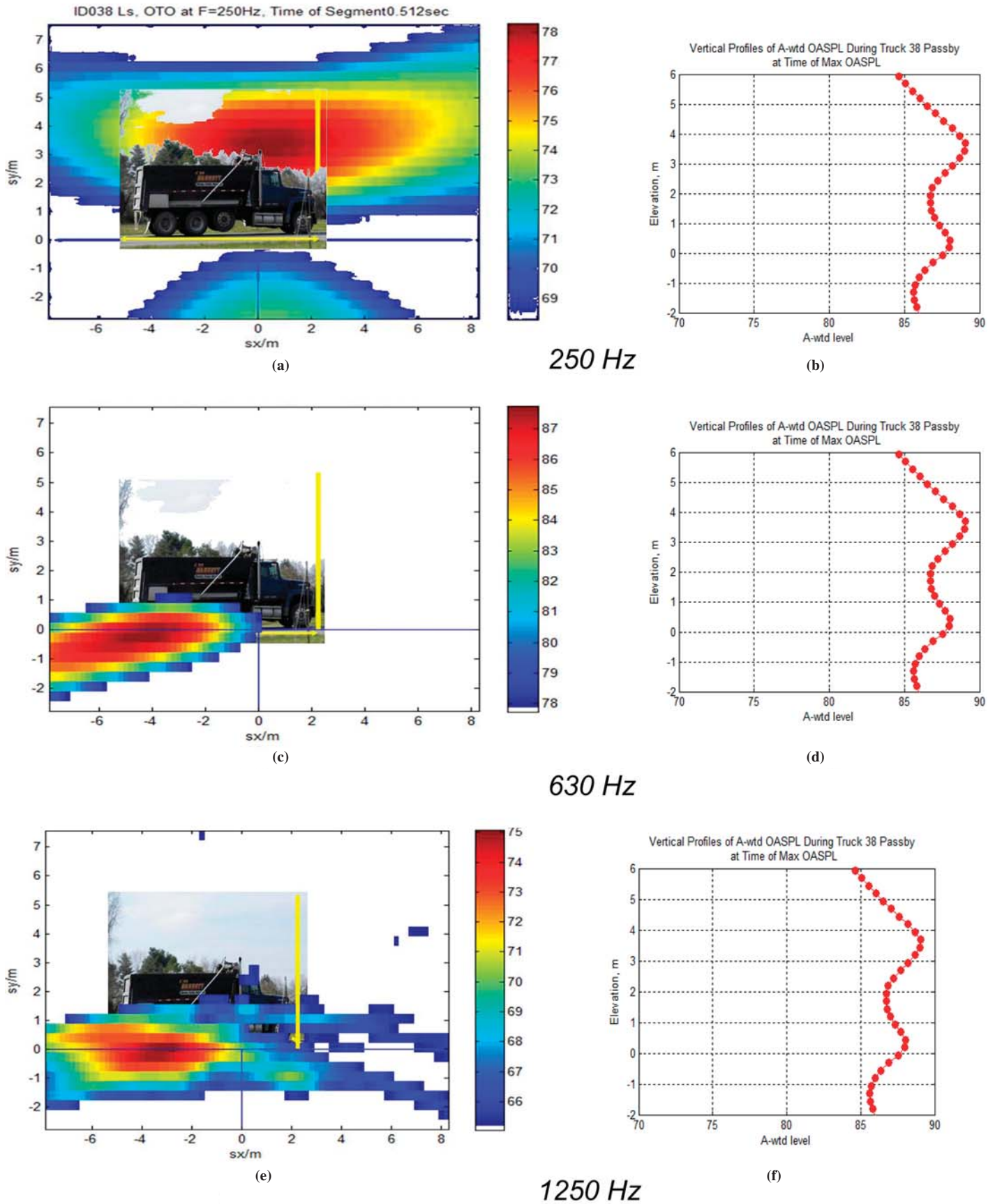
Figure 87. (a, c, e) Source images and (b, d, f) vertical profiles of OASPL for truck 38 in one-third octave bands centered at 250, 630, and 1250 Hz.
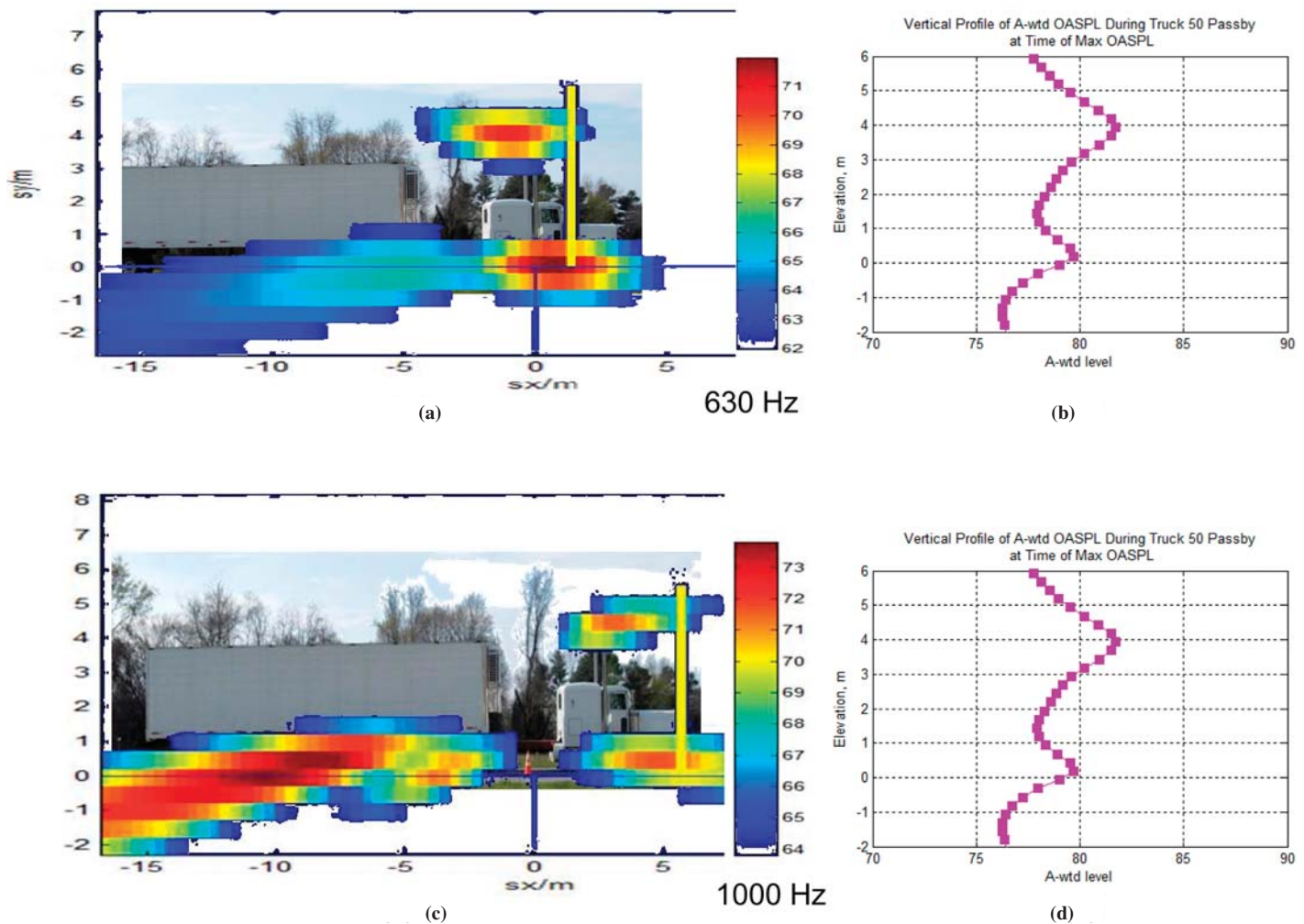
Figure 88. (a, c) Source images and (b, d) vertical profiles of OASPL for truck 50 in one-third octave bands centered at 630 and 1000 Hz.

levels of the population are significantly affected by the exhaust noise sources.

In an interesting case of truck 36, with the source distribution identified in Figure 85, the highest OASPL was localized below the road surface. Figure 89 shows three acoustic images of tanker truck 36 at various frequencies, which also reveal the source images located below the ground plane. The below-grade source image could be due to a combination of the direct-path tire noise and reflection of tire noise off the bottom of the tank. Close inspection of the photograph of this truck showed a distribution of piping and other structure below the tank between the axles, which may explain the presence of the additional weak source in the image at 800 Hz. Note also an increased level of sound in the area of the exhaust stack in the 500 Hz band. A slight shift of the source image from the exhaust stack forward, which can be observed in the figure, is likely a result of a gradual deceleration recorded for this truck.

3.7.3 Example Model of Truck Sources for Simulating Noise Propagation Results of the Vehicle Passbys

Figures 76, 77, and 80 through 88 show the vertical distributions of noise sources as determined by roadside measurements. The key figures are 76 and 80, which show the distributions for heavy trucks. Figure 76 shows the mean A-weighted spectral and overall levels, while Figure 80 shows the distribution of maximum levels. The data plotted in these two figures are presented in Appendix B.

The levels in Figures 76 and 80 and Appendix B are not normalized to absolute values. They are, rather, relative weightings. Application of these results to the Traffic Noise Model (*32*) requires that the levels be normalized to a 50 ft (15 m) passby distance. The scaling process would be as follows:

- At each height convert the levels in Table B-1 or B-2 to energy
- Sum the energies at all heights, then normalize to 1
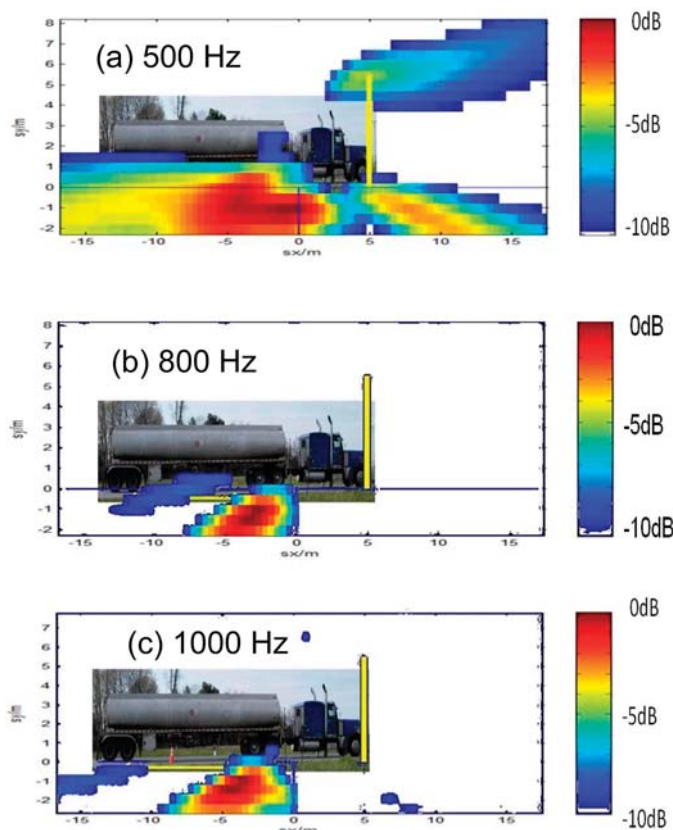
Figure 89. Source image for truck 36 in one-third octave bands centered at (a) 500 Hz, (b) 800 Hz, and (c) 1000 Hz.

Figure 90. Geometry of simulated truck noise sources. Simple sources S_1 and S_2 represent the tire and exhaust sources, respectively.

- Multiply the normalized energies by the energy of a total passby measurement [i.e., the levels in Appendix A of the Traffic Noise Model technical manual (32)]

This process can be carried out for any number of source heights, as a generalization of the upper and lower emission levels defined by Equations 7 and 8 in Appendix A of the Traffic Noise Model technical manual (32).

The apparent vertical distribution of truck noise sources can be effectively simulated by a simple system of two uncorrelated sources, similar to that presented in the Traffic Noise Model technical manual (32). This system is illustrated in Figure 90.

The ground is assumed to reflect sound from both sources with a reflection coefficient of 0.8, as suggested by the measurements made in this project with the calibration source. Note also that this model produced simulated source images that agree well with the measured ones, as was shown previously in Section 3.5.1 (see Figures 35 through 37). The source levels of S_1 and S_2 for the tires and exhaust, respectively, as well as the two heights y_{m1} and y_{m2} are frequency dependent. These quantities are also different for determining the mean sound levels and the maximum sound levels of the truck population. Table 15 gives the values of the parameters that were used to produce the vertical source distributions shown in Figures 91 and 92. The source levels in Table 15 are all relative to 20 µPa at 6 m and represent equivalent free-field source levels from the individual sources. The values shown are example values for two frequencies only. To extend these values to a broader range of frequencies, one would calculate by an inverse propagation method the levels and vertical locations of the elemental source distributions that are required to replicate the one-third octave band profiles. In general this calculation may require a continuum of sources.

The vertical profiles of the equivalent sources obtained for Figures 91 and 92 were produced using the same codes that are described in Sections 3.2.1 and 3.6.2 and used to process the

Table 15. Model parameters for simulation of vertical truck noise source distributions.

Sound Level Metric	Frequency Band (Hz)	Source Level S_1 (dBA)	Source Elevation y_{m1} (m)	Source Level S_2 (dBA)	Source Elevation y_{m2} (m)
Mean Levels	500	81	0.8	63	3.5
	1000	74	0.4	65	3.5
Maximum Levels	500	89	0.7	81	3.5
	1000	84	0.4	77	3.7

(a) Mean levels   **(b)** Maximum levels
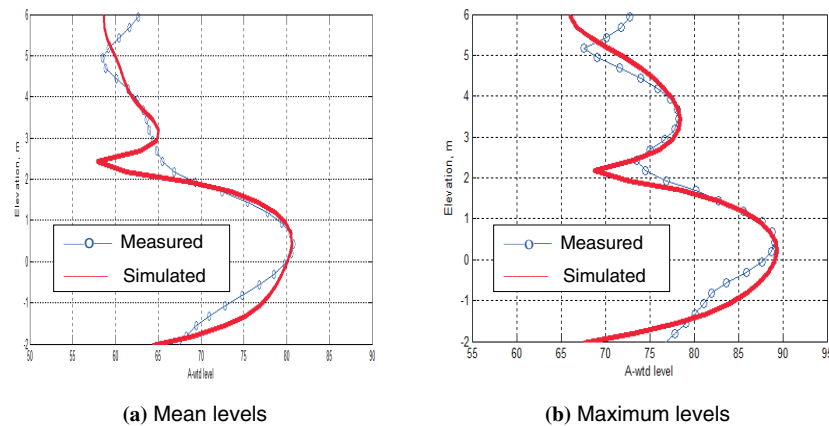
Figure 91. Vertical distributions of source levels for 500 Hz as measured at 6 m (20 ft) distance for heavy trucks: (a) mean levels, (b) maximum levels.

(a) Mean levels   **(b)** Maximum levels
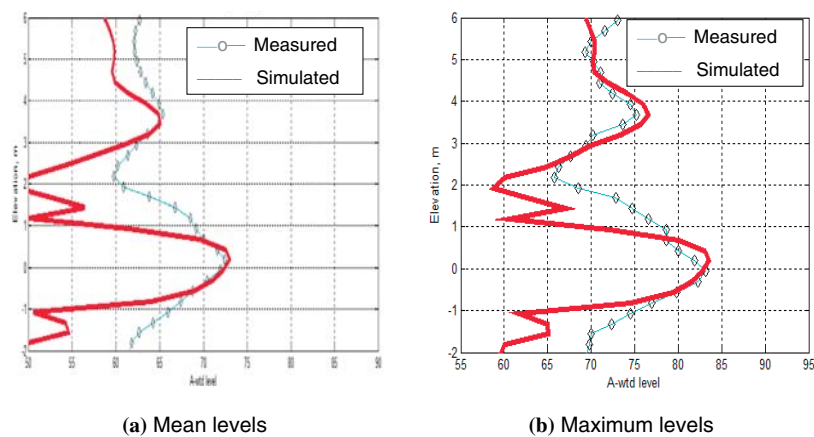
Figure 92. Vertical distributions of source levels for 1000 Hz as measured at 6 m (20 ft) distance for heavy trucks: (a) mean levels, (b) maximum levels.

measurement data. Note that the measured source distributions all match the simulated ones, although as frequency increases it is clear that additional sources would be necessary to "fill out" the profiles at intermediate elevations. These examples show, nevertheless, that a two-source model does provide a starting point that generally characterizes the apparent source profile quite well. To build a complete model of the truck noise sources with the requisite fidelity for a highway noise model, however, one should use the above model exam-

ple as a building block. Among other requirements for the adequate precision, such a model should use ground reflection coefficients as a function of frequency, improve fidelity in the vertical distribution at higher frequencies, and account for some beamforming factors inherent in the current data. These beamforming factors have to do with non-unity correlation coefficients between microphone pairs that determine the precise relationship between the steered array output and the sound levels at the reference microphone.

CHAPTER 4

Conclusions and Recommendations

4.1 Conclusions

Overall, the results of the study validated the beamforming measurement technique in the truck noise application. It is confirmed that the measurement system developed in the course of the project performed effectively in mapping and localizing typical noise sources for stationary and moving trucks in actual road conditions in a wide frequency range from 250 to 2000 Hz. Sound distribution images and maps obtained during truck passbys permitted examination of the time histories and spatial distributions of sources, as well as an analysis of the noise paths from the engine, exhaust, muffler, tires, and other body components for various trucks.

Statistical analysis of the vertical distribution of noise sources indicated that for the majority of truck passbys measured at highway speeds on an in-service highway, tire–pavement interaction was the dominant source generating sound close to the pavement. A small proportion of heavy trucks, however, exhibited significant noise generation in the area of the vertical exhaust stack, dominating at low frequencies and elevations around 3.6 m (12 ft). These results are in general agreement with the conclusions of the Caltrans study that used a commercial beamforming microphone array. The two studies provided essentially similar results in terms of sources identified, their relative contributions, and lack of higher elevation sources except in a few cases.

For the noise prediction modeling purposes, the current study indicated that a simple system of two uncorrelated sources, one located near the pavement and another at the exhaust stack elevation, can generally be used for simulating statistical vertical distributions (mean and maximum) of truck noise sources.

The results of the proof-of-concept testing have been published in two presentations (*33, 34*), and additional publications of the major results are anticipated.

4.2 Recommendations

Based on the key findings and conclusions for the project, the following future research and testing needs can be identified:

- Conduct nationwide roadside truck noise measurements on a wider range of pavement types in multiple states to establish a new truck noise source database (source height distributions and spectral content) for traffic noise models. Additional analysis of subsampling of the full beamforming microphone array may be necessary, based on the data obtained in the current project, to expand the technique, simplify the array, and speed up data collection for wider scale measurements at a practical degree of effort.
- The noise source distributions for trucks obtained in the current study, although based on a relatively small sample of the truck population, can be applied (if deemed appropriate) as interim source height adjustments to the reference emission levels in the FHWA Traffic Noise Model.
- Traffic noise prediction models updated using the noise source distributions obtained in the current study can serve as a resource for state and federal agencies to examine the effectiveness of highway noise mitigation strategies, such as the use of quieter pavements or barrier design.
- Novel information obtained for noise source distributions on trucks, as well as the measurement technique developed in the course of the study, are recommended to truck manufacturers for further studies of potential source- or path-targeting treatments.
- The beamforming measurement technique developed during the course of the study is also recommended for use in the analysis of noise-generating mechanisms and noise abatement measures for automobiles, buses, and motor-

cycles, as well as other noise sources such as construction equipment, etc.

- The approach developed in the study can be used for exploring in greater detail the effects of varying pavement types and terrains on noise generated by different vehicle types, including the effects on vertical noise source distribution and tire–pavement interaction.

References

1. Fleming, G., A. Rapoza, and C. Lee. *Development of National Reference Energy Mean Emission Levels for the FHWA Traffic Noise Model (FHWA TNM), Version 1.* Report DOT-VNTSC-FHWA-96-2, FHWA, U.S. Department of Transportation, 1996.
2. Coulson, R. *Vehicle Noise Source Heights & Sub-Source Spectra.* Report FL-ER-63-96. Florida Atlantic University, Boca Raton, Fla., December 1996.
3. Coulson, R. A Method for Measuring Vehicle Noise Source Heights & Sub-Source Spectra. *Proc., National Conference on Noise Control Engineering Noise-Con 96,* Seattle, Wash., Vol. 2, Institute of Noise Control Engineering, 1996.
4. Van der Toorn, J., T. van den Dool, and W. van Vliet. Sound Emission by Motor Vehicles on Motorways in The Netherlands: 1974–2000. *Proc., Inter-Noise 2001,* The Hague, Netherlands, Netherlands Akoestisch Genootschap, 2001.
5. Heutschi, K. New Swiss Source Model for Road Traffic Noise. *Proc., Inter-Noise 2001,* The Hague, Netherlands, Netherlands Akoestisch Genootschap, 2001.
6. Pallas, M. A. Acoustic Behavior of the Noise Sources of a Truck. *Proc., Inter-Noise 2004,* Prague, Czech Republic, International Institute of Noise Control Engineering, 2004.
7. Illingworth & Rodkin, Inc. *I-80 Davis OGAC Pavement Noise Study: Traffic Noise Levels Associated with an Aging Open Grade Asphalt Concrete Overlay.* Environmental Program—Noise and Vibration Studies, California Department of Transportation, Sacramento, Calif., 2002.
8. Scofield, L., and P. Donavan. Early Results of the Arizona Quiet Pavement Program. *Proc., 80th Meeting of the Association of Asphalt Paving Technologists,* Long Beach, Calif., March 7–9, 2005.
9. Donavan, P., and B. Rymer. Community Reaction to Noise from a New Bridge Span and Viaduct. Presented at 148th Meeting of the Acoustical Society of America, San Diego, Calif., November 2004.
10. Volpe Center Acoustics Facility (VCAF). *Caltrans Rte 138 Tire/Pavement Noise Study.* Environmental Program—Noise and Vibration Studies, California Department of Transportation, Sacramento, Calif., 2004.
11. Sharp, B. H. *Research on Highway Noise Measurement Sites.* Wyle Research Report WCR 72-1, Wyle Laboratories, El Segundo, Calif., March 1972.
12. *Background Document for Interstate Motor Carrier Noise Emission Regulations.* EPA 550/9-74-017, U.S. Environmental Protection Agency, Washington, D.C., October 1974.
13. Shrader, J. T., *Truck Noise IV-B: Identifying the Sources of Noise on a Heavy Duty Diesel Truck.* Report DOT-TST-75-109, U.S. Department of Transportation, May 1975.
14. Plotkin, K. J., D. B. Pies, and R. S. Helizon. *Light Vehicle Noise: Vol. III, Identification of Noise Source Components and Evaluation of Noise Reduction Techniques.* Wyle Research Report WR 79-20, Wyle Laboratories, Arlington, Va., October 1979.
15. Plotkin, K. J., and D. B. Pies. *Light Vehicle Noise: Vol. IV, The Effect of Partial Engine Enclosures on Light Vehicle Noise Levels and Operating Temperatures.* Wyle Research Report WR 79-22, Wyle Laboratories, Arlington, Va., October 1979.
16. Donavan, P., and L. Oswald. The Identification and Quantification of Truck Tire Noise Sources Under On-Road Operating Conditions. *Proc., Inter-Noise 80,* Miami, Fla., December 1980.
17. Rasmussen, P., and S. Gade. *Tyre Noise Measurement on a Moving Vehicle.* Application Note 96/04. Brüel & Kjær Sound & Vibration Measurement A/S, Naerum, Denmark, 1996.
18. Ruhala, R. J., and C. B. Burroughs. Tire-Pavement Interaction Noise Source Identification Using Multi-Planar Nearfield Acoustical Holography. *Proc., The Society of Automotive Engineers Noise and Vibration Conference and Exposition,* Paper No. 1999-01-1733, Traverse City, Mich., May 1999.
19. Crewe A., F. Perrin, V. Benoit, and K. Haddad. Real-Time Passby Noise Source Identification Using a Beam-Forming Approach. *Proc., The Society of Automotive Engineers Noise and Vibration Conference,* Paper No. 2003-01-1537, Traverse City, Mich., 2003.
20. Blake, W. K., and P. R. Donavan. A New Road-Side Array-Based Method for Characterization of Truck Noise During Passby. *Proc., NoiseCon 2008/ASME NCAD,* Dearborn, Mich., American Society of Mechanical Engineers, July 2008.
21. Barsikow, B. *The Snowflake Array—A New Development in Microphone-Array Technology.* Akustic-data Engineering, Berlin, 2002.
22. Christensen, J. J., and J. Hald. *Beamforming.* Technical Review No.1-2004. Brüel & Kjær Sound & Vibration Measurement A/S, Naerum, Denmark, 2004.
23. *PULSE Beamforming—Type 7768.* Product Data. Brüel & Kjær Sound & Vibration Measurement A/S, Naerum, Denmark, 2004.
24. Dougherty, R. P. Beamforming in Acoustic Testing. In *Aeroacoustic Measurements,* Chapter 2. T. J. Mueller, ed., Springer Verlag, 2002.
25. Meadows, K., T. Brooks, W. Humphreys, W. Hunter, and C. Gerhold. Aeroacoustic Measurements of a Wing-Flap Configuration, *Proc., 18th AIAA Aeroacoustics Conference,* Paper AIAA-97-1595, Atlanta, Ga., 1997.
26. Underbrink, J. R. *Practical Considerations in Focused Array Design for Passive Broad-Band Source Mapping Applications.* M.S. Thesis, The Pennsylvania State University, May 1995.
27. Underbrink, J. R. Aeroacoustic Phased Array Testing in Low Speed Wind Tunnels. In *Aeroacoustic Measurements,* Chapter 3. T. J. Mueller, ed., Springer Verlag, 2002.

74

28. Olsen, S. and T. J. Mueller. *An Experimental Study of Trailing Edge Noise.* Interim Report UNDAS-IR-0105, University of Notre Dame, Department of Aerospace and Mechanical Engineering, February 2004.

29. Donavan, P. Generation of Noise by Truck and Car Tires on Various Types of Asphalt Concrete Pavements. *Proc., Inter-Noise 2006,* Honolulu, Hawaii, December 2006.

30. Donavan, P. R., T. Dib, W. K. Blake, and B. Rymer. Determination of the Vertical Distribution of Noise Sources in Truck Pass-bys Using Acoustic Beam-forming. *Proc., Noise-Con 2008,* Dearborn, Mich., Institute of Noise Control Engineering, July 2008.

31. Donavan, P. R., and B. Rymer. Measurements of the Vertical Distribution of Truck Noise Sources During Highway Cruise Pass-bys Using Acoustic Beam-forming. In *TRB 2009 Annual Meeting* (CD-ROM), Transportation Research Board of the National Academies, Washington, D.C., January 2009.

32. Menge, C. W., C. F. Rossano, G. S. Anderson, and C. J. Bajdek. *FHWA Traffic Noise Model, Version 1.0, Technical Manual.* Report DOT-VNTSC-FHWA-98-2, FHWA, U.S. Department of Transportation, 1998.

33. Plotkin, K. J., Y. Gurovich, W. Blake, and P. Donavan. Noise Source Mapping for Trucks, Part 1: Development and Design. *Proc., Acoustics'08 Paris,* France, June–July 2008.

34. Blake W., K. J. Plotkin, Y. Gurovich, and P. Donavan. Noise Source Mapping for Trucks, Part 2: Experimental Results. *Proc., Acoustics'08 Paris,* France, June–July 2008.

APPENDIX A

Array Microphone Coordinates

Horizontal (*x*) and vertical (*y*) coordinates, in meters, of microphones vs. array center (0;0)

Microphone Number	*x* (m)	*y* (m)	Microphone Number	*x* (m)	*y* (m)
1	-0.204	0.465	40	0.490	-1.134
2	-0.276	0.632	41	0.113	-0.672
3	-0.347	0.799	42	0.152	-0.911
4	-0.418	0.966	43	0.191	-1.150
5	-0.490	1.134	44	0.230	-1.389
6	-0.113	0.672	45	0.269	-1.628
7	-0.152	0.911	46	0	-0.746
8	-0.191	1.150	47	-0.001	-1.010
9	-0.230	1.389	48	-0.002	-1.273
10	-0.269	1.628	49	-0.003	-1.537
11	0	0.746	50	-0.005	-1.801
12	0.001	1.010	51	-0.113	-0.672
13	0.002	1.273	52	-0.154	-0.908
14	0.003	1.537	53	-0.195	-1.145
15	0.005	1.801	54	-0.236	-1.381
16	0.113	0.672	55	-0.278	-1.616
17	0.154	0.908	56	-0.204	-0.465
18	0.195	1.145	57	-0.277	-0.627
19	0.236	1.381	58	-0.350	-0.789
20	0.278	1.616	59	-0.423	-0.951
21	0.204	0.465	60	-0.496	-1.112
22	0.277	0.627	61	-0.254	-0.166
23	0.350	0.789	62	-0.345	-0.222
24	0.423	0.951	63	-0.435	-0.278
25	0.496	1.112	64	-0.525	-0.333
26	0.254	0.166	65	-0.615	-0.387
27	0.345	0.222	66	-0.254	0.166
28	0.435	0.278	67	-0.344	0.227
29	0.525	0.333	68	-0.434	0.289
30	0.615	0.387	69	-0.524	0.351
31	0.254	-0.166	70	-0.613	0.414
32	0.344	-0.227	71	0	-0.241
33	0.434	-0.289	72	0	0
34	0.524	-0.351	73	0	0.241
35	0.613	-0.414	74	0	-0.467
36	0.204	-0.465	75	0	-0.114
37	0.276	-0.632	76	0	0.114
38	0.347	-0.799	77	0	0.467
39	0.418	-0.966	–	–	–

APPENDIX B

Vertical Distributions of Noise Sources for Heavy Trucks

Table B1. Vertical distribution of mean one-third octave band and overall A-weighted sound levels for 59 heavy trucks.

One Third Octave Band Levels re 20 microPascals at 6m Range   Generated by VertScanStatistics_Plotter1.m and includes y offset=.27m

	Frequency (Hz)															
Elevation (m)	100	125	169	200	250	315	400	500	630	800	1000	1250	1600	2000	2500	OASPL
-3.81	67.15	61.31	65.43	65.34	61.42	59.52	60.26	62.64	59.89	61.03	63.07	60.25	58.90	57.76	56.79	74.12
-3.56	67.22	61.43	65.58	65.54	61.79	60.04	60.78	62.95	60.23	61.16	62.82	60.31	59.18	57.52	56.75	74.28
-3.31	67.30	61.54	65.73	65.75	62.19	60.60	61.35	63.34	60.60	61.30	62.51	60.29	59.43	57.39	56.81	74.45
-3.06	67.38	61.66	65.89	65.97	62.62	61.18	61.97	63.87	60.98	61.44	62.14	60.19	59.65	57.37	56.98	74.66
-2.81	67.46	61.78	66.04	66.20	63.08	61.79	62.65	64.56	61.36	61.58	61.79	59.98	59.79	57.39	57.00	74.89
-2.56	67.53	61.89	66.20	66.45	63.58	62.41	63.39	65.38	61.73	61.72	61.53	59.68	59.73	57.29	56.74	75.15
-2.31	67.61	62.01	66.35	66.71	64.11	63.05	64.20	66.29	62.07	61.87	61.44	59.49	59.60	57.35	56.53	75.46
-2.06	67.69	62.13	66.51	66.98	64.66	63.69	65.08	67.24	62.39	62.09	61.51	59.66	59.50	57.54	56.46	75.84
-1.81	67.76	62.25	66.66	67.26	65.24	64.32	66.06	68.25	62.76	62.49	61.81	60.20	59.21	57.70	56.50	76.28
-1.56	67.83	62.36	66.81	67.55	65.83	64.92	67.15	69.44	63.42	63.19	62.67	60.75	58.96	57.67	56.41	76.84
-1.31	67.90	62.47	66.96	67.85	66.42	65.50	68.33	70.94	64.73	64.12	64.20	61.25	59.26	57.57	56.23	77.60
-1.06	67.96	62.59	67.10	68.14	66.99	66.02	69.58	72.79	66.86	65.15	65.93	62.11	60.09	58.00	55.99	78.61
-0.81	68.02	62.69	67.23	68.43	67.54	66.49	70.84	74.83	69.44	66.32	67.38	63.16	61.00	58.65	56.30	79.83
-0.56	68.07	62.80	67.36	68.70	68.04	66.91	72.04	76.80	71.96	67.90	68.75	63.86	61.41	58.77	56.34	81.16
-0.31	68.11	62.91	67.48	68.95	68.48	67.26	73.08	78.49	74.03	69.78	70.39	64.69	61.90	59.12	56.59	82.47
-0.06	68.14	63.01	67.60	69.17	68.85	67.54	73.89	79.78	75.48	71.29	71.90	66.27	64.21	60.82	57.83	83.59
0.19	68.16	63.11	67.70	69.34	69.12	67.76	74.41	80.57	76.18	71.86	72.44	67.06	65.63	62.23	59.04	84.22
0.44	68.16	63.21	67.79	69.46	69.28	67.89	74.58	80.81	76.04	71.26	71.60	65.92	63.99	60.61	57.64	84.21
0.69	68.15	63.30	67.87	69.52	69.32	67.92	74.34	80.46	74.95	69.69	70.03	64.51	62.50	59.61	57.14	83.68
0.94	68.13	63.39	67.93	69.52	69.24	67.82	73.66	79.46	72.86	68.08	69.17	64.55	62.33	59.60	57.24	82.78
1.19	68.09	63.47	67.98	69.46	69.03	67.55	72.50	77.78	69.93	67.01	68.52	64.13	62.32	59.97	57.30	81.56
1.44	68.03	63.55	68.02	69.33	68.69	67.08	70.89	75.42	67.14	65.57	66.74	62.68	61.32	58.91	56.62	80.05
1.69	67.96	63.62	68.04	69.15	68.24	66.39	68.89	72.46	65.67	63.19	63.76	60.75	60.45	58.07	55.97	78.51
1.94	67.87	63.67	68.04	68.92	67.70	65.50	66.77	69.33	64.60	60.62	60.92	59.41	60.34	57.99	55.32	77.29
2.19	67.76	63.71	68.03	68.67	67.12	64.47	64.96	66.85	62.74	58.97	59.79	58.92	60.25	57.71	55.30	76.47
2.44	67.63	63.73	67.99	68.39	66.53	63.47	63.83	65.51	60.35	58.17	60.20	59.98	60.28	57.19	55.55	76.00
2.69	67.49	63.72	67.93	68.12	66.00	62.72	63.36	64.83	59.04	57.97	61.37	61.03	59.83	57.12	55.63	75.76
2.94	67.34	63.70	67.85	67.85	65.55	62.37	63.32	64.34	59.44	58.76	62.35	61.43	59.45	57.25	56.04	75.65
3.19	67.17	63.64	67.75	67.59	65.18	62.32	63.48	63.95	60.38	60.58	63.61	61.39	59.15	57.30	56.58	75.64
3.44	66.99	63.57	67.62	67.34	64.87	62.36	63.60	63.63	61.19	62.29	64.90	61.32	59.11	57.69	57.00	75.71
3.69	66.80	63.46	67.45	67.08	64.58	62.29	63.51	63.23	61.56	63.32	65.34	61.10	59.39	58.43	57.47	75.68
3.94	66.60	63.33	67.26	66.82	64.26	62.00	63.08	62.56	61.34	63.71	64.92	60.39	59.09	58.05	57.46	75.42
4.19	66.39	63.18	67.03	66.53	63.88	61.44	62.28	61.50	60.68	63.61	64.15	59.76	58.77	58.19	57.32	75.04
4.44	66.18	63.00	66.77	66.21	63.41	60.61	61.09	60.13	60.15	63.25	63.39	59.63	58.98	58.75	57.06	74.63
4.69	65.96	62.80	66.48	65.86	62.84	59.52	59.58	58.87	60.31	62.82	62.79	59.74	59.09	59.10	57.03	74.25
4.94	65.74	62.59	66.17	65.46	62.18	58.18	57.78	58.49	60.97	62.40	62.42	59.82	59.04	59.41	56.86	73.92
5.19	65.52	62.36	65.82	65.03	61.41	56.62	55.80	59.20	61.65	61.92	62.19	59.71	59.36	59.63	56.55	73.65
5.44	65.30	62.12	65.45	64.56	60.57	54.88	53.78	60.42	62.16	61.37	62.11	59.57	59.98	59.86	56.32	73.45
5.69	65.09	61.86	65.06	64.06	59.64	53.02	52.03	61.63	62.54	60.83	62.29	59.69	60.53	59.77	56.10	73.30
5.94	64.88	61.61	64.66	63.52	58.65	51.15	50.96	62.65	62.86	60.39	62.70	59.93	61.11	59.51	55.99	73.22
6.19	64.67	61.34	64.24	62.97	57.61	49.42	50.79	63.47	63.11	60.04	63.13	60.12	61.47	59.29	56.20	73.17
6.44	64.47	61.08	63.81	62.39	56.54	48.03	51.28	64.11	63.28	59.76	63.44	60.21	61.75	59.20	56.36	73.12
6.69	64.27	60.81	63.37	61.79	55.46	47.11	52.03	64.61	63.33	59.54	63.67	60.30	62.08	59.15	56.32	73.08
6.94	64.08	60.55	62.93	61.19	54.39	46.65	52.77	64.98	63.26	59.35	63.89	60.50	62.19	58.96	56.31	73.02
7.19	63.89	60.29	62.50	60.58	53.35	46.51	53.42	65.27	63.10	59.21	64.16	60.81	62.18	58.70	56.33	72.97
7.44	63.72	60.04	62.06	59.97	52.37	46.55	53.98	65.48	62.87	59.12	64.47	61.17	62.26	58.60	56.32	72.94
7.69	63.55	59.79	61.63	59.37	51.46	46.65	54.46	65.63	62.62	59.08	64.77	61.50	62.31	58.58	56.45	72.92
7.94	63.39	59.55	61.20	58.76	50.65	46.77	54.89	65.74	62.36	59.09	65.03	61.79	62.22	58.44	56.66	72.88
8.19	63.23	59.31	60.79	58.17	49.95	46.88	55.28	65.82	62.12	59.15	65.21	62.02	62.03	58.29	56.77	72.84

Table B2. Vertical distribution of maximum one-third octave band and overall A-weighted sound levels for 59 heavy trucks.

One Third Octave Band Levels re 20 microPascals at 6m Range   Generated by VertScanStatistics_Plotter1.m and includes y offset=.27m

Frequency (Hz)

Elevation (m)	100	125	169	200	250	315	400	500	630	800	1000	1250	1600	2000	2500	OASPL
-3.81	83.18	70.08	78.99	81.44	74.61	72.64	73.52	73.46	70.75	70.73	71.05	66.39	66.03	63.66	63.27	85.62
-3.56	83.27	70.31	79.07	81.52	74.67	72.94	73.94	73.93	71.69	71.46	70.65	66.41	66.42	63.80	63.10	85.81
-3.31	83.36	70.54	79.15	81.59	74.70	73.20	74.30	74.32	72.53	72.16	69.81	66.50	65.84	63.28	63.43	86.00
-3.06	83.44	70.77	79.21	81.64	74.70	73.41	74.59	74.61	73.20	72.89	69.22	67.30	65.40	62.71	65.20	86.16
-2.81	83.53	71.00	79.27	81.69	74.64	73.57	74.79	74.76	73.66	73.72	69.70	67.36	66.35	63.00	65.43	86.26
-2.56	83.62	71.24	79.32	81.72	74.54	73.66	74.89	74.75	73.85	74.65	69.46	66.82	67.32	62.90	63.78	86.26
-2.31	83.70	71.47	79.35	81.74	74.38	73.68	74.88	75.02	73.70	75.62	68.30	66.23	67.94	62.77	62.43	86.18
-2.06	83.79	71.70	79.38	81.75	74.88	73.61	74.74	76.53	73.20	76.45	69.45	67.29	68.17	63.22	61.59	86.02
-1.81	83.87	71.93	79.39	81.74	75.81	73.45	74.45	77.89	72.41	76.94	69.77	68.24	66.75	64.03	61.64	85.83
-1.56	83.94	72.15	79.40	81.72	76.72	73.20	74.60	79.09	71.95	76.87	70.04	67.84	63.74	63.74	62.15	85.67
-1.31	84.01	72.35	79.39	81.69	77.59	72.83	76.37	80.13	73.01	76.05	72.30	67.22	63.71	62.56	62.95	85.61
-1.06	84.07	72.55	79.38	81.66	78.41	72.59	77.96	81.06	77.49	74.37	74.52	68.99	64.15	62.18	61.72	85.69
-0.81	84.13	72.73	79.37	81.62	79.16	72.60	79.30	81.94	81.82	74.80	76.96	70.38	65.25	64.18	63.00	85.96
-0.56	84.17	72.89	79.36	81.59	79.83	72.37	80.33	83.61	85.05	75.38	79.84	71.01	65.80	64.32	61.70	87.63
-0.31	84.20	73.03	79.36	81.57	80.40	72.58	81.49	85.96	87.30	78.45	82.23	72.50	66.67	63.09	62.98	89.77
-0.06	84.22	73.14	79.37	81.57	80.86	73.26	82.96	87.67	88.66	79.86	83.11	73.20	68.97	65.31	63.79	91.14
0.19	84.22	73.22	79.41	81.61	81.20	73.70	83.94	88.72	89.16	79.56	81.86	73.92	71.33	65.66	64.98	91.66
0.44	84.21	73.28	79.47	81.68	81.39	73.88	84.42	89.10	88.74	77.27	80.05	74.21	68.87	65.34	64.22	91.23
0.69	84.17	73.29	79.57	81.80	81.42	73.76	84.35	88.78	87.28	77.89	78.62	71.65	66.64	64.48	62.57	89.86
0.94	84.11	73.27	79.70	81.96	81.27	73.63	83.69	87.66	84.62	77.83	78.64	72.52	67.93	63.88	63.42	88.54
1.19	84.04	73.20	79.86	82.16	80.93	73.69	82.38	85.60	80.65	75.65	76.55	71.41	67.93	64.87	63.41	87.13
1.44	83.93	73.10	80.05	82.38	80.38	73.48	80.32	82.78	78.14	74.68	74.71	69.77	66.30	64.28	63.60	86.80
1.69	83.81	72.95	80.24	82.63	79.59	72.94	77.42	80.23	77.57	72.55	72.83	69.91	65.07	62.08	62.76	86.73
1.94	83.66	72.75	80.44	82.88	78.55	71.95	73.66	76.91	76.09	69.66	68.55	68.00	65.20	62.81	61.61	86.72
2.19	83.48	72.51	80.62	83.12	78.01	72.64	73.14	74.48	73.89	68.55	65.76	65.06	66.28	63.69	61.64	86.87
2.44	83.28	72.22	80.78	83.34	78.86	74.18	74.06	73.55	70.66	66.70	66.25	65.45	65.38	63.40	61.79	87.25
2.69	83.05	71.89	80.91	83.52	79.53	75.57	75.99	75.02	69.02	64.83	67.64	67.01	63.94	60.95	62.23	87.72
2.94	82.81	71.63	81.00	83.64	80.01	76.67	77.51	76.74	71.05	65.57	69.36	68.16	63.70	61.78	62.46	88.22
3.19	82.54	71.80	81.04	83.71	80.30	77.43	78.52	77.82	73.32	70.22	70.18	68.96	64.05	62.48	61.26	88.67
3.44	82.25	71.90	81.02	83.72	80.41	77.85	79.04	78.27	74.64	73.11	73.59	68.28	65.13	63.36	64.19	89.02
3.69	81.94	71.94	80.95	83.65	80.35	77.91	79.08	78.09	74.76	73.66	75.20	70.52	66.45	66.60	66.13	89.06
3.94	81.61	72.00	80.83	83.52	80.11	77.65	78.67	77.32	73.66	72.54	74.55	69.91	65.87	63.23	62.76	88.69
4.19	81.28	72.14	80.64	83.31	79.72	77.06	77.82	75.94	71.94	70.87	72.42	67.20	64.94	63.64	63.95	88.17
4.44	80.93	72.32	80.40	83.05	79.17	76.17	76.56	74.01	70.53	70.90	71.01	66.99	64.41	63.23	63.04	87.62
4.69	80.57	72.45	80.11	82.72	78.49	74.98	74.90	71.63	70.06	70.79	71.04	67.00	64.35	63.17	63.04	87.07
4.94	80.20	72.54	79.77	82.33	77.68	73.51	72.84	69.10	71.32	70.12	70.33	67.17	63.92	63.30	63.86	86.54
5.19	79.83	72.59	79.38	81.89	76.74	71.75	70.41	67.55	72.14	69.13	69.27	67.30	63.95	64.13	63.41	86.02
5.44	79.46	72.62	78.95	81.41	75.69	69.74	67.68	70.16	72.70	68.08	69.98	67.06	64.48	64.98	62.45	85.53
5.69	79.09	72.62	78.48	80.89	74.54	67.50	64.88	71.83	73.12	67.19	71.55	66.75	66.78	65.89	62.44	85.07
5.94	78.72	72.60	77.99	80.34	73.30	65.14	62.61	72.77	73.42	66.52	73.02	66.68	68.02	65.48	61.92	84.65
6.19	78.36	72.56	77.46	79.76	71.97	62.90	61.59	73.18	73.57	65.95	73.94	67.13	67.90	65.09	62.52	84.25
6.44	78.00	72.51	76.92	79.16	70.58	61.19	61.70	73.26	73.50	65.35	74.39	67.41	68.19	65.73	62.80	83.84
6.69	77.65	72.44	76.35	78.54	69.14	60.35	62.22	73.51	73.19	65.64	74.69	67.55	69.02	65.14	63.02	83.41
6.94	77.30	72.36	75.77	77.91	67.67	60.23	62.72	73.92	72.92	66.55	75.14	68.44	69.17	64.01	61.78	82.99
7.19	76.97	72.27	75.18	77.27	66.21	60.46	63.09	74.19	72.97	67.24	75.83	69.28	68.27	63.90	62.24	82.63
7.44	76.64	72.18	74.59	76.63	64.81	60.75	63.34	74.36	72.74	67.65	76.64	69.84	67.39	63.85	62.54	82.30
7.69	76.33	72.08	73.99	75.98	63.54	61.00	63.48	74.49	72.83	67.83	77.38	70.02	67.77	64.04	62.78	81.99
7.94	76.02	71.98	73.39	75.34	62.46	61.18	63.55	74.57	73.08	67.88	77.93	69.86	68.07	64.21	62.27	81.66
8.19	75.72	71.88	72.80	74.71	61.64	61.30	63.57	74.63	73.25	67.89	78.23	69.55	68.22	63.96	62.03	81.32

APPENDIX C

Glossary of Special Terms

1 Hz spectrum level: The level of a signal spectrum in a frequency band 1 Hz wide, often called spectral density.

Aperture: An opening in a microphone array through which sound waves travel.

Autospectrum: The averaged magnitude of multiple instantaneous spectra with the coefficients of the components expressed as the square of the magnitudes.

A-weighted sound level: The sound level obtained by use of A-weighting. A-weighting accounts for the frequency sensitivity of the human ear by decreasing the sound levels at very low and very high frequencies (below approximately 500 Hz and above approximately 10,000 Hz) to approximate the human ear's sensitivities to those frequencies [units: dBA].

Bandwidth: A frequency range of a segment of the frequency spectrum, which may be specified by its upper and lower cutoff frequencies.

Beam width (spot width): The width of the main lobe in the directivity pattern of a microphone array.

Beamforming: A signal processing technique used in sensor arrays for directional signal transmission or reception.

Cross spectrum: Cross-spectrum analysis is an extension of single-spectrum Fourier analysis (see *autospectrum, fast Fourier transform,* and *spectrum*) to the simultaneous analysis of two signals. The purpose of cross-spectrum analysis is to uncover the correlations between two signals at different frequencies.

Decibel (dB): The unit used to identify 10 times the common logarithm of two like quantities proportional to power, such as sound power or sound pressure squared, commonly used to define the level produced by a sound source. For the A-weighted sound levels, the unit symbol dBA is used.

Directivity: A measure of the directional characteristic of a microphone or a microphone array and its sensitivity to sound waves that arrive from various directions of propagation of the incident sound.

Doppler shift: The apparent change in frequency of sound waves, varying with the relative velocity of the source and the receiver: if the source and receiver are drawing closer together, the frequency is increased, and vice versa.

Equivalent sound level (Leq): The level of a constant sound that, in the given situation and time period, has the same average sound energy as does a time-varying sound. Specifically, equivalent sound level is the energy-averaged sound pressure level of the individual A-weighted sound pressure levels occurring during the specified time interval [units: dBA].

Fast Fourier transform (FFT): An efficient algorithm to compute the discrete Fourier transform of a signal, which decomposes a sequence of values into components of different frequencies (spectrum). This operation is useful in many fields but computing it directly from the definition is often too slow to be practical. An FFT is a way to compute the same result more quickly.

Free field: A sound field in a homogeneous isotropic medium whose boundaries exert a negligible influence on the sound waves. In practice, it is a field in which the effects of the boundaries are negligible over the frequency range of interest.

Frequency: The number of oscillations per second completed by a vibrating object [units: Hz].

Frequency resolution: Minimum difference in frequency between two components of the sound spectrum which still allows resolving two distinct peaks in the spectrum.

Grating lobe: A secondary projection in the directivity pattern of a microphone array caused by the interference of individual microphone directivities.

Hertz (Hz): The unit used to designate frequency. Specifically, the number of cycles per second.

Inverse square law: See *spherical spreading (divergence).*

Main lobe: A major projection or protuberance of rounded or globular form, specifically in the directivity pattern of a microphone array.

Microphone array: A collection or arrangement of multiple microphones in a certain order for conducting special measurements of sound.

Non-specular reflection: The change of direction which the ray of sound experiences when it strikes upon a surface and is thrown back into the same medium making the angle of reflection NOT equal to the angle of incidence, unlike in mirror reflection.

Octave: The interval between two sound frequencies having a ratio of 2.

Octave band: A frequency range which is one octave wide. Standard octave bands are designed by their center frequency.

Octave band center frequency: The geometric mean of the upper and lower frequencies of the octave band. Standard octave band center frequencies in the audible range are 31.5, 63, 125, 250, 500, 1000, 2000, 4000, 8000, and 16,000 Hz.

One-third octave: The interval between two sound frequencies having a ratio of the cube root of 2.

One-third octave band: A frequency range which is one-third octave wide. Standard one-third octave bands are designed by their center frequency.

One-third octave band center frequency: The geometric mean of the upper and lower frequencies of the one-third octave band. Standard one-third octave band center frequencies (in Hz) in the audible range are:

25.0	50.0	100	200	400	800	1,600	3,150	6,300	12,500
31.5	63.0	125	250	500	1,000	2,000	4,000	8,000	16,000
40.0	80.0	160	315	630	1,250	2,500	5,000	10,000	20,000

Overall sound pressure level (OASPL): The logarithmic level of the total energy contained in the noise spectrum, determined as the sum (based on energy) of the sound pressure levels of all frequency components [units: dB]. In this report this operation is applied to the A-weighted sound levels (in dBA).

Pink noise: Noise with a continuous frequency spectrum and with equal power per constant percentage bandwidth. For example, equal power in any one-third octave band.

Resonance: The tendency of a system to oscillate at its maximum amplitude, associated with specific frequencies known as the system's resonance frequencies (or resonant frequencies).

Sound exposure level (SEL): A time-integrated metric (i.e., continuously summed over a time period) which quantifies the total energy in the A-weighted sound level measured during a transient noise event. SEL represents the sound level of the constant sound that would, in one second, generate the same acoustic energy as did the actual time-varying noise event [units: dBA].

Sound intensity: The rate of flow of sound energy through a unit area normal to the specified direction at the point considered.

Sound (noise) source: The object which generates the sound.

Sound power: The rate per unit time at which sound energy is radiated from a source.

Sound power level (PWL): A measure in decibels of the rate at which sound energy radiates from a sound source. Specifically, it is the total energy per second produced by a sound source, and expressed in decibels, equal to 10 times the logarithm to the base 10 of the ratio of the power of a sound to the reference power of 10^{-12} watts [units: dB].

Sound pressure level (SPL): A measure in decibels of the magnitude of the sound. Specifically, the sound pressure level of a sound, in decibels, is 10 times the logarithm to the base 10 of the ratio of the squared pressure of this sound to the squared reference pressure. The reference pressure is usually taken to be 20 micropascals [units: dB].

Spatial resolution: Determination or breaking up of the image of a sound source into separate, constituent elements or parts in the space domain.

Spectrum: The frequency content of the noise produced by the source. The noise is broken into multiple periodic (frequency) components, each with an amplitude and phase.

Spherical spreading (divergence): The spreading of sound waves from a point source in a free field, resulting in a diminution in sound pressure level with increasing distance from the source. For waves having wave fronts that are concentric spheres (spherical waves), the sound pressure level decreases 6 dB for each doubling of distance from the source (inverse square law).

Spiral angle: The angle between a twisted spoke of a spiral microphone array and the array radial axis [see Figure 1(a)].

Wavelength: The physical distance between identical points on successive waves.

Weighting: An additive (or subtractive) factor by which the sound pressure level at certain frequencies in an acoustic measurement is increased (or reduced) in order for that measurement to be more representative of certain simulated conditions. See *A-weighted sound level*.

Abbreviations and acronyms used without definitions in TRB publications:

AAAE	American Association of Airport Executives
AASHO	American Association of State Highway Officials
AASHTO	American Association of State Highway and Transportation Officials
ACI–NA	Airports Council International–North America
ACRP	Airport Cooperative Research Program
ADA	Americans with Disabilities Act
APTA	American Public Transportation Association
ASCE	American Society of Civil Engineers
ASME	American Society of Mechanical Engineers
ASTM	American Society for Testing and Materials
ATA	Air Transport Association
ATA	American Trucking Associations
CTAA	Community Transportation Association of America
CTBSSP	Commercial Truck and Bus Safety Synthesis Program
DHS	Department of Homeland Security
DOE	Department of Energy
EPA	Environmental Protection Agency
FAA	Federal Aviation Administration
FHWA	Federal Highway Administration
FMCSA	Federal Motor Carrier Safety Administration
FRA	Federal Railroad Administration
FTA	Federal Transit Administration
IEEE	Institute of Electrical and Electronics Engineers
ISTEA	Intermodal Surface Transportation Efficiency Act of 1991
ITE	Institute of Transportation Engineers
NASA	National Aeronautics and Space Administration
NASAO	National Association of State Aviation Officials
NCFRP	National Cooperative Freight Research Program
NCHRP	National Cooperative Highway Research Program
NHTSA	National Highway Traffic Safety Administration
NTSB	National Transportation Safety Board
SAE	Society of Automotive Engineers
SAFETEA-LU	Safe, Accountable, Flexible, Efficient Transportation Equity Act: A Legacy for Users (2005)
TCRP	Transit Cooperative Research Program
TEA-21	Transportation Equity Act for the 21st Century (1998)
TRB	Transportation Research Board
TSA	Transportation Security Administration
U.S.DOT	United States Department of Transportation